Investigation of the Emergence and Elimination of Antibiotic Tolerant Variants in *Pseudomonas aeruginosa*

Dissertation

Presented in Partial Fulfillment of the Requirements for the Degree Doctor of Philosophy in the Graduate School of The Ohio State University

By

Devin Sindeldecker

Biomedical Sciences Graduate Program

The Ohio State University

2021

Dissertation Committee

Paul Stoodley, Advisor

John S. Gunn

Daniel J. Wozniak

Matthew Anderson

Abstract

Pseudomonas aeruginosa is an opportunistic pathogen commonly associated with lung infections of patients with cystic fibrosis as well as infections in wounds and post-surgical sites. These infections are often difficult to treat due to the rise of antibiotic resistance including multi-drug resistance. *P. aeruginosa* is also able to form biofilms which increase tolerance to antimicrobials and provide a high-density population which increases the probability of the emergence of antibiotic resistant or tolerant variants.

In order to combat infections of wounds and surgical sites, local antibiotic therapy is often used to allow for higher concentrations of antibiotic to be achieved at the site without having to worry about the toxicity associated with systemic treatment. In investigations of the local antibiotic treatment method's ability to kill biofilm infections, it was noted that variant colonies emerge within the zone of clearance (ZOC) of the antibiotic source. Here, we describe our efforts to: 1) characterize the phenotypes which emerge as variant colonies within the ZOC, 2) investigate the novel tolerance phenotype identified emerging within the ZOC, using RNAseq, and 3) identify the area under the curve (concentration vs time) necessary to achieve complete biofilm eradication as exhibited in the zone of killing (ZOK) of an antibiotic source.

We report the presence of classically resistant mutants, persister cells, viable but non-cultureable like cells, and phoenix colonies emerging from within the ZOC of a

tobramycin impregnated calcium sulfate bead. Phoenix colonies are a novel, antibiotic tolerant phenotype which are able to survive and maintain high levels of metabolic activity while high concentrations of tobramycin are present in the environment but return to wild-type levels of susceptibility once the antibiotic pressure is removed. Both whole genome sequencing and RNAseq were performed on phoenix colony isolates in an attempt to understand the mechanisms behind their survival. Phoenix colonies were found to be transcriptionally different from controls and differentially expressed genes (DEGs) were identified which may give clues to the mechanism behind phoenix colony development.

Lastly, the ZOK of tobramycin was investigated using a combination of *in vitro* and computational techniques to determine if there was an area under the curve (AUC, concentration vs time) associated with the complete killing of the biofilm lawn and antibiotic resistant and tolerant variants. We report a consistent AUC, regardless of starting mass of antibiotic or biofilm substrate, that is able to eradicate *P. aeruginosa* biofilms.

Collectively, the findings presented here serve to further our understanding of antibiotic tolerance and the phenotypes associated with it. Additionally, through our AUC findings, we have made progress towards the goal of eliminating antibiotic resistance. These findings demonstrate the importance for continued research into methods and therapeutics to combat the rising rate of antibiotic resistance and tolerance.

Dedication

I dedicate this thesis to my wife, Madalyn Sindeldecker, my parents, Jeffrey and Dana Sindeldecker, my brothers, Dillon, Dalton, and Deacon Sindeldecker, and my mentor, Paul Stoodley.

Acknowledgments

I would like to begin by thanking my advisor, Dr. Paul Stoodley, for providing a place in your lab for me to grow, both as a student and a person. You often encouraged me to be the best that I could and provided countless opportunities to push myself further. The lessons that I have learned under your mentorship and guidance will stay with me not only in my scientific career but also my life. It has been an honor being your student. I could not have asked for a better mentor, and I cannot thank you enough for all that you have done for me.

I would also like to thank my thesis committee, Dr. John Gunn, Dr. Daniel Wozniak, and Dr. Matthew Anderson. I truly appreciate all of the work and support that you have put into me and my project. From feedback after presentations, experiment discussions, and opening up your lab and resources to me, you were crucial to my development as a student and the success of my project. Additionally, I would like to thank all of the past and current members of the Stoodley lab. I have enjoyed not only working alongside each of you but also learning from you as well. I have many fond memories and will never forget the experiences that we have shared. A special thanks to Kelly Moore and Anthony Li, two incredible undergraduate researchers that I had the pleasure of working with and mentoring. I greatly appreciate all of the effort and time that you put into helping me throughout my project.

Lastly, I would like to thank my wife Maddy, my parents, my brothers, and my grandparents. I would not be where I am today without all of your unconditional support, love, and encouragement in my academic career as well as in the rest of my life. Even when you were unaware, you helped me through the most challenging parts of this journey. You all have made me who I am, and I am eternally grateful for each of you.

Vita

2016……..B.S. Biology, West Liberty University

2016-Present……Graduate Research Associate, The Ohio State University

Publications

Sindeldecker, D., Prakash, S., & Stoodley, P. (2021). Exploration of the Pharmacodynamics for *Pseudomonas aeruginosa* Biofilm Eradication by Tobramycin. *Antimicrobial agents and chemotherapy*.

Sindeldecker, D., & Stoodley, P. (2021). The Many Antibiotic Resistance and Tolerance Strategies of *Pseudomonas aeruginosa*. *Biofilm*, 100056.

Sindeldecker, D., Moore, K., Li, A., Wozniak, D. J., Anderson, M., Dusane, D. H., & Stoodley, P. (2020). Novel aminoglycoside-tolerant phoenix colony variants of *Pseudomonas aeruginosa*. *Antimicrobial agents and chemotherapy*, *64*(9), e00623-20.

Dusane, D. H., Brooks, J. R., **Sindeldecker, D.**, Peters, C. W., Li, A., Farrar, N. R., ... & Stoodley, P. (2019). Complete killing of agar lawn biofilms by systematic spacing of antibiotic-loaded calcium sulfate beads. *Materials*, *12*(24), 4052.

Dusane, D. H., Lochab, V., Jones, T., Peters, C. W., **Sindeldecker, D.**, Das, A., ... & Stoodley, P. (2019). Electroceutical treatment of *Pseudomonas aeruginosa* biofilms. *Scientific reports*, *9*(1), 1-13.

Lehnig, A. C., Dewal, R. S., Baer, L. A., Kitching, K. M., Munoz, V. R., Arts, P. J., **Sindeldecker, D.**, ... & Stanford, K. I. (2019). Exercise training induces depot-specific adaptations to white and brown adipose tissue. *Iscience*, *11*, 425-439.

Loughman, K., Hall, J., Knowlton, S., **Sindeldecker, D.**, Gilson, T., Schmitt, D. M., ... & Horzempa, J. (2016). Temperature-dependent gentamicin resistance of *Francisella tularensis* is mediated by uptake modulation. *Frontiers in microbiology*, *7*, 37.

Robinson, C. M., Kobe, B. N., Schmitt, D. M., Phair, B., Gilson, T., Jung, J. Y., ..., **Sindeldecker, D.**, & Horzempa, J. (2015). Genetic engineering of *Francisella tularensis* LVS for use as a novel live vaccine platform against *Pseudomonas aeruginosa* infections. *Bioengineered*, *6*(2), 82-88.

Fields of Study

Major Field: Biomedical Sciences

Area of Emphasis: Microbial Pathogenesis

Table of Contents

List of Tables

List of Figures

Chapter 1. Introduction

Figures and excerpts adapted from: Sindeldecker, D., & Stoodley, P. (2021). The Many Antibiotic Resistance and Tolerance Strategies of *Pseudomonas aeruginosa*. *Biofilm*, 100056.

The Many Antibiotic Resistance and Tolerance Strategies of *Pseudomonas aeruginosa*.

Devin Sindeldecker and Paul Stoodley

1.1. Introduction to *Pseudomonas aeruginosa*

Pseudomonas aeruginosa is a Gram-negative, opportunistic, bacterial pathogen associated with a wide range of infections including cystic fibrosis (CF) associated lung disease, post-surgical infections, and chronic wound infections (1-4). *P. aeruginosa* has several strategies which it uses to establish and maintain infection including biofilm production, multidrug resistance, and antibiotic tolerance (5-8). Along with several other bacterial pathogens, multidrug resistance in *P. aeruginosa* is a growing concern (9-13). In addition, *P. aeruginosa* CF isolates have been shown to be hypermutable, further raising the concern for antimicrobial tolerance and resistance to develop (14). Aminoglycoside resistance, in particular, is a growing concern in *P. aeruginosa* (15-17) and is something which must be understood and accounted for in clinical treatment plans.

P. aeruginosa has multiple antibiotic resistance and tolerance phenotypes which could allow survival of a bacterial population during antibiotic treatment of an infection. These phenotypes are highly diverse in not only their mechanisms of development but also in the extent to which they are able to survive in the presence of antibiotics. Antibiotic tolerance has also been found to allow for development of complete antibiotic resistance (18), further showing the importance of understanding how these phenotypes develop and function in order to prevent recurrent and recalcitrant infections. In this review, various resistance and tolerance phenotypes will be summarized in terms of their mechanisms of development and survival despite the presence of antibiotics.

1.2. Antibiotic Resistance

Antibiotic resistance is characterized primarily by genetic alterations which allow cells to actively resist killing by antibiotics. This can be accomplished through antibiotic target site modification, enzymatic degradation of the antibiotic, or an increase in expression of efflux pump genes (19-21). Additionally, there are other mechanisms which confer antibiotic resistance, including heteroresistance and adaptive resistance.

1.2.1. Mutation Driven Antibiotic Resistance

"Classical" antibiotic resistance is driven by either stable mutations or horizontal gene transfer of plasmids harboring resistance genes, both of which allow bacteria to survive in the presence of antibiotics at both high concentrations and over repeated

exposures. Treatment of *P. aeruginosa* is primarily accomplished using aminoglycosides such as gentamicin or tobramycin. Aminoglycoside resistance through modifying enzymes which inactivate the aminoglycoside has been known to exist since the 1960's and 1970's (21-23). These enzymes often phosphorylate or adenylate the antibiotics and multiple modifying enzymes are often harbored in a single genome, allowing for broad-spectrum antibiotic disruption (24-26). In addition, modification of membrane permeability can lead to a decrease in the uptake of antibiotics (27, 28), and, additionally, the presence of efflux pumps such as the MexXY pump (in aminoglycosides) or the MexCD-OprJ and MexEF-OprN pumps (in fluoroquinolones) serve to further prevent antibiotics from accumulating intracellularly (24, 29-32). Target site modification (ribosomal in the case of aminoglycosides, or DNA gyrase in fluoroquinolones) has also been noted, leading to a lack of binding of the antibiotic to its target (27, 33). Antibiotic resistance can also be conferred through horizontal gene transfer, in which antibiotic modifying enzyme genes can be acquired by plasmid transfer from other species of bacteria (34, 35). Clinically, antibiotic resistance is a growing concern. A recent study on 60 *P. aeruginosa* strains isolated from burn patients found that 90% were resistant to at least one antibiotic and 94% of the isolates were multidrug resistant (25). Another study on *P. aeruginosa* clinical isolates found overexpression of MexXY-OprM in 53% of strains, indicating the importance of efflux pumps as well in a clinical setting (24).

1.2.2. Heteroresistance

In additional to classical antibiotic resistance, in which a complete population exhibits the phenotype, heteroresistance is a classification characterized by a small subset

of genetically resistant bacteria hiding within a population which is overall susceptible to the antibiotic (36, 37). During antibiotic exposure, the majority of the population is killed leaving the resistant subset behind to recolonize as an antibiotic recalcitrant infection (38, 39). Although this is similar to the early stages of classical resistance development, it is important to note that heteroresistance is unstable and can revert to an antibiotic susceptible population where the antibiotic pressure is removed (36). This instability, combined with the low frequency of resistant cells within the population, leads to difficulties in detection of heteroresistance (36). Clinically, antibiograms are charts used to determine the susceptibility of a culture to various antibiotics. The most commonly used methods to generate an antibiogram are by disc diffusion or Etest assays. Unfortunately, heteroresistance is difficult to identify using traditional antibiogram methods due to the possibility of the overall population appearing susceptible during the initial assay if the resistant population is too small to be detected (40, 41) and it is possible that this could lead to treatment failure (41, 42). Population assay profiling (PAP) uses a dilution series of antibiotic concentrations to allow the heteroresistant population to emerge and be visualized (43). Heteroresistance has also been linked to spontaneous, unstable tandem amplifications of known resistance genes across different bacterial species and in response to various antibiotics (44). In order to combat the presence of these resistance mechanisms in a heteroresistant population, Band et al. propose using combination antibiotic therapy to exploit these populations in a clinical setting (45). Combination antibiotic therapy would be effective in treating a population containing multiple heteroresistant subpopulations by targeting multiple subcellular sites.

This would overcome the resistance mechanism of each subpopulation and allow for complete killing of all of the bacteria regardless of the presence of heteroresistance.

1.2.3. Adaptive Resistance

Another antibiotic survival mechanism of *P. aeruginosa*, termed adaptive resistance, is characterized by a transient resistance to antibiotics. Adaptive resistance in *P. aeruginosa* was first identified clinically in sputum samples from CF patients in 1996 (46). While the molecular mechanisms of resistance are not fully understood, this phenotype is primarily driven by environmental stimuli such as antimicrobial exposure, pH changes, anaerobic environments, and starvation. Adaptive resistance has also been highly linked to swarming motility, biofilm development, and a transient upregulation of the MexXY-OprM efflux pump (47-49). Once the antibiotic pressure is removed, the adaptive resistance bacteria are able to revert to a wild-type level of antibiotic susceptibility (48). Currently, the presence of an adaptive resistance phenotype being present in a clinical setting is speculative, and further research is needed to explore the danger which this phenotype may present.

1.3. Antibiotic Tolerance

In addition to antibiotic resistance, antibiotic tolerance is an area of increased concern, especially given the potential of tolerance leading to population resistance over time (18). Antibiotic tolerance is generally differentiated from antibiotic resistance by a lack of a stable phenotype. Tolerance is characterized as an ability to survive transient

exposure to high concentrations of antibiotic without a change in the minimum inhibitory concentration (MIC) for the organism. This is often achieved by altering essential bacterial processes (50).

1.3.1. Persister Cells

Persister cells are an antibiotic tolerant phenotype of bacteria which enter a metabolically inactive state of dormancy but return to a wild-type level of antibiotic susceptibility once antibiotic concentrations drop below the MIC leading to a population which is again susceptible to the antibiotic (Figure 1.1) (5, 51, 52). They were first described in *Staphylococcus aureus* by Hobby et al. in 1942 (53). Two years later, Joseph Bigger further described the phenotype in *Staphylococcus pyogenes*, adding that while persister cells were able to survive antibiotics (penicillin), they were not genetically different than wild-type (54). Further studies have implicated toxin-antitoxin (TA) systems in the mechanism behind persister cell tolerance (5, 55-57). TA systems are comprised of a stable, protein toxin which disrupts essential cellular processes as well as an antitoxin which prevents toxicity (57). Overproduction of the toxin portion of a TA system relative to antitoxin production leads to an autotoxicity induced dormancy state. Two TA systems have been identified in *Escherichia coli* which led to the development of the persister cell phenotype, the MqsR/MqsA system and the TisB/IstR-1 system (58, 59). Within the MqsR/MqsA system, MqsR leads to diminished translation and ability to respond to cellular stresses leading to a state of dormancy (60-63). For the TisB/IstR-1 system, the TisB toxin decreases both the proton motive force and ATP leading to

cellular dormancy (22). Although *E. coli* persister cells have been studied extensively, these TA systems do not have homologs in *P. aeruginosa* and little is known about the mechanisms behind *P. aeruginosa* persister cell development despite a high level of emergence specifically within CF patients (64). Persister cells develop at a low rate (~1% of the population, (65)), however, it is a major concern due to the possibility of them leading to recurrent infections (8), although this has yet to be confirmed in a clinical study.

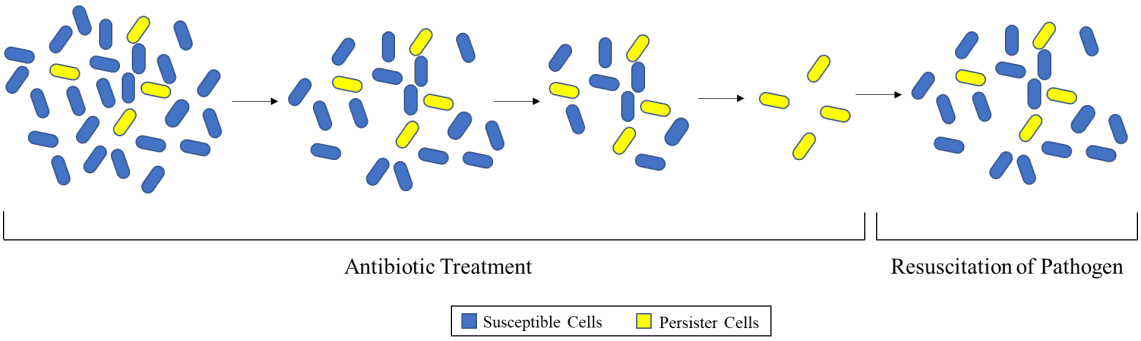

Figure 1.1 Progression of persister cells during antibiotic treatment.

1.3.2. Small Colony Variants

Small colony variants (SCV) are phenotypic variants directly associated with antibiotic tolerance and persistent infections. In *P. aeruginosa*, they were first described in CF associated *P. aeruginosa* respiratory tract infections (66). After their discovery, the first clinical investigation was performed from 1996 to 1998 (67). After testing sputum from 86 CF patients for *P. aeruginosa* SCVs, it was found that 33 patient samples contained isolates from this phenotype. SCVs are typically characterized by their small size relative to wild-type. This small colony size is due to either a slower growth rate like that exhibited by *Staphylococcus aureus* SCVs (68, 69), or more commonly by extracellular matrix overproduction in *Pseudomonas*' rugose SCVs (RSCVs), which also allow SCVs to be tolerant to a range of antibiotic classes (67, 69). SCVs can be differentiated from RSCVs by their appearance. SCVs are typically small and smooth colonies, whereas RSCVs, also known as wrinkly spreader colonies, have a rough appearance due to the overproduction of matrix components (69, 70). Drenkard and Ausubel showed that *P. aeruginosa* RSCVs could be induced by the addition of kanamycin to culturing media and were able to link the phenotype to the cyclic-di-GMP (cdG) phosphodiesterase gene, pvrR (71). Additionally, D'Argenio et al. identified another gene implicated in RSCV formation within the lab strain *P. aeruginosa* PAO1, the WspR diguanylate cyclase (DGC) (72). cdG is produced when DGC joins two molecules of GTP (73). cdG is highly promiscuous and binds to transcriptional regulators (74-76). Within RSCVs, intracellular levels of cdG have been found to be elevated, leading to transcriptional changes including the overproduction of exopolysaccharides,

fimbrial adhesins, Psl, Pel, and alginate (77-82). These changes contribute to both the rough, morphological presentation of RSCVs as well as the antibiotic tolerance phenotype which allows RSCVs to survive therapeutic interventions. Antibiotic tolerance of RSCVs is likely due to the hyperbiofilm state produced by overproduction of the extracellular matrix components. Clinically, RSCVs have been seen for decades and continue to be a concerning issue, particularly within the field of cystic fibrosis. Additionally, RSCVs have been associated with prolonged antibiotic treatment and poor clinical outcomes (67).

1.3.3. Metabolic Alterations

In addition to the aforementioned, well described, antibiotic tolerant phenotypes, other metabolic variants have been identified which are tolerant to antibiotics. In 2019, Schiessl et al. described an antibiotic tolerant phenotype of *P. aeruginosa* which is driven by an alternative metabolism induced in anaerobic or microaerobic environments (83). This paper proposed that the alternate metabolism uses phenazines which are produced by the *Pseudomonas* cells as an alternative electron acceptor due to the lack of available oxygen. Further research has shown that when glucose and pyruvate are converted into acetate by fermentation, phenazines are able to regenerate the oxidant NAD(P)H by acting as an extracellular electron shuttle and alleviating the redox constraints on the metabolic pathway (84). While the link is not fully understood, this metabolic phenotype confers tolerance to ciprofloxacin, allowing for survival until oxygen is present again (83). An overproduction of agmatine has also been associated with antibiotic tolerance in

P. aeruginosa. Agmatine is a pre-poly-amine intermediate metabolite of the arginine decarboxylase pathway. After observing a correlation between agmatine concentration and CF disease severity, McCurtain et al. further explored the effects of this metabolite on antibiotic tolerance and virulence. It was found that cells harboring an increased amount of agmatine were tolerant to positively charged aminoglycosides and polymyxins but were still susceptible to antibiotics with a neutral charge. It is believed that this is due to membrane stabilization since agmatine is also positively charged (85). Further studies are needed to better characterize these and other metabolic variants of *P. aeruginosa* including the mechanisms conferring this type of antibiotic tolerance, particularly their role in a clinical setting.

1.3.4. Phoenix Colonies

In 2020, Sindeldecker et al. described a novel antibiotic tolerant phenotype which they have termed phoenix colonies (Chapter 2, (86)). Phoenix colonies are able to grow and remain metabolically active in the presence of antibiotics, even when the antibiotic concentration is >10 times the MIC. However, after being removed from the antibiotic environment from which they emerged, the phoenix colonies return to a wild-type level of antibiotic susceptibility (86). The molecular mechanisms behind this phenotype are currently unknown and much work is needed to better characterize and understand their antibiotic survival and its implications. Similar to heteroresistance, phoenix colonies appear to have avoided detection until now due to the limitations of conventional assays. Anecdotally, due to relatively short incubations times (~24 hours), colonies do not

typically arise within the zone of inhibition or zone of clearance of a bacterial population. Those which do arise have been considered to be resistant mutants. The methods used to detect phoenix colonies, involved incubating the bacteria for an extended period of time (120 hours) before replica plating onto both media containing and lacking antibiotic in order to differentiate between resistant colonies and any tolerance mechanisms which may be present (86). Additionally, the PAP assay for heteroresistance uses cultures equivalent to a 0.5 McFarland standard, which are approximately $1x10^8$ CFUs/mL (87). The higher concentrations of bacteria (~$5x10^9$ CFU/mL) used to detect phoenix colonies provide a more sensitive system which may be able to further detect heteroresistance (86). As phoenix colonies have only recently been discovered, it has yet to be confirmed whether or not they may exist in a clinical setting. It is also important to note that the field of antibiotic tolerant phenotypes is still advancing, leading to new tolerant phenotypes continuing to be discovered.

In addition to phoenix colonies, Sindeldecker et al. also identified viable but non-culturable (VBNC)-like colonies emerging as antibiotic tolerant variants (86). This colonies were able to grow in the presence of tobramycin on initial exposure but were unable to be cultured through replica plating. Due to the unculturable nature of VBNC-like colonies, further studies have yet to be completed to identify the mechanism behind their emergence and antibiotic survival.

1.3.5. Biofilm Populations

In addition to phenotypes which occur in single cells of a population, antibiotic tolerance can also be conferred at the population level though mechanisms such as biofilm formation. Biofilms are populations of bacteria which conglomerate and encase themselves in an extracellular polymeric substance (EPS) (88). The EPS matrix is comprised of polysaccharides, proteins, eDNA, and lipids and provides a scaffolding structure for the bacteria within the biofilm (89, 90). In *P. aeruginosa* specifically, the main components of the EPS are Pel, Psl, and alginate, three exopolysaccharides (89-92). cdG is an important transcriptional regulator for the biofilm phenotype and causes an increase in production of adhesins and EPS components (93-95). Quorum sensing is also an important function for control of biofilm formation (96) and consists of two major systems, Las and Rhl (97). One important characteristic of biofilms is their ability to survive high concentrations of antibiotics. This antibiotic tolerance is conferred through a number of mechanisms (4), the most basic of which is a restriction in antibiotic penetration into the biofilm (Figure 1.2a). This restriction primarily effects charged antibiotics as they are bound up by other charged components of the EPS (98, 99). This antibiotic binding protects bacteria which are deeper within the biofilm, as the antibiotics are hindered from reaching them. In addition to antibiotics being unable to effectively penetrate the biofilm, nutrients and oxygen are also limited deep within the biofilm leading to a slower growth phenotype (Figure 1.2b). Nutrient depletion also leads to an increase in the SOS and stringent responses (Figure 1.2b) which have also been shown to play a role in tolerance (4, 100, 101). Additionally, the large population increases the

chance for the emergence of persister cells, phoenix colonies, resistant mutants, and any other small population phenotype (Figure 1.2c). Both the slow growth and persister cell phenotypes exhibit an increased tolerance to antibiotics (55, 102). As mentioned previously, the survival of persister cells could possibly lead to a recurrent infection (8). Clinically, biofilm related *P. aeruginosa* infections are commonly observed in chronic obstructive pulmonary disorder, cystic fibrosis, urinary tract infections, catheterization, intubation, and surgical site infections (2, 103-105). Biofilm related infections are considered especially serious due to the difficult in achieving complete killing and clearance of the biofilm.

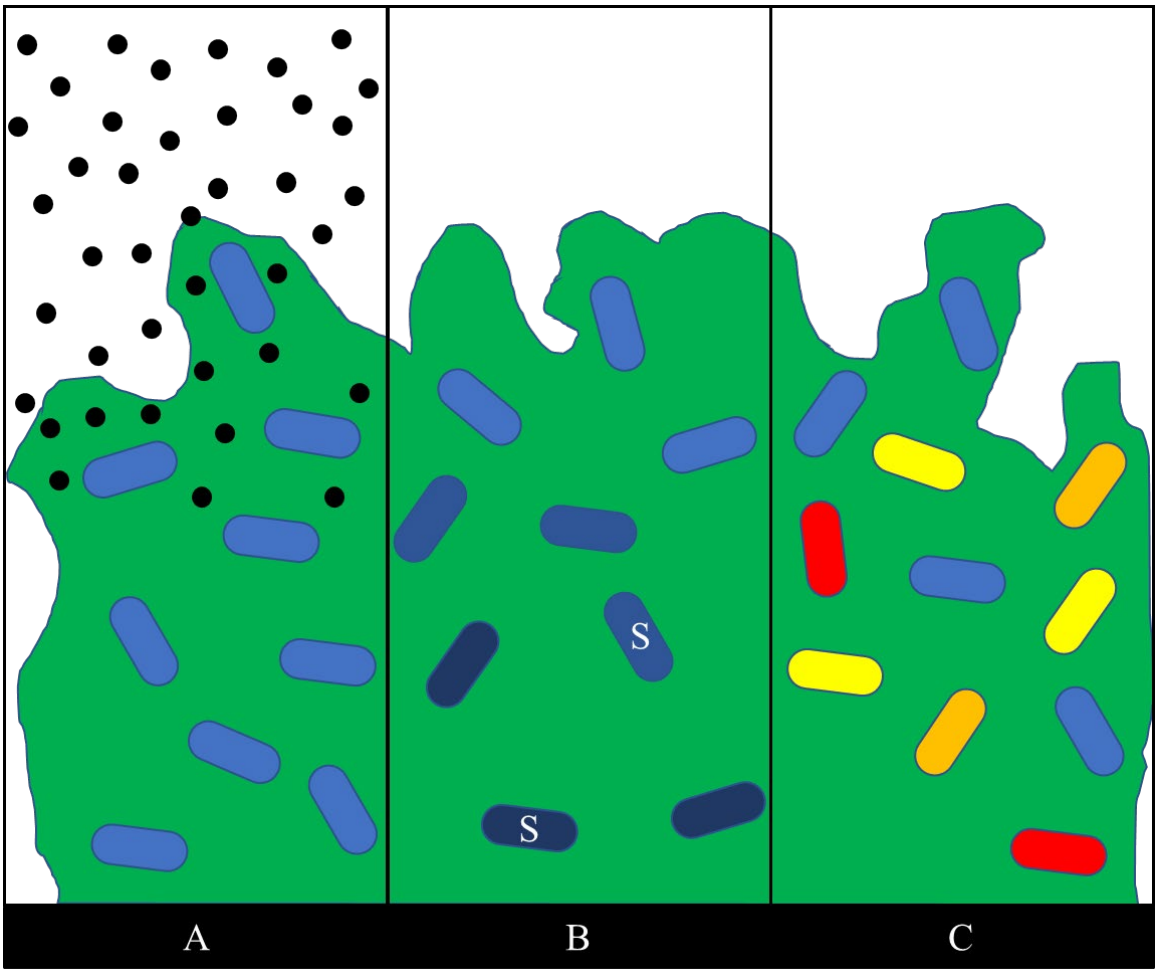

Figure 1.2 Four mechanisms of antibiotic survival in *P. aeruginosa* biofilms.

A – Antibiotic (black circles) penetration is restricted, preventing complete killing of biofilm cells; B – a concentration gradient of oxygen and nutrients leads to regions of slow or non-growing bacteria (shaded cells) deeper within the biofilm, some cells within the biofilm may also exhibit an increase in the SOS response (white "S") due to nutrient depletion; C – the large population of cells in the biofilm increase the chances for persister cells (yellow), phoenix colonies (red), or resistant mutants (orange) to emerge. Adapted from P. S. Stewart (106).

1.4. Conclusions

Numerous antibiotic tolerant and resistant phenotypes exist in *P. aeruginosa*, at both the single cell (Figure 1.3) and population levels. Both antibiotic tolerance and antibiotic resistance are growing issues throughout many pathogenic species, including *P. aeruginosa*. Clinically, classical antibiotic resistance, heteroresistance, RSCVs, and biofilms have been implicated in *P. aeruginosa* infections (25, 41, 67, 107-109). The presence of these antibiotic resistance and antibiotic tolerance phenotypes is extremely concerning not only due to the difficulty in treating infections of this nature but also due to the increased severity of these infections (67, 89). As antibiotic resistance and tolerance continues to emerge, the morbidity and mortality associated with these infections will also likely increase. An understanding of the mechanisms by which *P. aeruginosa* is able to survive antibiotic therapeutics is fundamental in not only the clinical setting but also in the laboratory setting, as it is important to be able to differentiate between the various phenotypes when performing any research related to antibiotic therapies. It is also important to further characterize these phenotypes and to continue to evaluate antibiotic surviving isolates for novel driving mechanisms, so that we may be able to further our knowledge and combat the rising number of reoccurring, persisting, and recalcitrant infections.

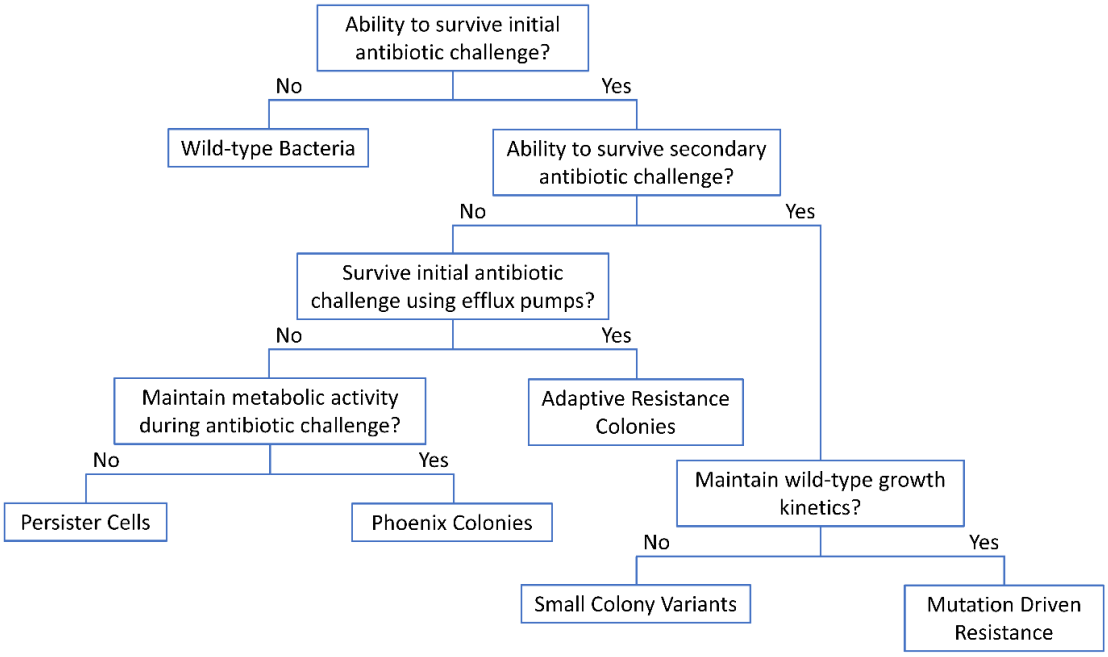

Figure 1.3 Antibiotic tolerant and resistant phenotype comparisons.

Flow chart comparing the differences between the most common antibiotic tolerant and resistant phenotypes in *P. aeruginosa*. The range of phenotypes span fully susceptible wild-type bacteria, transiently tolerant phenotypes, and fully resistant bacteria driven by genetic mutations.

1.5. Aims and Hypotheses

Antibiotic resistance and tolerance are a growing concern in *P. aeruginosa,* particularly in the context of biofilm related infections. Preliminary data from our lab while investigating the ability of tobramycin impregnated calcium sulfate beads and bone cements had demonstrated colonies emerging within the zone of clearance of the antibiotic source. While it was likely that these colonies were resistant mutants, we believed that antibiotic tolerant variants could also be present. The work described herein sought to identify the phenotypes which could emerge in the zone of clearance as well as to investigate the ability to prevent variant colony emergence. These goals are outlined in the following aims:

1.5.1. Aim 1 (Chapter 2) – Investigate variant colony development in the presence of tobramycin antibiotic therapy, as well as in the presence of other antimicrobial agents.

Hypothesis: In addition to resistant mutants, antibiotic tolerant variants also arise with the zone of clearance of a tobramycin loaded calcium sulfate bead.

Preliminary data had shown the emergence of colonies within the zone of biofilm clearance of a tobramycin loaded calcium sulfate bead. While we believed that most of these colonies were likely to be resistant mutants, we hypothesized that antibiotic tolerant variant colonies were also present. In order to investigate whether antibiotic tolerant variants existed, and if so, what phenotypes were present, we isolated colonies and tested their MIC on a second exposure to tobramycin. After identifying antibiotic tolerant colonies, we further characterized the various phenotypes using growth curves, a

heritability study, anaerobic studies, and alternate classes of antibiotics. These studies determined that four variant colony phenotypes emerged within the zone of clearance: resistant mutants, persister cells, viable but non-culturable-like colonies, and a novel tolerant phenotype which we refer to as phoenix colonies.

1.5.2. Aim 2 (Chapter 3) - Examine transcriptomic changes as a basis for the mechanism behind phoenix colony development.

Hypothesis: Transcriptional changes lead to the antibiotic tolerant phenotype of phoenix colonies.

Due to the transient nature of phoenix colonies, we hypothesized that changes in gene transcription were likely the mechanism used by phoenix colonies to survive initial tobramycin exposure. RNAseq was performed on the phoenix colonies and identified general transcriptional changes compared to controls as well as numerous differentially expressed genes. These genes were screened using transposon mutants and two genes were identified which may play a role in phoenix colony development, one of which is a hypothetical protein. Additionally, whole genome sequencing was performed and a single SNP was identified in the phoenix colony genome. Structural modeling was completed for the RNAseq identified hypothetical protein as well as the SNP containing gene.

1.5.3. Aim 3 (Chapter 4) – Investigate the pharmacodynamics of the eradication of lawn biofilms and antibiotic resistant and tolerant variants.

Hypothesis: An area under the curve value exists that is able to eradicate all *P. aeruginosa* biofilm bacteria including antibiotic resistant and tolerant variants.

In addition to the variant colonies which emerge within the zone of clearance of a tobramycin source, there was also a consistent region immediately adjacent to the antibiotic source from which nothing emerged or was able to be cultured. We referred to this region as the zone of killing. Due to the presence of this zone of killing, we hypothesized that the junction at the outer edge of the zone of killing represents a antibiotic concentration vs time constraint (area under the curve (AUC)) which is able to eradicate the biofilm fully, including any antibiotic resistant or tolerant variants. To address this, we used a combination of *in vitro* zone of killing measurements as well as computational modeling to determine if there was a consistent AUC. The results of these studies determined that regardless of the starting mass of tobramycin, a consistent AUC was present for the zone of killing. Additionally, this AUC can eradicate biofilms grown on both agar and hydroxyapatite, indicating that biofilm substrate rigidity does not affect the measured AUC.

Chapter 2. Novel Aminoglycoside-Tolerant Phoenix Colony Variants of *Pseudomonas aeruginosa*

Devin Sindeldecker, Kelly Moore, Anthony Li, Daniel J. Wozniak, Matthew Anderson, Devendra H. Dusane, and Paul Stoodley

Data and figures represented in this chapter have been previously published:

Sindeldecker, D., Moore, K., Li, A., Wozniak, D. J., Anderson, M., Dusane, D. H., & Stoodley, P. (2020). Novel aminoglycoside-tolerant phoenix colony variants of *Pseudomonas aeruginosa*. *Antimicrobial agents and chemotherapy*, *64*(9), e00623-20.

2.1. Abstract

Pseudomonas aeruginosa is an opportunistic bacterial pathogen and is known to produce biofilms. We previously showed the emergence of colony variants in the presence of tobramycin-loaded calcium sulfate beads. In this study, we characterized the variant colonies, which survived the antibiotic treatment, and identified three distinct phenotypes— classically resistant colonies, viable but nonculturable colonies (VBNC), and phoenix colonies. Phoenix colonies, described here for the first time, grow out of the zone of clearance of antibiotic-loaded beads from lawn bio- films while there are still very high concentrations of antibiotic present, suggesting an antibiotic-resistant phenotype. However, upon subculturing of these isolates, phoenix colonies return to wild-type levels of antibiotic susceptibility. Compared with the wild-type, phoenix

colonies are morphologically similar aside from a deficiency in green pigmentation. Phoenix colonies do not recapitulate the phenotype of any previously described mechanisms of resistance, tolerance, or persistence and, thus, form a novel group with their own phenotype. Growth under anaerobic conditions suggests that an alternative metabolism could lead to the formation of phoenix colonies. These findings suggest that phoenix colonies could emerge in response to antibiotic therapies and lead to recurrent or persistent infections, particularly within biofilms where microaerobic or anaerobic environments are present.

2.2. Introduction

Pseudomonas aeruginosa is a Gram-negative, opportunistic pathogen responsible for a wide range of infections ranging from those in surgical sites, chronic wounds, and the cystic fibrosis (CF) lung (2, 3, 110). *P. aeruginosa* utilizes several methods to establish and maintain an infection including biofilm production, multidrug resistance, and antibiotic tolerant persister cell formation (5-8). Multidrug resistance is a growing problem worldwide and is found in numerous bacterial species including *P. aeruginosa* (9-13). Additionally, *P. aeruginosa* isolates have been shown to be hypermutable in the context of infection, which further raises concerns for the development of antimicrobial tolerance and resistance (14). Specifically, aminoglycoside resistance is a growing concern in *P. aeruginosa* (15-17) and should be considered in all *P. aeruginosa* related infections including periprosthetic joint infections (PJIs), CF, and wounds.

Several antibiotic tolerance mechanisms have been identified which could allow for survival of a bacterial population, and tolerance can provide a mechanism to develop

full antibiotic resistance (18). Persister cells are bacteria that enter a state of dormancy in which they become metabolically inactive. This dormancy allows for the survival of these bacteria in the presence of antibiotic treatment, but once the antibiotic has dropped below the minimum inhibitory concentration (MIC), these bacteria can regrow with the resulting population demonstrating wild-type antibiotic susceptibility (5). Although this is a low frequency event (~1% of the population, (65)), it is a major concern and it has been hypothesized that they could lead to recurrent infections in humans (8). Another antibiotic survival mechanism of *P. aeruginosa*, termed adaptive resistance, allows for transient antibiotic resistance through a temporary up-regulation of efflux pumps when antibiotics are present. Once the antibiotic pressure is removed, the bacteria down-regulate their efflux pumps and return to a wild-type level of antibiotic susceptibility (15, 48). Heteroresistance is another possible survival mechanism, which could allow colonies to grow in an environment with antibiotic levels above the MIC. In a heteroresistant population of bacteria, the overall population appears to be susceptible to antibiotics but contains a hidden, resistant subset of bacteria. During antibiotic exposure, the majority of the population is killed leaving the resistant subset behind to recolonize as an antibiotic recalcitrant infection (38). The prevalence of these and other antibiotic tolerance and resistance mechanisms may allow bacterial populations to evade complete killing and lead to recurrent and recalcitrant infections.

Previous work in our lab focused on the use of vancomycin and tobramycin loaded calcium sulfate ($CaSO_4$) bone void filler beads to treat PJIs in a Kirby-Bauer type test (111, 112). After extended culture, variant colonies emerged in the zone of clearing

(ZOC) of a *P. aeruginosa* lawn biofilm (113). In the present study, these variant colonies which emerged in the cleared zone of the lawn biofilm around a tobramycin-loaded calcium sulfate bead were characterized to determine if these were classically resistant mutants, persister cells, adaptive resistance colonies, heteroresistant colonies, or if they belonged to another variant colony type of *P. aeruginosa*.

2.3. Materials and Methods

Bacterial strain and culture conditions

The bioluminescent strain *P. aeruginosa* Xen41 (Xenogen Corp., USA) and its parent *P. aeruginosa* PAO1 were used in this study. Glycerol stock cultures were stored at -80°C and streaked onto fresh Luria-Bertani (LB) agar plates that were incubated for 24 hours. Isolated colonies from the LB agar plate were transferred to 20 mL of LB broth and incubated overnight on an incubator shaker set at a temperature of 37°C and at a speed of 200 rpm.

Preparing lawn biofilms of P. aeruginosa

Spreading the overnight culture on LB agar generated lawn biofilms of *P. aeruginosa* Xen41 and PAO1. Briefly, the overnight *P. aeruginosa* Xen41 or PAO1 culture grown in LB broth was diluted to an OD_{600} of 0.1. 100 µL of the diluted culture was spread onto a 100 mm diameter, polystyrene Petri plate (Fisher Scientific, USA) containing LB agar. The petri-plates were incubated at 37°C for 24 hours to develop a lawn biofilm of *P. aeruginosa*. Additionally, the CFU/cm^2 of the lawns was measured to be used as a reference value. In short, a biofilm lawn was generated, and a 1 cm by 1 cm

area was marked and isolated using a sterile plastic loop into 1 mL of sterile phosphate-buffered saline (PBS). A dilution series was generated and plated onto LB agar by dripping 5 μL of each dilution onto the agar surface and allowing it to dry. The plates were then incubated at 37°C with 5% CO_2 overnight. Colonies were then counted and the CFU/cm^2 of the lawn was calculated to be $5 \pm 2*10^9$ CFU/cm^2.

Preparation of tobramycin containing calcium sulfate beads

All experiments conducted required the preparation of $CaSO_4$ (Sigma-Aldrich) beads containing tobramycin. We used 240 mg of tobramycin (Sigma-Aldrich) per 20 g of $CaSO_4$, a ratio commonly used by orthopedic surgeons when mixing antibiotics into pharmaceutical grade $CaSO_4$ bone void filler for local release at the surgical site in PJIs (114). Once the tobramycin and $CaSO_4$ were mixed together, sterile water was added and mixed for approximately one minute until a thick paste was produced. This paste was spread into silicone molds (Biocomposites Ltd.) to form hemispherical beads of 4.5 mm diameter and allowed to dry overnight.

Exposure of lawn biofilms to antibiotic loaded beads

After generation of a 24 hour lawn biofilm a tobramycin-loaded bead was placed in the center of the plate using sterile forceps. The forceps were used to also push the bead into the agar. Once the bead was placed, the plate was incubated at 37°C, 5% CO_2 in a humidified incubator (Heracell 150i, Thermo Scientific) for 3 days and checked daily for the appearance and spread of a ZOC as well as any colonies appearing in this zone. *In*

vitro imaging system (IVIS) images were taken daily to monitor bioluminescence, which is an indicator for metabolic activity within *P. aeruginosa* Xen41. Photographic images were also taken at the same time. After 3 days, IVIS and photographic images were taken again and variant colonies in the zone of lawn clearing were manually counted.

Bioluminescence Imaging

Bioluminescence imaging was performed using IVIS imaging. Thirty second exposures were obtained for each plate imaged. A pseudo-color heatmap was applied where red indicates high light intensity, blue indicates low levels of light intensity, and black indicates no light present. While a black color indicates a lack of activity, it cannot be used to rule out cell viability.

Determination of sensitive and resistant strains using replica plating

To characterize the colonies in the cleared zone and to screen for persisters we used replica plating (115). A sterile, cotton velveteen square (150 × 150 mm) was aseptically draped over a PVC replica plater and locked in place with an aluminum ring. The tobramycin-loaded bead was removed from the center of the plate after five days of incubation using a sterile, plastic loop. The plate was then marked to indicate the 12 o'clock position and gently placed onto the velveteen square and tapped gently to ensure complete contact of the plate with the velveteen. The plate was then removed from the replica plater, and a fresh, sterile LB agar plate containing 5 μg/mL of tobramycin and marked at the 12 o'clock position was placed on the velveteen square. This plate was also

tapped gently to ensure complete contact with the velveteen surface and then removed. Finally, a fresh, sterile LB agar plate marked at the 12 o'clock position was placed on the velveteen square and tapped gently to ensure complete surface contact. Both of the fresh replica plates were incubated for 24 hours at 37°C in an incubator with 5% CO_2. After incubation, the pattern of the plates was compared and colonies, which appeared on both plates, were deemed to be resistant mutants. Total colony counts were compared between the original plate and replica plates. The difference between the two can be explained by the presence of persister cells and thus persister cell calculations were completed in this manner. Colonies, which appeared on the original plates but on neither of the replica plates, were deemed to be VBNCs. An additional population of colonies was observed which appeared on the LB agar replica plate but not on the LB agar replica plate containing tobramycin. Because they do not fit into any of the other categories, we termed these phoenix colonies. All phoenix colonies were isolated and subjected to MIC testing for confirmation of susceptibility to tobramycin. In addition to replica plating, colonies were isolated into LB broth to confirm the lack of growth of VBNCs in the replica plating results. In short, variant colonies were generated as above and then isolated using sterile pipette tips and dipped into 200 µL of LB broth containing 5 µg/mL of tobramycin in a well of a 96-well plate (Corning, Sigma-Aldrich). The pipette tip was then dipped into the corresponding well of another 96-well plate containing 200 µL of LB broth. 96 colonies were isolated from three different plates for a total of 288 colonies. The plates were then incubated for 96 hours at 37°C with 5% CO_2. After incubation, turbidity in the wells of each plate was compared. VBNCs were determined by lack of

growth in the LB broth as well as the corresponding well of LB broth containing the tobramycin. Percentages for the phoenix and resistant were found to be consistent in the VBNC broth study when compared to replica plating. The data presented in Table 2.1 was derived by combining both replica plating counts and VBNC broth data. Briefly, the VBNC percentage was taken directly from the VBNC broth data. This value was then subtracted from 100%, and the remaining percentage was used to calculate the phoenix, resistant, and persister cell proportions based on colony counts from replica plating.

Alternative Antibiotic Testing

In addition to tobramycin, additional clinically relevant antibiotics were tested for the emergence of phoenix colonies. Gentamicin, ciprofloxacin, and colistin are routinely used to treat *P. aeruginosa* infections (116, 117). Each of these antibiotics were examined in similar studies as above including variant colony generation and replica plating. Phoenix colonies emerged within the ZOC of gentamicin (Figure 2.1), but not in the ZOC of ciprofloxacin (Figure 2.2) or colistin (Figure 2.3) indicating that this may be an aminoglycoside exclusive phenotype.

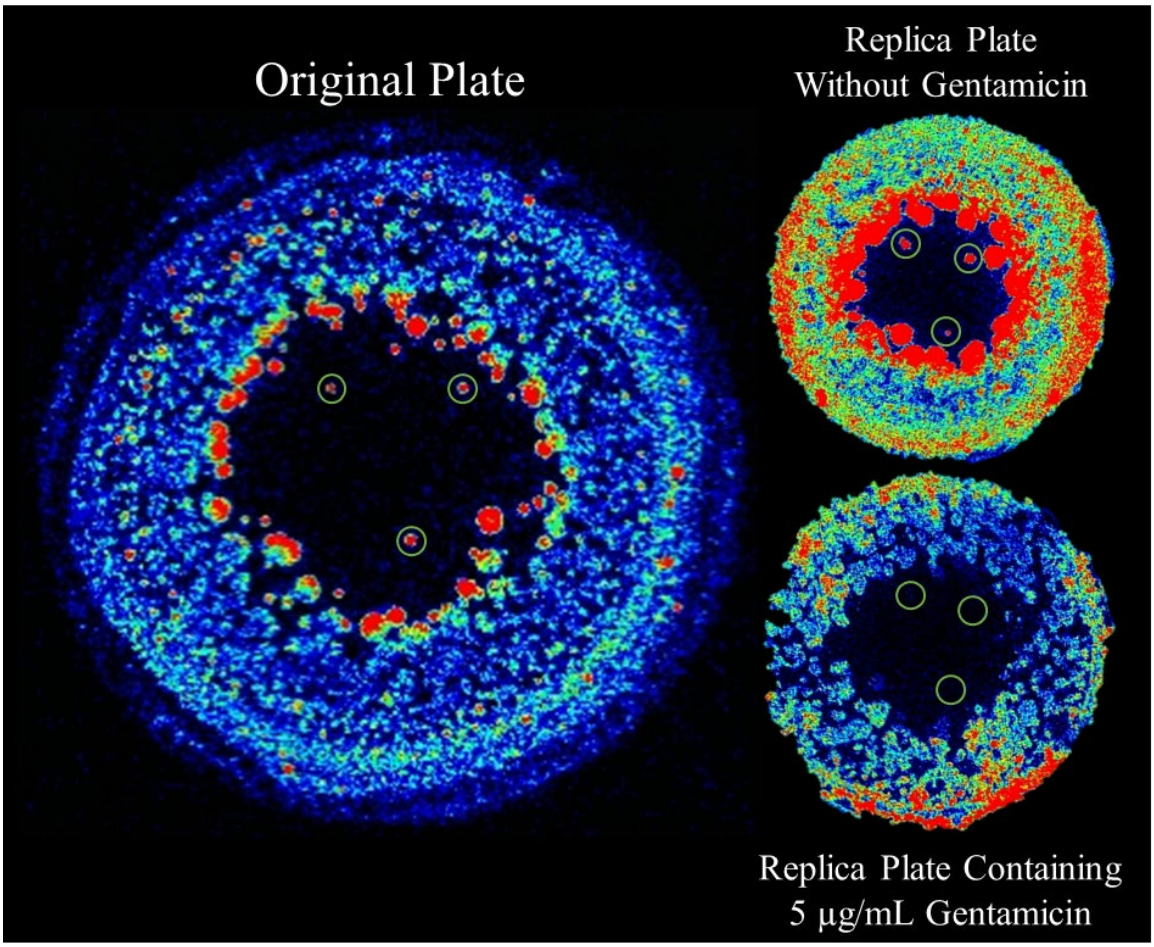

Figure 2.1 Phoenix colonies emerge in the presence of gentamicin.

IVIS imaging of a representative *P. aeruginosa* plate six days post a gentamicin-loaded $CaSO_4$ bead as well as images of the antibiotic lacking and antibiotic containing replica plates derived from the original plate. Green circles contain colonies which grew on the original plate and appear on the antibiotic lacking replica plate but do not appear on the antibiotic containing replica plate and are thus phoenix colonies. Red indicates high levels of metabolic activity and blue indicates low levels of metabolic activity.

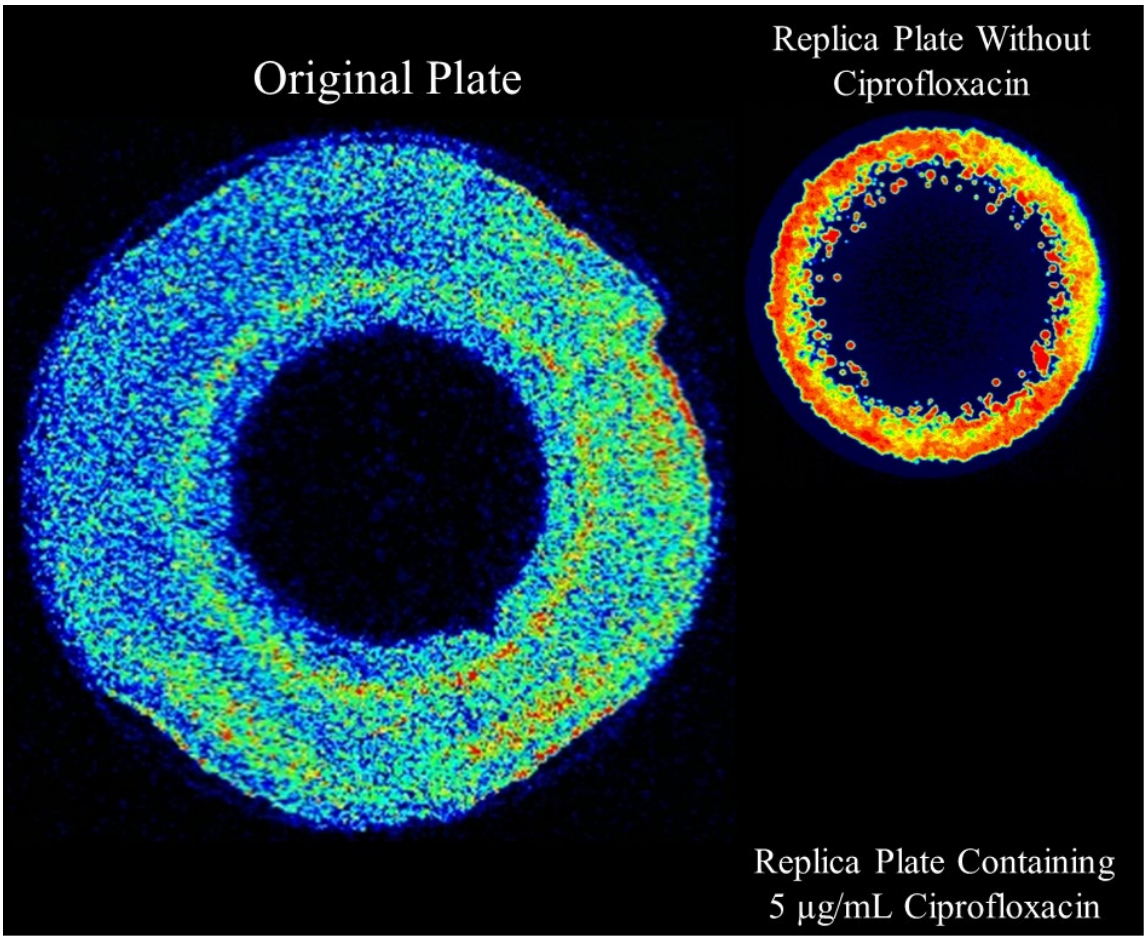

Figure 2.2 Phoenix colonies do not emerge in the presence of ciprofloxacin.

IVIS imaging of a representative *P. aeruginosa* plate six days post a ciprofloxacin-loaded $CaSO_4$ bead as well as images of the antibiotic lacking and antibiotic containing replica plates derived from the original plate. No variant colonies were seen emerging within the ZOC on the original plate. Additionally, only background lawn which had not been cleared on the original plate was able to grow on the replica plate lacking antibiotics. The replica plate containing ciprofloxacin showed no growth. Red indicates high levels of metabolic activity and blue indicates low levels of metabolic activity.

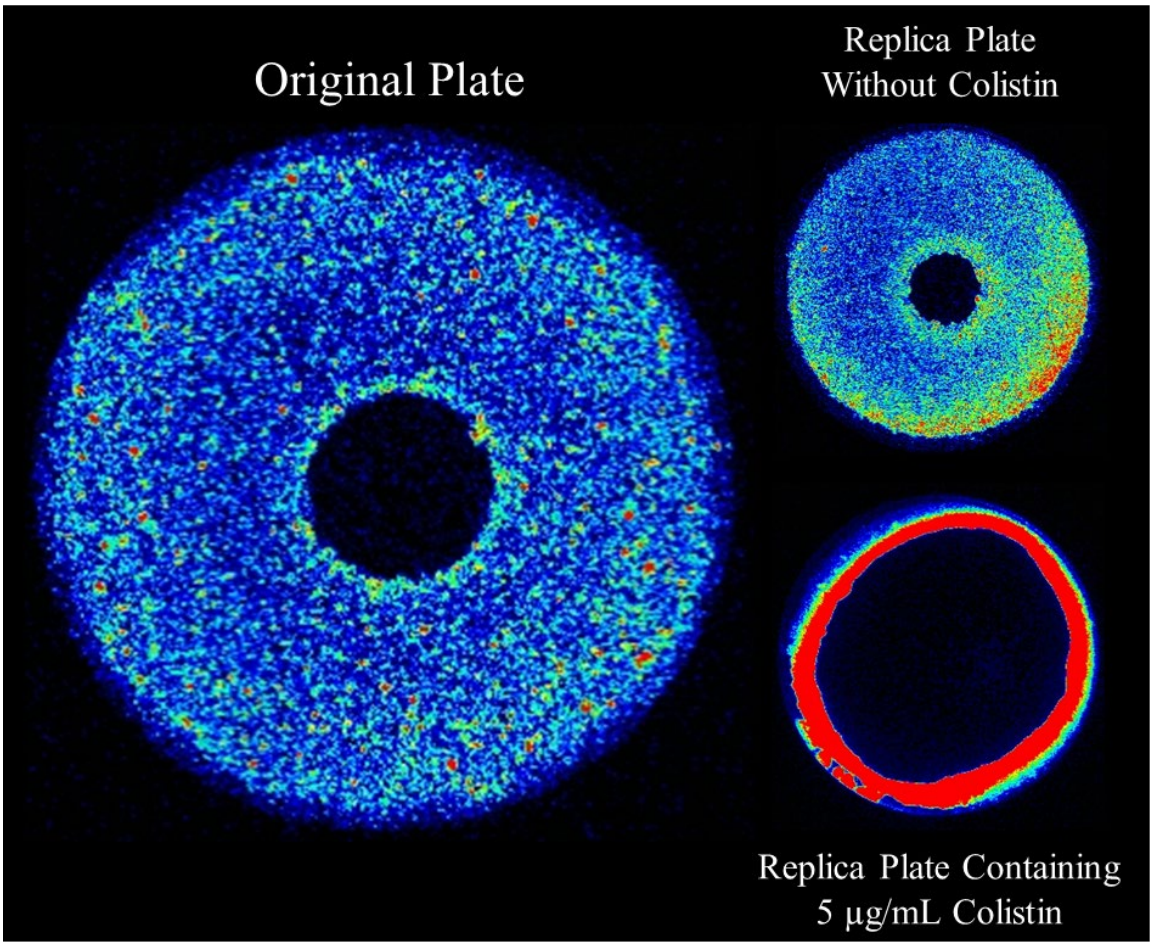

Figure 2.3 Phoenix colonies do not emerge in the presence of colistin.

IVIS imaging of a representative *P. aeruginosa* plate six days post a colistin-loaded $CaSO_4$ bead as well as images of the antibiotic lacking and antibiotic containing replica plates derived from the original plate. No variant colonies were seen within the ZOC of the original plate. Variant colonies were also not found on either of the replica plates. Red indicates high levels of metabolic activity and blue indicates low levels of metabolic activity.

Comparison of the emergence of phoenix colonies by strain and antibiotic delivery method

In order to examine the emergence of phoenix colonies in different strains of *Pseudomonas* as well as to determine if $CaSO_4$ directly linked this emergence to antibiotic delivery, comparison studies were completed. Overnight cultures of *P. aeruginosa* Xen41 and PAO1 were generated as above. Each culture was diluted to an OD_{600} of 0.1, and 100 μL of the solution was spread onto sterile, LB agar. Six plates were spread with Xen41 and six plates were spread with PAO1. All plates were incubated at 37°C with 5% CO_2 overnight. After 24 hours, a sterile filter disk (7 mm, Remel, Thermo Scientific) was placed in the center of three of the Xen41 and three of the PAO1 plates, and 10 μL of a 10 mg/mL tobramycin solution was placed on the disk to match the tobramycin potency in a tobramycin-loaded bead. Tobramycin-loaded beads were placed in the center of each of the six remaining plates as above. All plates were incubated at 37°C with 5% CO_2 for five days post initial antibiotic exposure. Replica plating was performed, and colony counts were obtained for each plate and are represented by mean ± SD.

Growth rate studies of isolates

To determine whether the phoenix colonies might have a growth defect and to rule out the presence of small colony variants (SCVs), we performed growth curves and also measured colony diameter as a function of time on the plates. Variant colony generation was performed as above, after generation and characterization of the variant

isolate MIC, growth curves were generated for each isolate along with wild-type *P. aeruginosa* Xen41 growth curves. In short, isolates were placed in 200 µL of LB broth in a well of a 96-well plate. The plates were then placed in a plate reader (SpectraMax i3x, Molecular Devices) and incubated statically at 37°C for 15 hours. OD_{600} readings were taken every ten minutes with five seconds of orbital shaking occurring before each read. After the growth curves had been generated, growth curve data from phoenix colony replicates were averaged to determine the mean OD_{600} at each time point. The same was done for resistant isolates and wild-type samples. The data were plotted as mean ± SD. The maximum growth rate for each of these mean curves was also calculated from the maximum slope during exponential phase, and is presented as mean ± SD. *In situ* growth on the plate was also measured for variant colonies. Variant colonies were generated as above and once colonies began to be visible, images were taken of the plates at various time points. After five days, the plates were replica plated and each colony's phenotype was determined. In addition to variant colonies, a dilution series of *P. aeruginosa* PAO1 was made and spread on several plates. These plates were then observed for the emergence of colonies and once colonies were visible, images were taken of the plates at various time points. The images of all of the plates were then analyzed using image analysis software to measure the diameter of each colony. Measurements were grouped together based on variant colony phenotype and the data was plotted as mean ± SD.

Calculation of tobramycin concentration in agar plates and biofilm lawn

To measure the concentration of tobramycin in the agar and the biofilm as a function of time and radial distance from the tobramycin-loaded bead, we first generated a standard curve and then excised portions of both a biofilm lawn and agar exposed to a tobramycin-loaded bead in order to calculate the concentration of tobramycin in each by using a Kirby-Bauer type assay. First, we generated calibration curves by diluting an overnight culture of *P. aeruginosa* PAO1 to an OD_{600} of 0.1 and spreading the dilution onto sterile, LB agar. A sterile filter disk was then placed in the center of the plate and 10 µL of varying tobramycin potencies (8-500 µg/mL) was placed onto the disk. The plate was incubated for 24 hours at 37°C with 5% CO_2. After incubation, the zones of inhibition were measured and plotted to produce a standard curve ($y=5.2384\ln(x) – 2.3996$, $R^2=0.9994$).

Once the standard curve had been generated, the tobramycin concentration in the agar at various radii and time points was measured. Tobramycin-loaded beads were placed into sterile LB agar plates. The plates were incubated at 37°C with 5% CO_2 and at various time points, plates were removed and marked with 5 mm x 5 mm squares from the edge of the bead to the edge of the plate. Each of these squares was excised using a razor blade and forceps. The excised plug was then melted at 100°C. An overnight culture of *P. aeruginosa* PAO1 was diluted to an OD_{600} of 0.1 and spread onto sterile, LB agar. A sterile filter disk was then placed in the center of the plate and 10 µL of the melted plug was placed onto the disk. The plate was incubated for 24 hours at 37°C with 5% CO_2. After incubation, the zone of inhibition was measured and compared to a standard

curve for tobramycin in LB agar to determine the concentration in the melted plug. This process was repeated at the various time points using different plates each time.

To quantify the amount of antibiotic that might have portioned into the biofilm we measured both the free antibiotic concentration in the lawn as well as the concentration trapped in the cells and biofilm extracellular polymeric substance (EPS). Variant colony generation was performed as above. On day four post tobramycin-loaded bead placement, the plates were removed from the incubator and marked with 5 mm x 5 mm squares from the edge of the bead to the edge of the plate. The biofilm lawn overlying each of the squares was isolated using a sterile plastic loop and placed in 1 mL of sterile ddH_2O. The sample was then vortexed for 10 seconds before being centrifuged at 21.1 x g for 2 minutes. The supernatant was collected, and the pellet was resuspended in 1 mL of sterile ddH_2O. The resuspended pellet was boiled at 100°C for 10 minutes to lyse the cells and denature proteins. An overnight culture of *P. aeruginosa* PAO1 was diluted to an OD_{600} of 0.1 and spread onto sterile, LB agar. A sterile filter disk was then placed in the center of the plate and 10 µL of either the supernatant or boiled pellet was placed onto the disk. The plate was incubated for 24 hours at 37°C with 5% CO_2. After incubation, the zone of inhibition was measured and compared to a standard curve for tobramycin in LB agar to determine the concentration in the respective components. Data are presented as mean ± SD.

Population analysis profiling of background P. aeruginosa strains

To assess for the presence of heteroresistance (i.e. a small population of resistant cells that might go undetected by routine clinical antibiogram assays (38, 40)) in our background strains we used population analysis profiling (PAP, (40)). First 20 mL of LB broth was inoculated with either *P. aeruginosa* PAO1 or *P. aeruginosa* Xen41. The cultures were incubated at 37°C with 200 rpm shaking for 24 hours. After incubation, the cultures were diluted to an OD_{600} of 0.1 and spread onto LB agar containing a two-fold dilution series of tobramycin. The plates were then incubated at 37°C with 5% CO_2 for 24 hours. After incubation, colony growth on each plate was analyzed. If heteroresistance is present in the population, colonies should appear on the dilution plate with an 8x higher concentration than the highest non-inhibitory concentration. No heteroresistance was found in our background strains (Data not shown).

Effect of efflux pump inhibitor on phoenix colony emergence

To assess the role of efflux pumps in the emergence of phoenix colonies, phe-arg-β-naphthylamide (PAβN), a broad-spectrum efflux pump inhibitor (30), was used. Lawn biofilms of *P. aeruginosa* PAO1 were generated as above on LB agar containing 27 μM of PAβN as well as LB agar without PAβN. Tobramycin-loaded bead placement and variant colony quantification was completed as above. Mean ± SD of the colony counts was obtained and plotted.

Heritability study of phoenix colonies

To assess whether it is possible to enrich for the phoenix colony phenotype within a population, heritability studies on phoenix colony isolates were performed. Variant colonies were generated as above. Variant colony plates were replica plated and all phoenix colonies were isolated and used to inoculate 20 mL of LB broth. The broth cultures were incubated for 24 hours at 37°C with 200 rpm shaking. After incubation, each of the cultures was diluted to an OD_{600} of 0.1. Variant colonies for each isolate were again generated as before and replica plated. Isolation of phoenix colonies, overnight growth, and variant colony generation for each isolate were repeated. Data are presented as mean ± SD.

Anaerobic chamber studies

A previous study has shown the importance of alternative metabolic pathways in antimicrobial tolerance (83). In order to assess the effects of other metabolic pathways on the emergence of phoenix colonies, studies were performed in an anaerobic chamber to deprive the bacteria of oxygen. Variant colonies were generated as above aside from incubation parameters on both LB agar plates and LB agar plates containing 100 mM KNO_3. The plates were incubated at 37°C in an anaerobic chamber at all times. Inside of the chamber, the plates were also placed in a sealable bag containing a paper towel soaked in water to prevent dehydration of the agar. The plates were allowed to grow for five days and were removed from the chamber. Biofilm lawn growth was observed on the plate, imaged by IVIS, and the plates were immediately replica plated as above onto both LB agar and LB agar containing 5 μg/mL of tobramycin. These plates were incubated at

37°C with 5% CO_2 in a standard aerobic incubator. After 24 hours, growth on these plates was examined and IVIS images were taken.

Eradication of planktonic tolerant, resistant, and phoenix phenotypes

The results from our replica plating studies indicate that there is a zone surrounding the antibiotic source in which everything including persister cells appears to be sterilized. To determine whether all cells truly could be killed with high enough concentration of antibiotics, we performed a planktonic assay to look for the concentration at which bacterial eradication occurs. 100 mL of LB broth was used to prepare an overnight broth culture of *P. aeruginosa* PAO1. The culture was incubated at 37°C with 200 rpm of shaking for 24 hours. 5 mL aliquots of the overnight culture were placed into 15 mL conical tubes and tobramycin was added to each tube in order to produce a triplicate dilution series of antibiotics at 400, 500, 600, 700, 800, 900, and 1000 μg/mL.

Due to the very high concentrations of tobramycin in our studies, we were concerned that there may be an osmolarity effect causing the lysing of bacteria. To control for this a separate triplicate was prepared with 0.385 mg/mL of dextrose to produce an equivocal maximum osmolarity solution. The new cultures were then incubated for 48 hours at 37 °C with 200 rpm of shaking. After incubation, 1 mL of each culture was centrifuged at max speed for 5 minutes. The supernatant was then removed, and the pellet was resuspended in 200 μL of sterile LB broth. The resuspension was used to prepare a ten-fold dilution series in a 96-well plate containing sterile LB broth. 5 μL

aliquots were then dropped onto a sterile LB agar plate. The plates were incubated at 37°C with 5% CO_2 for 7 days in order to allow any dormant or slow growing phenotypes to appear before being counted. The plates were then counted and CFU's were calculated. Data are presented as mean ± SD.

Statistical analysis

All experiments were performed in a minimum of triplicates. ANOVA analysis was completed by GraphPad Prism Version 8.2.1 for all studies with a p-value of 0.05 being considered significant. Data represented in graphs is plotted as mean ± SD.

2.4. Results

Variant colonies emerge in the presence of tobramycin-loaded beads

The model used in our assay was similar to that used by Gefen et al. (118) to quantify persister cells in a population by first allowing a zone of inhibition to form in response to an antibiotic loaded filter paper disk and then replacing the antibiotic disk with a nutrient disk. By switching out the disks, the antibiotic levels dropped below MIC, and persister cells and other tolerant phenotypes grew within the zone of inhibition (118). In the present study, we modified Gefen *et al.*'s (118) protocol to investigate these late appearing resistant or tolerant phenotypes by first allowing a biofilm lawn to grow for 24 hours before placing an antibiotic carrier (a $CaSO_4$ bead or filter paper) in the center and then using an extended incubation to monitor for the appearance of colonies in the ZOC. The emergence of both resistant and susceptible colonies was observed when a 24-hour

lawn biofilm of *P. aeruginosa* Xen41 was treated with a tobramycin-loaded bead placed at the center of the plate and incubated for 96 hours (Figure 2.4a). On days one and two, two distinct zones were visualized by *in vivo* imaging system (IVIS) bioluminescence imaging: a ZOC surrounding the bead, which demonstrated temporal expansion, and the background lawn. On days three and four post-tobramycin-loaded bead placement, a third zone of colonies within the ZOC became visible. This zone grew rapidly from day three to four and began to encroach on the inner zone of biofilm clearance as well as expand further towards the outer edge of clearance. Images taken on day five post-tobramycin-loaded bead placement showed that all colonies, which grew within the ZOC, were bioluminescent, and, thus, metabolically active (Figure 2.4b). A pigmentation defect was evident in the variant colonies causing them to appear white instead of the yellow-green of wild-type. However, this phenotype was transient, and the pigmentation was restored upon sub-culturing. Additionally, over time, a haze appeared immediately adjacent to the bead within the agar. This haze has been seen before in association with $CaSO_4$ beads (113) and is thought to be a precipitate. The region overlying this haze was swabbed, however, no bacterial growth was derived from cultures.

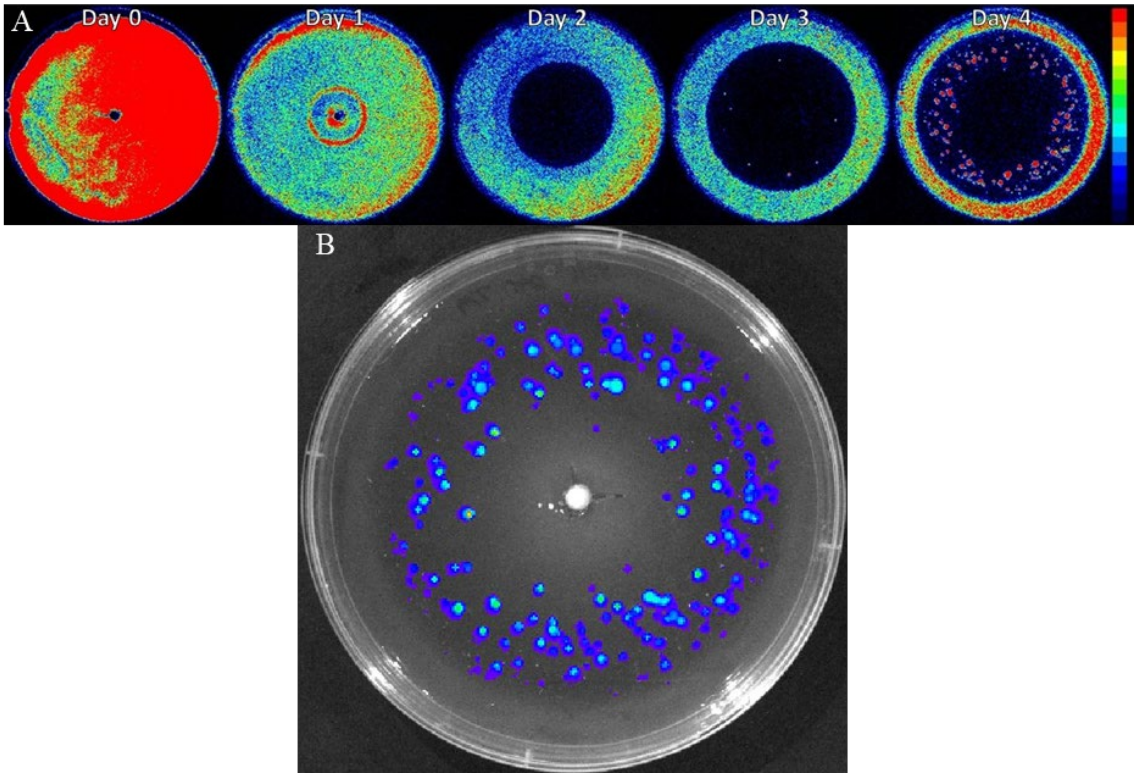

Figure 2.4 *In vitro* imaging system (IVIS) images of *P. aeruginosa* Xen41 biofilm plates.

A. IVIS imaging was performed on day 0 of the tobramycin-loaded bead placement and daily thereafter until emergence of phoenix colonies was observed at day 4. Scale is at the right of the panel. Red indicates high levels of metabolic activity and blue indicates low levels of metabolic activity. B. IVIS imaging overlay on a black and white photo of the plate showing high levels of metabolic activity in all colonies at five days post tobramycin-loaded bead placement.

Replica plating reveals both antibiotic sensitive and resistant colonies

Replica plating was used to determine if variant colonies growing within the zone of biofilm killing were susceptible or resistant to tobramycin (Figure 2.5). While there was a large population of resistant colonies present, a susceptible population of colonies was also identified. Persister cells were found within the variant colony population (Table 2.1). In addition to replica plating, colonies were also isolated from the ZOC of a tobramycin-loaded bead five days post treatment using sterile pipette tips and placed into both LB broth and LB broth containing 5 μg/mL of tobramycin. These counts revealed an additional population of colonies, which grew and were active on the original plates but were unable to be cultured either in the presence of tobramycin or the lack thereof (Table 2.1). We refer to these colonies as viable-but-not-culturable colonies (VBNCs). We refer to the susceptible colonies as "phoenix" colonies because they arise from the dead bacterial lawn and proliferate in the presence of antibiotic treatments. In order to ensure that phoenix colony development is not a $CaSO_4$ bead specific or a strain specific phenomenon, colony counts were also obtained for the equivalent concentration of tobramycin placed on sterile, filter paper disks as well as for *P. aeruginosa* PAO1. While these differences between resistant colony emergence rates were significant, there was no significant difference in the number of phoenix colonies produced between either strain or either antibiotic delivery method (Figure 2.6).

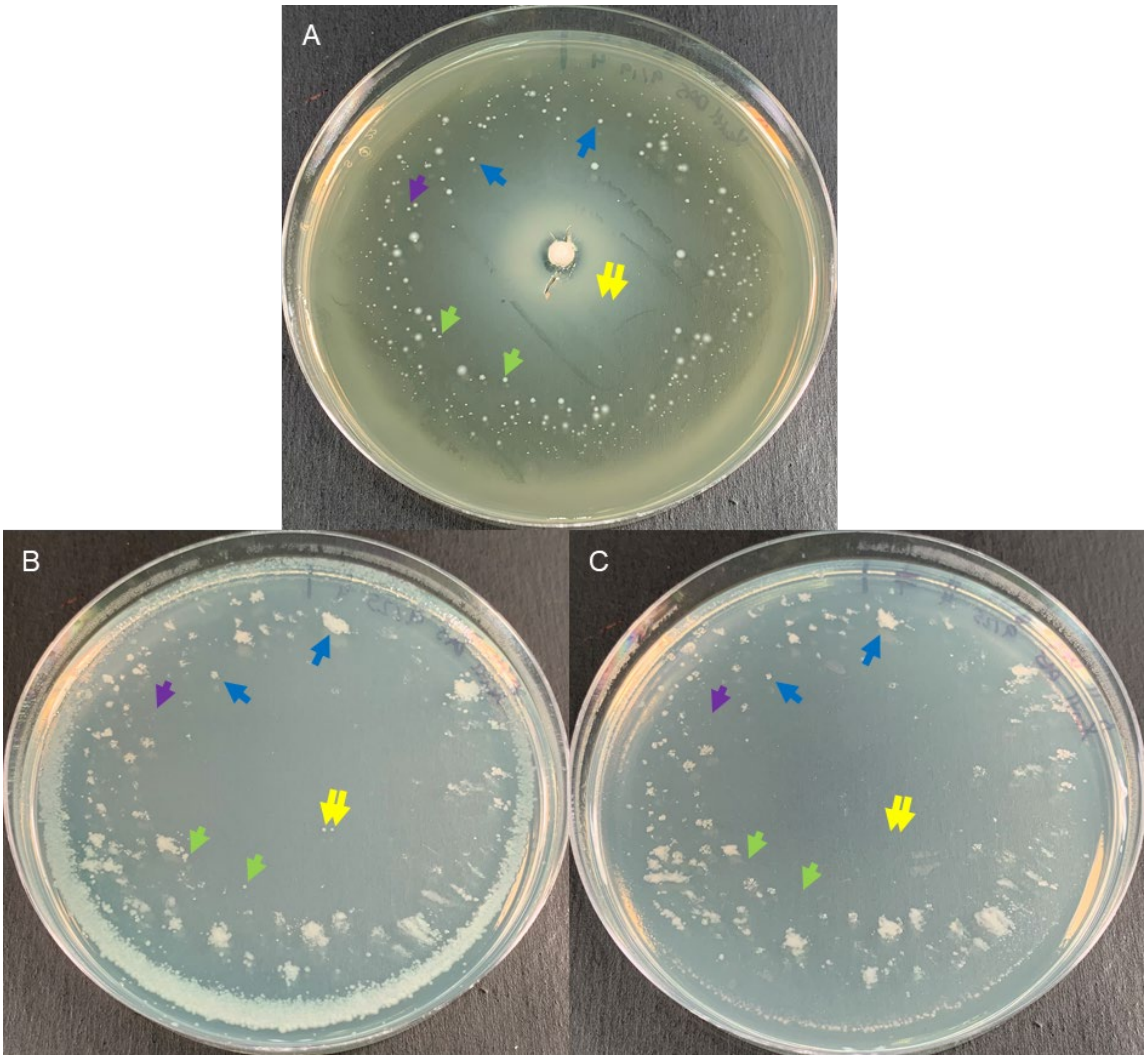

Figure 2.5 Replica plating reveals resistant, phoenix colony, viable but non-culturable (VBNC), and persister cell variants.

Images are of representative replica plates (n=3). A. Original plate before replica plating. B. LB replica plate. C. LB + tobramycin replica plate. A-C. Blue arrows represent colonies, which grow on all three plate types and are thus resistant colonies. Green arrows represent colonies, which appear on the original and LB replica plate but not the LB replica plate containing tobramycin and are thus phoenix colonies. Purple arrows represent colonies, which only grow on the original plate and thus are VBNCs. Yellow

arrows represent likely persister cells, which did not appear on the original plate but grew on the LB replica plate only.

Table 2.1 Colonies emerging from zone of clearance are comprised of various phenotypes.

Variant phenotype colony counts for *P. aeruginosa* PAO1 exposed to tobramycin for 5 days. Data are reported as mean ± SD.

Total Colonies	Resistant Colonies	Phoenix Colonies	Persister Cells	VBNC Colonies
364 ± 23	81.7% ± 4.6%	2.8% ± 2.6%	8.6% ± 6.5%	6.9% ± 9.5%

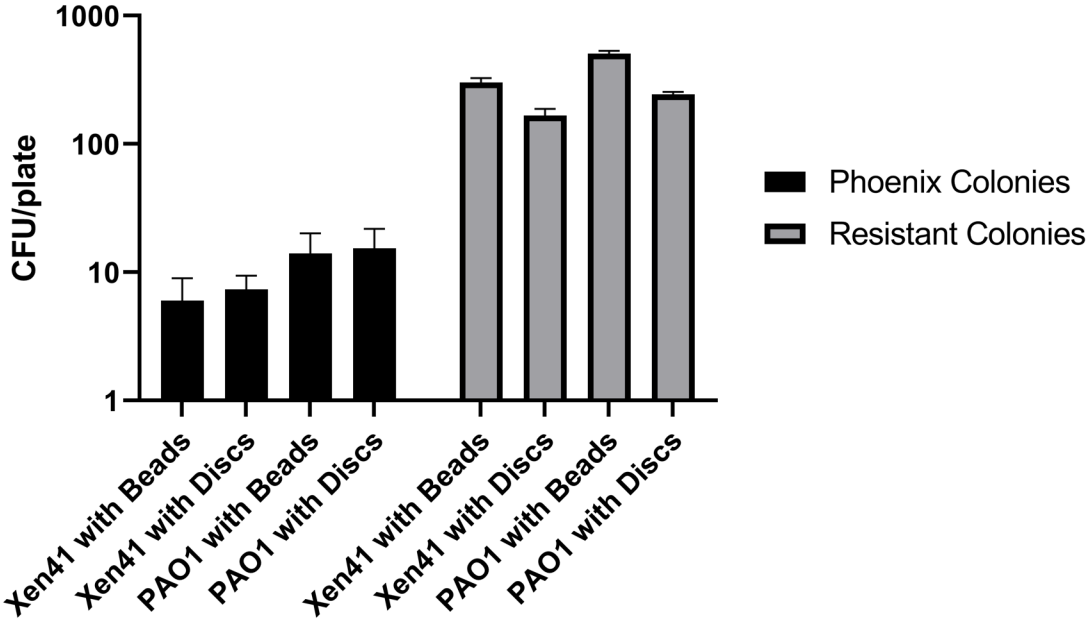

Figure 2.6 *P. aeruginosa* variant colonies emerge regardless of antibiotic delivery method.

Colony counts were obtained of variants, which emerged in response to tobramycin-loaded beads in each strain as well as by a 1 mg of tobramycin in solution placed on a sterile filter disk in each strain. There was no significant difference in the number of phoenix colonies produced across all condition comparisons. Data are reported as mean ± SD (n=3).

Phoenix colonies have no defect in growth kinetics

Growth curves were generated for each isolate which emerged on the agar plate after treatment with antibiotic. Phoenix and resistant colonies were each compared with wild-type *P. aeruginosa* Xen41 (Figure 2.7a). No significant difference in the maximum specific growth rate was observed for either phoenix colonies ($p=0.2981$) or resistant colonies ($p=0.3168$) as compared to the wild-type (Figure 2.7b). We also measured the *in situ* growth of variant colonies. Colonies were measured over time as they appeared within the zone of biofilm killing and the phenotypes were compared (Figure 2.7c). No significant difference was observed among the variants.

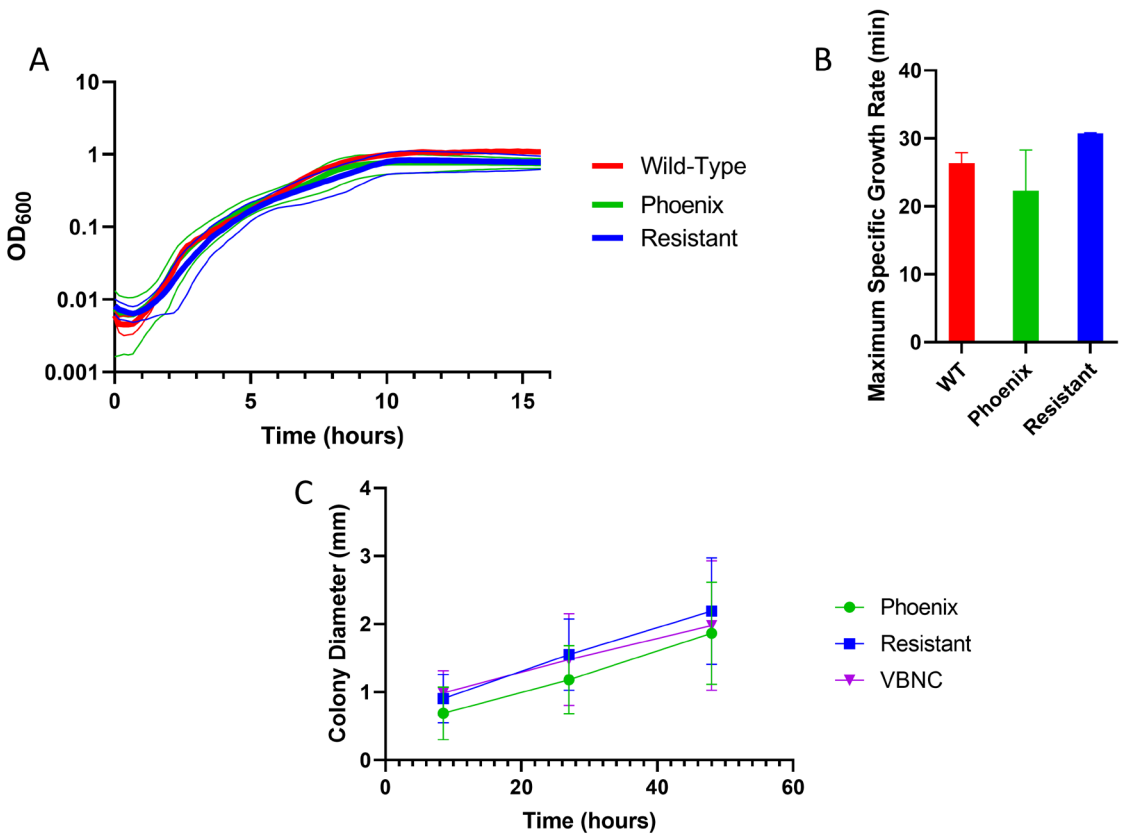

Figure 2.7 Phoenix colonies have no defect in growth kinetics.

A. OD_{600} was measured every 10 minutes for wild-type and phoenix isolates. Mean values (thick lines) and SD (thin lines) were plotted for resistant isolates (n=7), phoenix colonies (n=20), and wild-type *P. aeruginosa* Xen41 (n=3). B. Maximum specific growth rates were measured for each of the panel A curves. There was no significant difference between wild-type and resistant isolates (p=0.3168) or between wild-type and phoenix colonies (p=0.2981). C. *In situ* colony growth was measured over time for resistant colonies (n=29), phoenix colonies (n=11), and VBNCs (n=4) exposed to antibiotics. Time 0 represents the time at which the colonies were first noted. Although the phoenix colonies were consistently smaller, there was no significant difference found in colony size between any of the other groups at any time point. Data are reported as mean ± SD.

Tobramycin concentrations remain above MIC during emergence of variant colonies

In order to examine the possible phenotype of phoenix colonies, various studies were performed. First, it was important to define the concentration of tobramycin to which the variant colonies were exposed in order to determine if phoenix colonies could simply be persister cells. Tobramycin concentrations from the beads could diffuse to sub-MIC levels after clearing the biofilm lawn and could allow persister cells to emerge. Tobramycin levels were measured both in sterile agar (Figure 2.8a) and in biofilm lawns that had been exposed to tobramycin-loaded bead (Figure 2.8b). After five days post tobramycin-loaded bead placement, the tobramycin concentration in the agar was five times higher than the MIC at the edge of the variant colony radius. Additionally, the tobramycin concentration was twenty times higher than MIC within the lawn biofilm, itself. The amount of tobramycin within the biofilm was similar between free, unbound tobramycin and tobramycin that was trapped either inside of cells, on the cell surface, or bound within the biofilm extracellular polymeric substance (EPS). In these high concentrations of antibiotic, persister cells would be predicted to not grow (8).

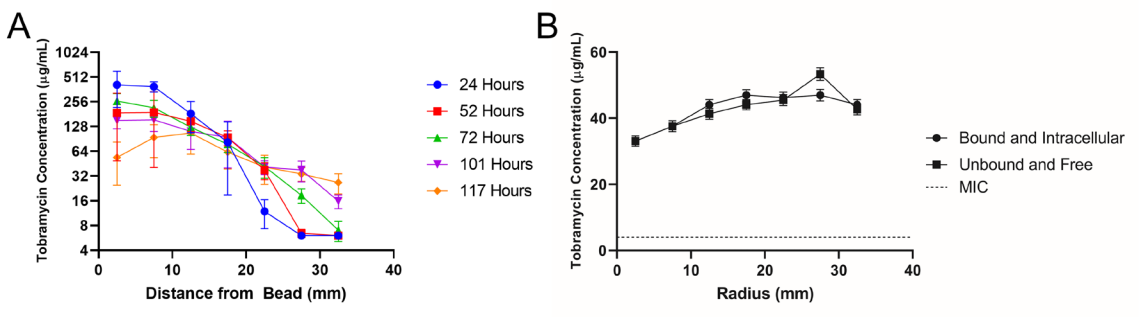

Figure 2.8 Tobramycin concentration remains above MIC during phoenix colony emergence.

A (Data reanalyzed from (113)). A tobramycin-loaded bead was placed in sterile LB agar, and at various time points, agar plugs were extracted at various radii to examine the concentration of tobramycin by plating for MIC (n=3). MIC zones were compared to a standard curve to calculate the tobramycin concentrations in the agar plugs. B. At varying radii, the lawn of a day four-post bead placement plate was resuspended, separated into fractions of freely diffusible and bound tobramycin, plated, and plotted against a standard curve to calculate the concentration of tobramycin. In the variant zone, both the intracellular and extracellular concentrations remain higher than MIC. Data are reported as mean ± SD.

Phoenix colonies are different than an adaptive resistance phenotype

In order to assess the potential for phoenix colonies to be the result of adaptive resistance through transient efflux pump up-regulation (48), bacteria were exposed to phe-arg-β-naphthylamide (PAβN), a broad-spectrum efflux pump inhibitor, in conjunction with a tobramycin-loaded bead. No significant difference ($p=0.5377$) was observed between the number of phoenix colonies which developed in the presence of (8.3 ± 6.6) or absence of (5.3 ± 4.0) exposure to PAβN. Since phoenix colonies are unable to be properly categorized in a known resistance, tolerance, or persistence phenotype, phoenix colonies appear to be a distinct, tolerant phenotype, able to survive and remain metabolically active despite the presence of high concentrations of antibiotics; however, once they are removed from the antibiotic containing environment, they return immediately to a wild-type level of antibiotic susceptibility.

Phoenix colony progeny produce consistent numbers of phoenix colonies

A heritability study was performed in order to determine if the phoenix colony phenotype could be selected for and passed on to the progeny. Phoenix colonies were isolated as per standard procedure (Figure 2.9a) and plated to obtain a second-generation population (Figure 2.9b) and third-generation population (Figure 2.9c). While there was no significant difference in resistant colonies produced from the first to second generations ($p=0.1024$), there was a significant increase in resistant colonies from the second to third generations ($p<0.0001$). There was no significant difference when comparing phoenix colony counts from the first to second generations ($p=0.9300$) or

from the second to third generations ($p=0.4529$). This indicates that phoenix colony emergence remains stable and cannot be selected for or enriched.

Figure 2.9 Phoenix colony heritability is stable.

A. Variant colonies were generated as described, replica plated, and enumerated. Replica plating was performed, and counts were taken of the number of resistant and phoenix colonies. Phoenix colonies were isolated and grown overnight before being plated again. B. Isolate cultures were then plated and allowed to grow for five days in the presence of a tobramycin-loaded bead. These plates were replica plated and colony counts were obtained. Phoenix colonies were again isolated and grown in overnight broth cultures. C. Isolate cultures from step B were plated and allowed to grow for five days in the presence of a tobramycin-loaded bead. Replica plating was again performed and colony counts obtained. No significant difference was seen in the number of phoenix colonies produced for each generation. Data are reported as mean ± SD.

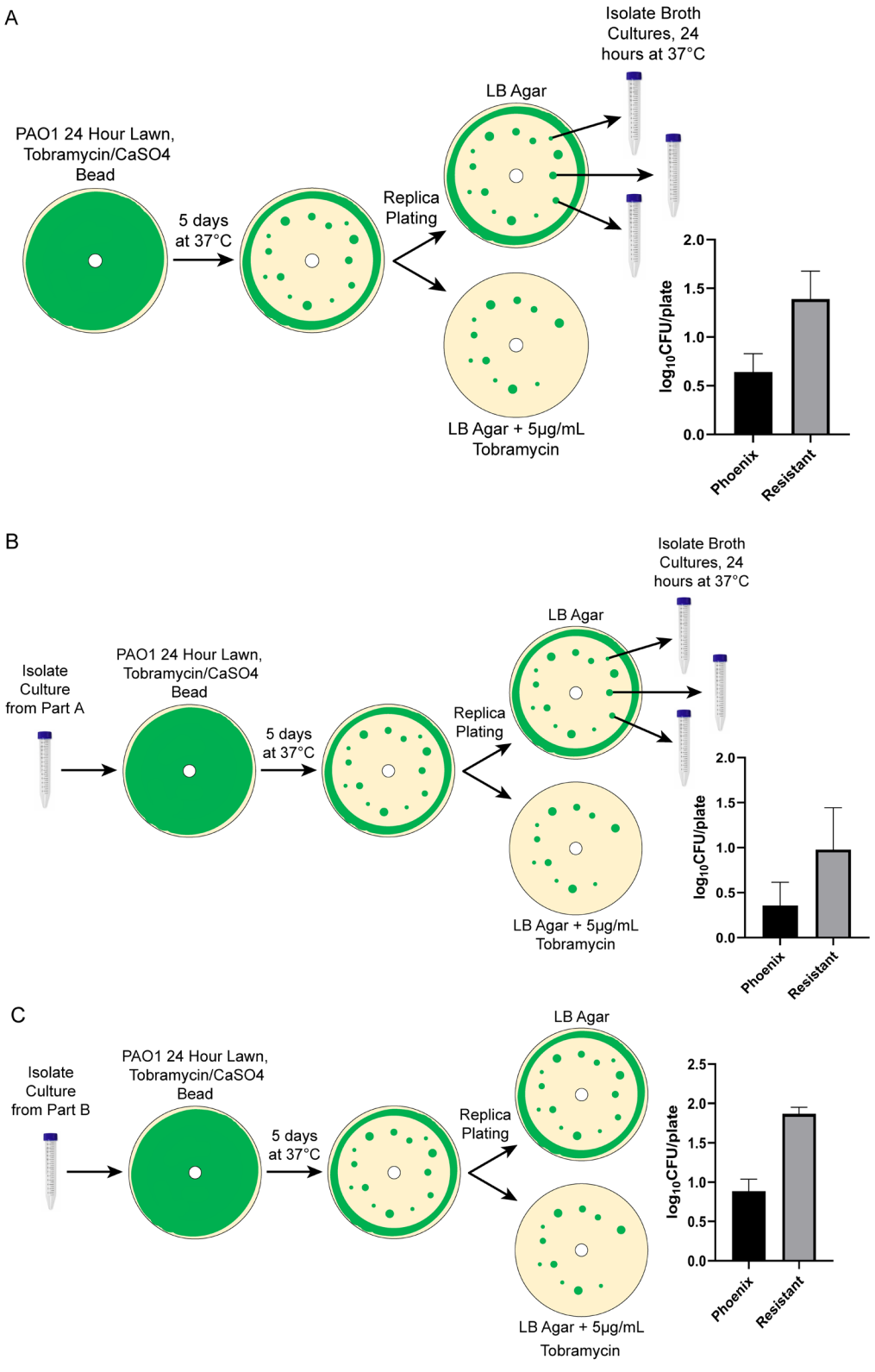
A
Isolate Broth Cultures, 24 hours at 37°C
LB Agar
PAO1 24 Hour Lawn, Tobramycin/CaSO4 Bead
5 days at 37°C
Replica Plating
LB Agar + 5µg/mL Tobramycin
log10CFU/plate
2.0
1.5
1.0
0.5
0.0
Phoenix
Resistant
B
Isolate Broth Cultures, 24 hours at 37°C
LB Agar
Isolate Culture from Part A
PAO1 24 Hour Lawn, Tobramycin/CaSO4 Bead
5 days at 37°C
Replica Plating
LB Agar + 5µg/mL Tobramycin
log10CFU/plate
2.0
1.5
1.0
0.5
0.0
Phoenix
Resistant
C
LB Agar
Isolate Culture from Part B
PAO1 24 Hour Lawn, Tobramycin/CaSO4 Bead
5 days at 37°C
Replica Plating
LB Agar + 5µg/mL Tobramycin
log10CFU/plate
2.5
2.0
1.5
1.0
0.5
0.0
Phoenix
Resistant

Anaerobic environments provide protection from killing by tobramycin

Previous studies have linked antibiotic tolerance in *P. aeruginosa* to anaerobic environments (83), which led us to evaluate the effect of oxygen depletion on the emergence of variant colonies. In order to examine the possibility that an altered metabolic state could select for the emergence of phoenix colonies, biofilm lawns of *P. aeruginosa* PAO1 were generated in an anaerobic chamber. After 24 hours of biofilm lawn growth in the anaerobic chamber on either LB agar and LB agar containing 100 mM KNO_3, to serve as an alternative terminal electron acceptor, a tobramycin-loaded bead was placed into its center. The plates were incubated anaerobically for five additional days. After removing the plates from the anaerobic chamber, there was no visible ZOC, despite the lawn growth on LB agar plates, indicating that the anaerobic environment had led to protection of the biofilm lawn. In contrast, complete clearance of the lawn on LB agar plates containing KNO_3 occurred, indicating that with supplementation with a terminal electron acceptor, the lawn was active and able to be killed by tobramycin to an even higher degree than plates in an aerobic environment. The plates were immediately replica plated onto LB agar with and without tobramycin. After 24 hours, a confluent lawn was observed on each of the LB agar replica plates derived from the original plates lacking KNO_3, and there was no growth on the replica plates containing tobramycin. This indicates that while the anaerobic environment had protected the biofilm lawn from the original tobramycin treatment, the lawn had returned to wild-type levels of susceptibility once placed in an aerobic environment. Replica plates derived from the LB agar plates containing KNO_3 produced slight growth on the LB agar plate and no growth on

antibiotic containing plates, further confirming the killing of the original LB agar plate containing KNO_3 in the anaerobic chamber (Figure 2.10). This data indicates that phoenix colonies may be protected by an anaerobic microenvironment within the biofilm, and also that denitrification is not the metabolic process utilized by phoenix colonies to remain active and survive antibiotic exposure. It is possible that phoenix colonies utilize either fermentation or an alternative metabolic process to be able to grow in an anaerobic environment and survive antibiotic exposure.

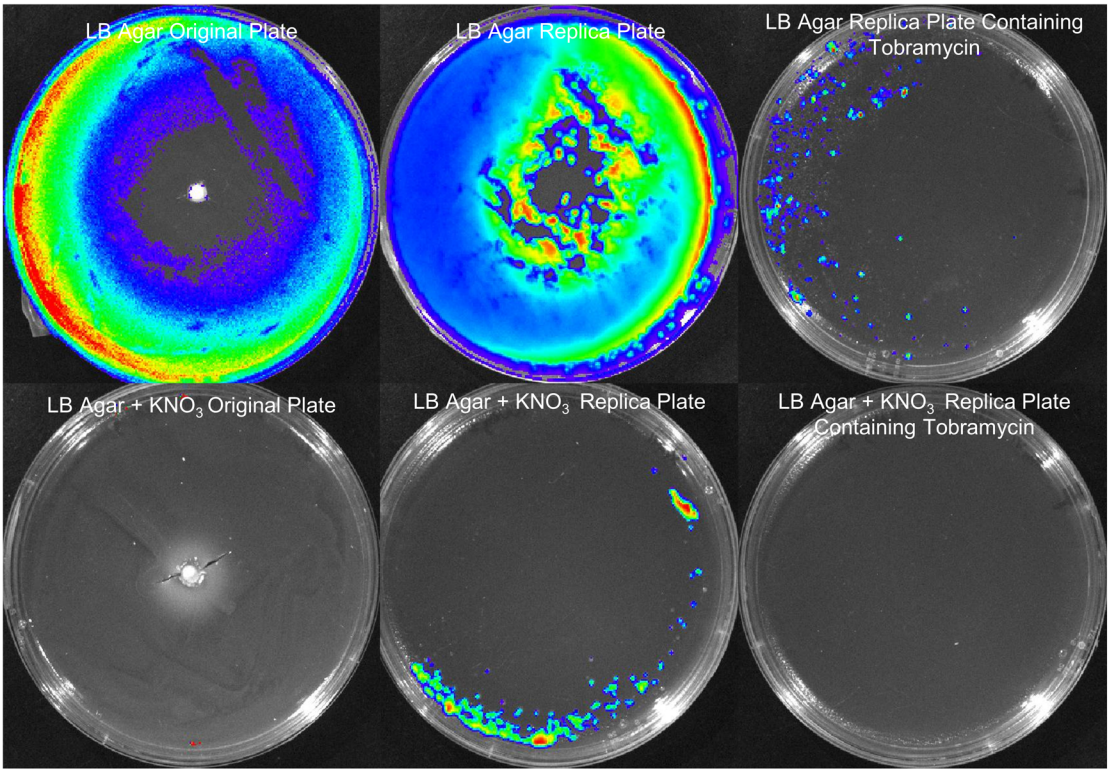

Figure 2.10 Anaerobic environments provide bacterial protection from antibiotics. Tobramycin-loaded beads were placed in the center of 24-hour lawn biofilms grown on LB agar and LB agar containing 100 mM KNO_3 in an anaerobic environment. The plates remained in the anaerobic environment for 5 days before being imaged using IVIS and replica plated on LB agar and LB agar containing 5 μg/mL of tobramycin. The replica plates were grown aerobically for 24 hours before IVIS imaging was performed. While the anaerobic environment protected the lawn from killing, supplementing the plates with KNO_3 allowed for the lawn to be killed across most of the plate.

Planktonic populations are eradicated by high concentrations of tobramycin

In both a previous (113) and the current study, biofilm lawns showed an area of complete bacterial eradication immediately adjacent to the highly, concentrated antibiotic source from which no resistant, tolerant, or persister cell variants could be cultured. In order to test if similarly efficient eradication could occur in a planktonic state, stationary phase cultures of *P. aeruginosa* PAO1 were incubated for 48 hours with varying high concentrations of tobramycin. After incubation, broth culture samples were plated for CFU counts and incubated for 7 days in order to allow any dormant or slow growing phenotypes to appear before being counted. In all tested concentrations (400-1,000 μg/mL), no bacteria were recovered despite the long incubation. Due to the very high concentrations of tobramycin, there was concern that an osmolarity effect may be causing bacterial cells to lyse. A control study was performed to determine if the high, solution osmolarity caused by the large amount of tobramycin could account for the total eradication as opposed to cell death being exclusive caused by the aminoglycoside mechanism of action. Dextrose was used to produce equivalent osmolarity in additional bacterial samples lacking tobramycin. The dextrose samples showed growth of 2.7 ± 0.5 x 10^9 CFU/mL indicating that the bacteria are able to survive despite the high osmolarity exposure when such high concentrations of tobramycin are present.

2.5. Discussion

Pseudomonas aeruginosa is an important, bacterial pathogen, which is able to cause infections in several human-associated environments including the lungs, wounds, and post-surgical sites. Its ability to form biofilms and resist antibiotic therapy is

something, which must be better understood to help clear infections and deal with the rise of multidrug resistance (5, 7, 9, 10, 119, 120). Calcium sulfate beads, cements, and bone fillers are routinely impregnated with antibiotics and placed at the surgical site during orthopedic revision surgeries to provide local therapy to treat infections (111). It is also important to note that each of these methods allow an antibiotic gradient to develop in which the region immediately adjacent to the antibiotic source contains high enough drug concentrations to eradicate bacterial biofilms and antibiotic variants, but diffusion limitation leads to areas with lower concentrations including those at sub-MIC concentrations. While these local antibiotic therapy methods may effectively kill a large amount of planktonic or biofilm-associated bacteria, the presence and gradient of antibiotics could also facilitate emergence of antibiotic tolerant variants, potentially resulting in a chronic or recurrent infection (121). Three variant colony phenotypes of *P. aeruginosa* were identified in this study: i) classically resistant mutants, ii) phoenix colonies, and iii) VBNCs, all of which emerged in the presence of tobramycin. This is not due to a calcium sulfate chemistry specific phenomenon but, instead, likely occurs in any antibiotic release mechanism in which gradients form due to diffusion limitation. It is important to note that the variant colonies take 3-5 days to emerge and only do so after the surrounding, wild-type bacterial lawn has been killed. We propose that the death of the wild-type bacteria allows the variant colonies, which presumably exist as small proportions in the lawn, to emerge and generate discrete, visible colonies.

The observed resistant mutants are heritable and therefor likely caused by a genetic mutation. Acquired antibiotic resistance in *P. aeruginosa* is well documented and

can occur by a number of mechanisms including increase in efflux pump expression and modification of the antibiotic target site (6, 13, 16, 29, 122, 123). The phoenix colonies, however, appear to be driven by a new mechanism as they are able to maintain metabolic activity and growth in the presence of high concentrations of tobramycin, but revert to wild-type susceptibility once they are removed from the environment and sub-cultured (Figure 2.11). Similar studies were performed by Gefen *et al.* (118) where they studied the emergence of tolerant phenotypes by allowing the antibiotic concentration to drop below MIC levels. The concentration of antibiotic used in their study was significantly lower than in our study. In the current study, we have shown that phoenix colonies are different from persister cells. The persister cells survive antibiotic therapy by entering a state of dormancy, which allows survival while the antibiotic is present. Once the antibiotic concentration drops below MIC, the persister cells are able to reactivate and grow (8), while phoenix colonies thrive in the antibiotic laden environment and do not seem to enter any dormancy phase. The phoenix colonies also exhibit a non-heritable change in pigmentation from yellow-green to white. This loss of pigmentation suggests a reduction in pyocyanin production, which may also give clues to the molecular mechanism behind the production of the phoenix colonies. While the phoenix colonies emerge at a very low frequency, it is still possible that they could survive antibiotic therapy and cause re-colonization and perpetuation of an infected site.

In addition to tobramycin, gentamicin, another aminoglycoside antibiotic, also showed an emergence of phoenix colonies (Figure 2.1) while ciprofloxacin and colistin did not (Figures 2.2 and 2.3). While inhibition of DNA replication activity

(ciprofloxacin) or membrane integrity (colistin) did not produce growth of the phoenix phenotype, it is possible that the mechanisms behind phoenix colony emergence may be linked to disruption of ribosome assembly and translation. Further studies, including transcriptomic and genomic sequencing, are needed to elucidate the mechanisms responsible for the emergence of phoenix colonies.

Previous studies have shown that an alternate metabolism caused by an anaerobic environment could lead to antibiotic tolerance in *P. aeruginosa* (83). Due to the presence of anaerobic microenvironments within a biofilm, it is possible that phoenix colonies originate in an anaerobic or microaerobic portion of the biofilm lawn and enter an alternate metabolic state, which then confers tolerance to the presence of antibiotics. The anaerobic chamber data presented here support the likelihood of this possibility as there was no apparent killing of the biofilm lawn grown in the anaerobic chamber, but once removed to an aerobic environment, the biofilm lawn returned to being tobramycin susceptible. In addition, when given a terminal electron acceptor (nitrate), the lawn was able to utilize denitrification but regained susceptibility to the tobramycin suggesting a different alternate metabolism is responsible for the protection of the phoenix colonies.

While VBNCs were noted in our experiments, it was difficult to study them due to the lack of an ability to culture them following their initial appearance. This population could play a role in infection, but this remains purely speculative. It is likely that the VBNCs are dependent on a compound in the plate environment released from dead or dying cells that is not present once the colonies are sub-cultured. Further study is needed to better understand this phenotype as well as to examine the spatial distribution of

VBNCs and phoenix colonies during development within the biofilm. With advancements in live single cell imaging, as well as the development of viability and metabolic reporter stains, further insight into these rare sub-populations found within biofilms should be achievable, which is a topic of our current study.

Although phoenix colonies, resistant mutants, and persister cells could lead to chronic or recurrent infections, it is important to note that high concentrations of tobramycin were able to eradicate these variant colonies near the tobramycin-loaded beads. This is supported by the lack of growth in the ZOC on replica plates as well as by the lack of growth in cultures taken from the zone immediately surrounding the tobramycin-loaded bead where there would initially be very high concentrations of antibiotic. This suggests that closely packed antibiotic-loaded $CaSO_4$ beads or high enough concentrations of antibiotics may be able to kill all phoenix colonies, resistant mutants, persister cells, and any other *P. aeruginosa* colony variants.

In conclusion, we have identified a novel, tolerant phenotype known as phoenix colonies which emerge along with other antibiotic resistant and tolerant variants from the ZOC of high concentrations of tobramycin. Further study, including transcriptomic or genomic sequencing, is needed to understand the complete mechanism behind the emergence of phoenix colonies and other phenotypic *P. aeruginosa* variants including VBNCs to understand how best to approach prevention and treatment strategies for patients with chronic or recurrent infections while also combating the increasing occurrence of multidrug resistance.

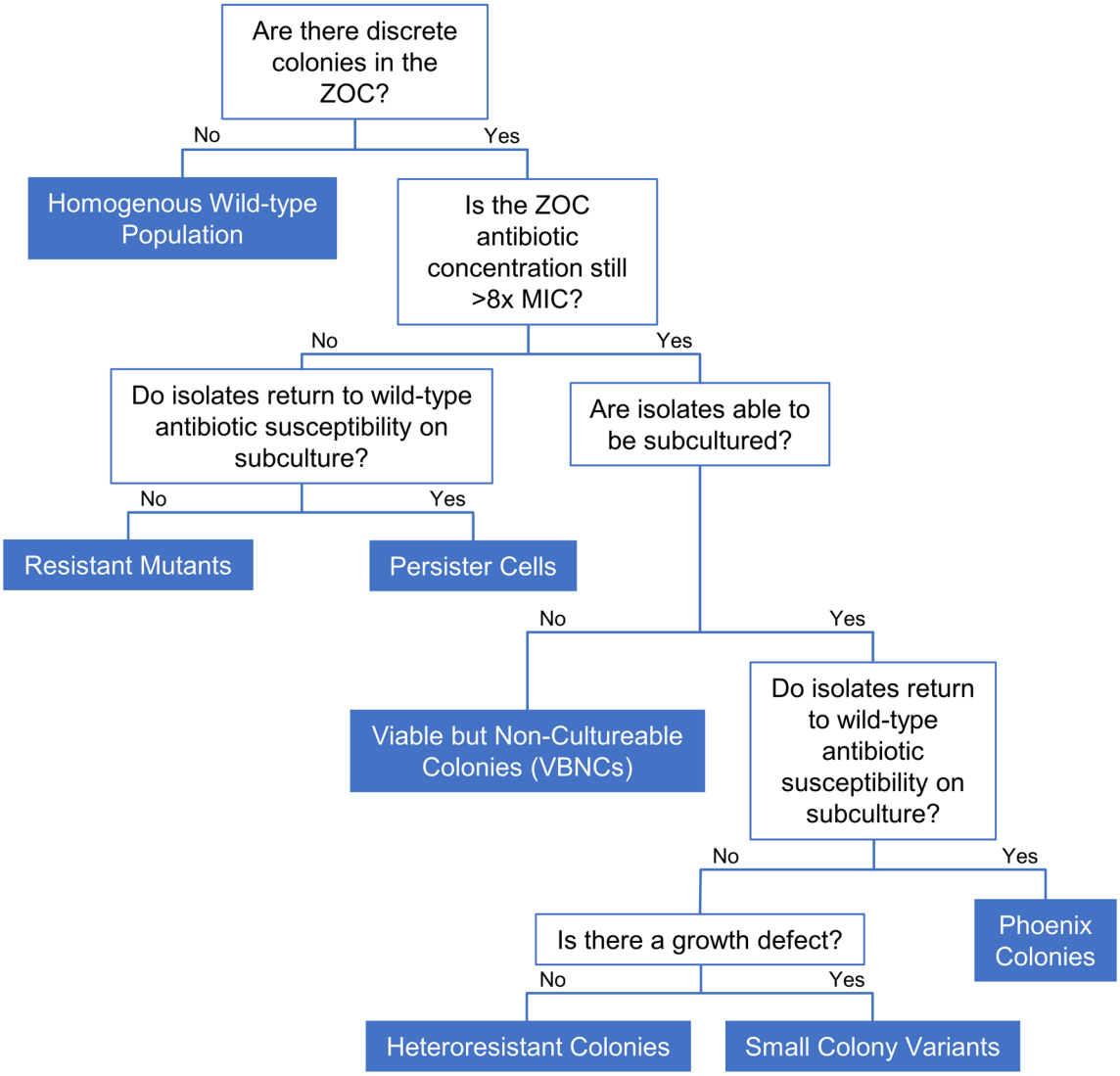

Figure 2.11 Antibiotic variant flow chart.

Following the flow chart allows one to easily determine the antibiotic variant classification of cultures and isolates. Although this chart is based on a pre-grown biofilm lawn of *P. aeruginosa* exposed to tobramycin, it can easily be adapted to other antibiotics, strains, and culturing techniques.

2.6. Acknowledgements

This work was supported in part by the Ohio State University College of Medicine and R01 NIH- GM124436 (PS). Conflict of interest - None declared.

Chapter 3. Genomic and Transcriptomic Profiling of Phoenix Colonies

Devin Sindeldecker, Matthew Dunn, Matthew Anderson, and Paul Stoodley

3.1. Abstract

Pseudomonas aeruginosa is a Gram-negative bacterium responsible for numerous human infections. Previously, novel antibiotic tolerant variants known as phoenix colonies as well as variants similar to viable but non-culturable (VBNC) colonies were identified in response to high concentrations of aminoglycosides. In this study, the mechanisms behind phoenix colony and VBNC-like colony emergence were further explored using both whole genome sequencing and RNA sequencing. Phoenix colonies were found to have a single nucleotide polymorphism (SNP) in the PA4673 gene, which is predicted to encode a GTP-binding protein. No SNPs were identified within VBNC-like colonies compared to the founder population. RNA sequencing did not detect change in expression of PA4673 but revealed five differentially expressed genes that may play a role in phoenix colony emergence. Three of the genes encode hypothetical proteins, one encodes a tRNA pseudouridine synthase D, and the last encodes the sRNA P27 that is known to inhibit *rhlI*, an important protein in the RhlR regulatory pathway of *Pseudomonas*. Although not immediately clear whether the identified genes in this study may have interactions which have not yet been recognized, they may contribute to the

understanding of how phoenix colonies are able to emerge and survive in the presence of antibiotic exposure.

3.2. Introduction

Pseudomonas aeruginosa is a Gram-negative bacterium found throughout the natural environment. As an opportunistic pathogen, it is most commonly associated with cystic fibrosis (CF) infections but can also reside in chronic wounds and post-surgical site infections (2, 3, 110). Additionally, *P. aeruginosa* has been found to rapidly adapt to its environment within the context of infection (14), leading to concerns of emerging antimicrobial tolerance or resistance. Formation of biofilms, persister cells, and development of multidrug resistance mechanisms also reduce the effectiveness of antimicrobial agents in eradicating *P. aeruginosa* (5-8).

In a previous study, our lab identified a novel, tolerant phenotype of *P. aeruginosa*, which we have termed phoenix colonies. Phoenix colonies are able to survive and thrive in an antibiotic laden environment, specifically in the presence of aminoglycosides, which are commonly used to treat *Pseudomonas* infections. Once removed from the antibiotic environment, phoenix colonies revert to a wild-type level of antibiotic susceptibility (86). Phoenix colonies differ from traditional tolerance in that they are able to maintain high levels of metabolic activity throughout antibiotic exposure, whereas traditional tolerance is typically the result of slow growth or a decrease in metabolism (50). Additionally, another identified phenotype in the same study was similar to the viable but non-culturable colonies (VBNCs, (124)) phenotype. The identified VBNC-like colonies were also able to grow in the antibiotic environment but

were unable to be cultured outside of the environment in which they arose, including cultures of the same antibiotic (86). While the significance of these phenotypes in a clinical setting is currently unknown, it is possible that phoenix colonies or VBNC-like colonies could lead to chronic or recurrent infections, similar to persister cells (8). Furthermore, the molecular and genetic mechanisms leading to phoenix colony and VBNC-like emergence are unknown. Understanding the genetic alterations in these cells or alterations to gene expression may allow for better preventative or treatment options in the management of chronic or recurrent infections.

In this study, whole genome sequencing (WGS) of phoenix colonies and VBNC-like colonies identified a single nucleotide polymorphism (SNP) which may be associated with the emergence of phoenix colonies in the presence of high concentrations of aminoglycosides. Additionally, RNA sequencing was performed on phoenix colonies as well as VBNC-like colonies and identified differentially expressed genes (DEGs) which could account for the antibiotic adaptation phenotypes portrayed by both phoenix colonies and VBNC-like colonies.

3.3. Materials and Methods

Bacterial strains and culture conditions

The bioluminescent strain *P. aeruginosa* Xen41 (Xenogen Corp., USA) was used for the imaging portion of this study (Figure 3.1). Additionally, *P. aeruginosa* PAO1 (125), which is also the parent strain for *P. aeruginosa* Xen41, was used in this study. Stock culture plates were prepared by streaking from glycerol stock cultures which were stored at -80°C onto fresh Luria-Bertani (LB) agar plates. The streaked plates were

incubated at 37°C for 24 hours before being examined for individual colony growth and proper morphology. Individual colonies were isolated from stock culture plate and transferred to 20 mL of LB broth. Broth cultures were incubated overnight in a shaking incubator set to 37°C and 200 rpm.

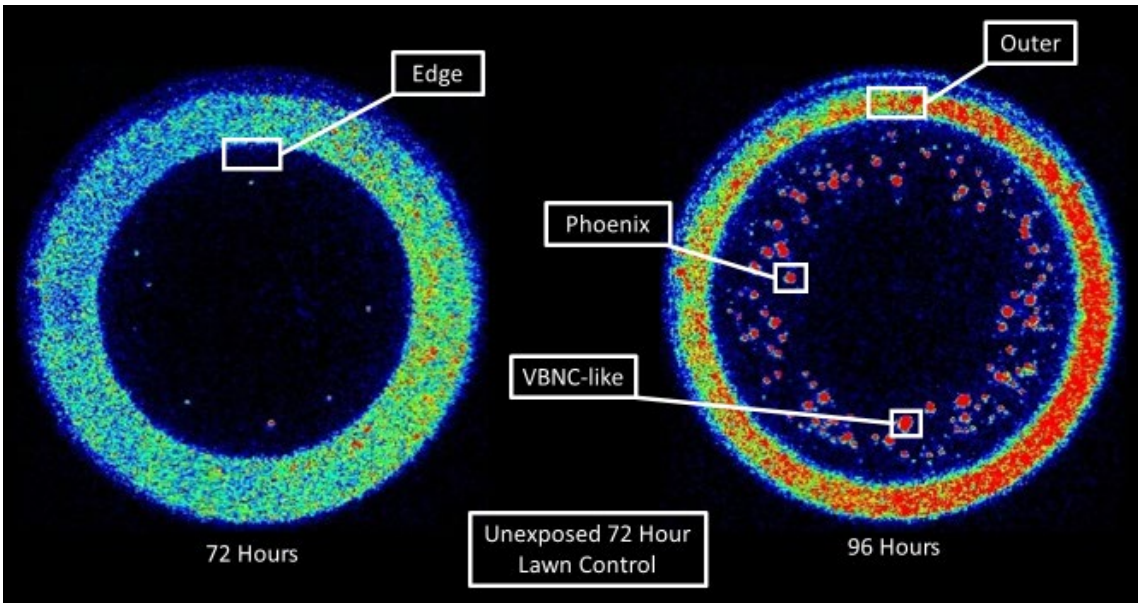

Figure 3.1 Isolation of *P. aeruginosa* colony variants for assaying the genome and gene expression.

In vitro imaging system (IVIS) images of representative phoenix colony plates show areas of bacterial sampling. Seventy-two hours post tobramycin bead placement, samples were taken from the edge of the zone of clearance (ZOC) where phoenix colonies would be expected to arise the following day after continued incubation. Ninety-six hours post tobramycin bead placement, samples were taken from phoenix colonies, VBNC-like colonies, and the outer background lawn. Additionally, samples were taken from bacterial lawns grown for 72 hours that had not been exposed to antibiotics to be used as comparative controls. Red indicates high levels of metabolic activity, blue indicates low levels of metabolic activity, black indicates no metabolic activity.

Preparation of tobramycin loaded calcium sulfate beads

Antibiotic loaded calcium sulfate beads were added to pre-formed biofilm lawns. 240 mg of tobramycin (Sigma-Aldrich) per 20 g of $CaSO_4$ hemi-hydrate (Sigma-Aldrich), a ratio commonly used by orthopedic surgeons for treatment of periprosthetic joint infections (PJIs), was used (114). After mixing of the tobramycin and $CaSO_4$ powders, sterile water was added and mixed to produce a thick paste. The paste was then spread into silicone molds (Biocomposites Ltd.) to form 4.5 mm diameter, hemispherical beads. The beads were allowed to dry at room temperature overnight before being removed from the mold and stored at 4°C before use.

Preparation of phoenix and VBNC-like colonies of P. aeruginosa

Phoenix colonies were obtained as per Sindeldecker et al. (86). Briefly, an overnight bacterial culture of *P. aeruginosa* PAO1 was diluted to an OD_{600} of 0.1 using sterile LB broth. One hundred µL of the diluted culture was spread onto LB agar contained in 100 mm diameter, polystyrene plates (Fisher Scientific, USA). The plates were incubated at 37°C with 5% CO_2 for 24 hours in a humidified incubator (Heracell 150i, Thermo Scientific) to allow a lawn biofilm of *P. aeruginosa* to develop. After the 24 hour lawn biofilm was prepared, a tobramycin-loaded calcium sulfate bead was placed in the center of the plate and pushed into the agar using sterile forceps. The plates were then incubated further at 37°C with 5% CO_2 for an additional 96 hours. Plates were visually checked daily for the appearance of a zone of clearance (ZOC) as well as

colonies emerging within this zone. Additionally, 72 hour lawn biofilms were prepared in the same fashion but without tobramycin beads for use as a control lawn.

Isolation of Samples to be used for Whole Genome Sequencing

Phoenix colonies, VBNC-like colonies, and wild-type *P. aeruginosa* PAO1 colonies were isolated for whole genome sequencing. In short, phoenix colony plates were generated as above. After the emergence of the variant colonies on three replicate plates, 96 colonies from each plate were isolated into individual aliquots of 100 µL of PBS and stored at -20°C. Before placing the colony isolate samples at -20°C, 5 µL was used to inoculate 200 µL of LB broth containing 5 µg/mL of tobramycin in a well of a 96-well plate (Corning, Sigma-Aldrich). An additional 5 µL was added to a corresponding well of another 96-well plate containing 200 µL of LB broth. The plates were then incubated for 96 hours at 37°C with 5% CO_2. After incubation, turbidity in the wells of each plate was visually compared. Variants which showed a lack of growth in the LB broth as well as the corresponding well of LB broth containing the tobramycin were defined to be VBNC-like colonies. Phoenix colonies were defined as those showing a lack of growth in the LB broth containing tobramycin while having growth in the LB only wells. An overnight broth culture of *P. aeruginosa* PAO1 was also grown as above to provide a wild-type sample for DNA extraction.

Determination of Variant Colony Antibiotic Susceptibility

Isolates which grew from the previous section were subjected to a Kirby-Bauer assay to determine whether they were resistant or susceptible to tobramycin. Each isolate was diluted to an OD_{600} of 0.1. 100 µL of each diluted culture was spread onto sterile LB agar plates. A sterile, filter paper disk was placed in the center of each plate and 10 µg of tobramycin was placed on each disk. These plates were incubated at 37°C with 5% CO_2 for 24 hours. After incubation, the diameter of the zone of inhibition produced was measured and compared to the Clinical and Laboratory Standards Institute (CLSI) guidelines to determine if they were resistant or susceptible (phoenix colonies). Four phoenix colonies and four VBNC-like colonies were randomly selected to be used in RNA extraction.

Whole Genome Sequencing

DNA extraction was performed for each of the above isolated samples by following manufacturer's instructions using the GenElute™ Bacterial Genomic DNA kit (Sigma-Aldrich). After gDNA extraction, samples were pooled to obtain samples of 400 ng gDNA to identify conserved driver mutations. Library preparation and barcoding was completed using the Rapid Barcoding Kit (Nanopore). A Nanopore MinION Sequencer was then used to complete bacterial whole genome sequencing using default settings. After sequencing was completed, quality control was performed using the software Epi2ME (Nanopore). Reads were then trimmed using Porechop (126) and aligned to a reference *P. aeruginosa* PAO1 genome (GCF_000006765.1, available for download from the Pseudomonas Genome database, (127)) using graphmap (128). Reads were sorted and

indexed using samtools (129). Structural variants were identified using sniffles (130) and SNPs were identified using BCFtools (131).

Isolation of Samples to be used for RNAseq

Once phoenix colony plates had been prepared, samples were taken for use in RNA sequencing. Seventy-two hours post tobramycin bead placement, triplicate samples were taken from the edge of the zone of clearance (ZOC) where phoenix colonies would arise on the following day. Ninety-six hours post tobramycin bead placement, triplicate samples from the outer background lawn were taken and variant colonies which had emerged in the ZOC were isolated for phenotype characterization (phoenix colonies, VBNC-like colonies, or resistant mutants). Additionally, triplicate samples were taken from bacterial lawns grown for 72 hours that had not been exposed to antibiotics. All samples and isolates were placed into 100 µL of RNAlater (Ambion) and stored at -20°C to protect the RNA from degradation until needed for RNA extraction. A control study was done in which 40 colonies of wild-type *P. aeruginosa* PAO1 were isolated into LB broth and 40 colonies were isolated into RNAlater before being transferred to LB broth. No significant difference was seen in viability of the colonies exposed to RNAlater ($p=1.0$). For the variant colony isolates, immediately after being mixed in the RNAlater, a 5 µL sample was taken and used to inoculate 15 mL of sterile LB broth. These broth cultures were incubated at 37°C with 200 rpm shaking overnight. Cultures which did not grow in the overnight broth cultures were deemed to be VBNC-like colonies. The

cultures which did grow were then further examined to determine their level of susceptibility to tobramycin.

RNA Sequencing

RNA extraction was performed for each sample using the Direct-zol RNA Miniprep Kit (Zymo) following manufacturer's instructions. RNA quantity was measured using Qubit 3.0. In order to remove ribosomal RNA from isolated samples, the RiboZero Bacteria Kit (Illumina) was used as per manufacturer's instructions. Barcoded RNAseq libraries were then generated using the ScriptSeq™ v2 Kit (Illumina) per the manufacturer's instructions. Samples were sequenced using paired-end (2 x 150 bp) sequencing on an Illumina HiSeq 4000 device. Sequencing reads were quality controlled using FastQC (132) and mapped to the reference genome for *P. aeruginosa* PAO1 (GCF_000006765.1, available for download from the Pseudomonas Genome database, (127)) using STAR (133). After read mapping, sequences were visualized to ensure adequate genome coverage using IGV (v2.4.13, (134)). Transcript counts were obtained using HTseq (135) and were further analyzed for differential gene expression using the R package edgeR (v3.24.3, (136)). Multi-dimensional scaling plots were also generated using the plotMDS function within edgeR. Volcano plots were generated using the plot function in R. Genes found to be differentially expressed when comparing phoenix colony and VBNC-like colony samples to 72 hour unexposed lawn samples were submitted to DAVID 6.8 (137, 138) and KEGG (139) for pathway analysis.

Screening DEG Transposon Mutants

Transposon mutants (obtained from the lab of Dr. Colin Manoil, (125)) corresponding to each of the identified differentially expressed genes were screened in triplicate replicates for their ability to produce phoenix colonies. A biofilm lawn was generated for each mutant, a tobramycin loaded $CaSO_4$ bead was placed, and phoenix colonies were generated as described above. Upon phoenix colony emergence, phoenix colonies were distinguished from resistant colonies and VBNC-like colonies using replica plating as per Sindeldecker et al. (86). Briefly, a sterile, cotton velveteen square (150 × 150 mm) was draped over a PVC replica plating block and held in place using an aluminum replica plater ring. The tobramycin loaded $CaSO_4$ bead was removed from the plate using a sterile, plastic loop. The plate was marked to indicate a 12 o'clock position and gently placed on the velveteen square. The plate was then gently tapped down before being removed from the replica plater. A fresh, sterile LB agar plate containing 5 μg/mL of tobramycin and marked at the 12 o'clock position was placed on the velveteen square and tapped down in the same fashion before being removed. A fresh, sterile LB agar plate marked at the 12 o'clock position was placed on the velveteen square and tapped down before being removed. Replica plates were incubated for 24 hours at 37°C with 5% CO_2. After incubation, the colony pattern on the plates was compared and colonies which appeared on the LB agar replica plate but not on the LB agar replica plate containing tobramycin were determined to be phoenix colonies. Transposon mutant phoenix colony counts were obtained and compared to control *P. aeruginosa* PAO1 counts.

Creation of a PA3626 Complementation Plasmid

P. aeruginosa PAO1 gDNA was extracted using the GenElute™ Bacterial Genomic DNA kit. After extraction, PCR was performed to amplify the PA3626 gene using the manufacturer's protocols for Phusion Taq polymerase (New England Biolabs) and forward (5'-GCGCGGATCCATGAGCGTTCTCGGCGAA) and reverse (5'-GCGCTCTAGATCAGTATGCGCATGGGTT) primers (Integrated DNA Technologies). After amplification, the PA3626 product was run on an agarose gel and extracted using the GenElute™ Gel Extraction kit. A DNA digestion was then completed using the restriction enzymes BamHI and XbaI (New England Biolabs) on both the PA3626 product and pUCP18 plasmid following the New England Biolabs protocol. DNA ligation was then completed using manufacturer's protocol for the T4 DNA ligase (Thermo Fisher) and a 7:1 ratio of insert to plasmid. After ligation, the plasmid was electroporated into *P. aeruginosa* PAO1 PA3626::Tn5. Briefly, 1 mL of an overnight culture of PAO1 PA3626::Tn5 was centrifuged at max speed in a microcentrifuge for 1 min. The pellet was then washed three times in 10% sucrose in sterile water before being resuspended in 100 µL of 10% sucrose. 5 µL of the ligated plasmid was added and the mixture was transferred to a 2 mm electroporation cuvette. The cuvette was then electroporated at 25 µF, 200 Ω, and 2.5 kV. 1 mL of sterile LB was then added to the cuvette and the culture was transferred to a 1.5 mL tube and incubated at 37°C with 200 rpm shaking for 1 hr. After incubation, the culture was spread on LB agar containing 100 µg/mL of carbenicillin and incubated overnight at 37°C with 5% CO_2. Isolates were then cultured and plasmids were extracted using the Qiagen Spin Miniprep kit. Plasmids were

then digested using BamHI and XbaI restriction enzymes, and an agarose gel was run to confirm the appropriately sized bands were present.

Screening Complementation Strain for Phoenix Colony Emergence

The PA3626 complementation strain was plated and exposed to 1 mg of tobramycin as above in order to allow variant colonies to emerge. After variant colony emergence, the plates were replica plated onto fresh LB agar and LB agar containing 5 μg/mL of tobramycin. Replica plates were incubated for 24 hours at 37°C with 5% CO_2. After incubation, plates were compared to each other and colonies which grew on the original plate and LB only replica plate but did not grow on the replica plate containing tobramycin were counted as phoenix colonies.

Protein Modeling

Amino acid sequences for wild-type PA4673 and PA4673 containing the identified SNP were submitted for protein structure and functional modeling to the Phyre2 server (140) using the intensive modeling mode. Amino acid sequences for the hypothetical proteins associated with phoenix colony DEGs were also submitted for protein structure and functional modeling to the Phyre2 server using the intensive modeling mode. Models were visualized using RasMol (141).

Statistical analysis

All experiments were performed with a minimum of triplicate technical replicates. ANOVA analysis was completed in edgeR for differentially expressed genes with significance set at a q-value of 0.05. ANOVA analysis was completed by GraphPad Prism (v8.2.1) for all other studies with a p-value of 0.05 being considered significant.

Bioluminescence Imaging

Bioluminescence imaging was performed using an *in vitro* imaging system (IVIS). Plates were exposed for thirty second exposures to obtain images. A pseudo-color heatmap was then applied to aid in visualization.

3.4.3.4. Results

Phoenix Colonies Contain a SNP in PA4673

As shown previously (86), antibiotic resistant and tolerant variant colonies were cultured by exposing a *P. aeruginosa* PAO1 biofilm lawn to high concentrations of tobramycin (Figure 3.1). Genomic DNA was isolated from phoenix colonies, VBNC-like colonies, and the founder population of *P. aeruginosa* PAO1. Whole genome sequencing (WGS) was performed using a Nanopore MinION Sequencer, and the reads were mapped to the PAO1 reference genome. Mapped reads were analyzed for the presence of SNPs as well as insertions or deletions (indels). Only the phoenix colony sample encoded any SNPs compared to the PAO1 reference genome and no samples (phoenix colony, VBNC-like colony, or control colony) contained indels. The single guanine to thymine

(GCF_000006765.1:c.353G>T) variant occurred within the PA4673 gene, a hypothetical cytosolic protein, to produce a serine to isoleucine (S118I) amino acid change.

PA4673 is Predicted to Encode a GTP-binding Protein

To determine the impact of the S118I polymorphism in PA4673, *de novo* protein modeling was performed using Phyre2 (140). The structural models of both the wild-type and mutant proteins show a change in the secondary structure of the mutant protein, specifically, the formation of a predicted β sheet at the mutation site, which is located in an external area of the protein. This modification may lead to alteration of a binding site or protein function (Figure 3.2). Identification of functional domains in both PA4673 isoforms predicted domains between AA001 and AA363, indicating they likely function as GTP-binding proteins as they align with 100% confidence to the YchF GTP-binding protein of *Schizosaccharomyces pombe* (142, 143).

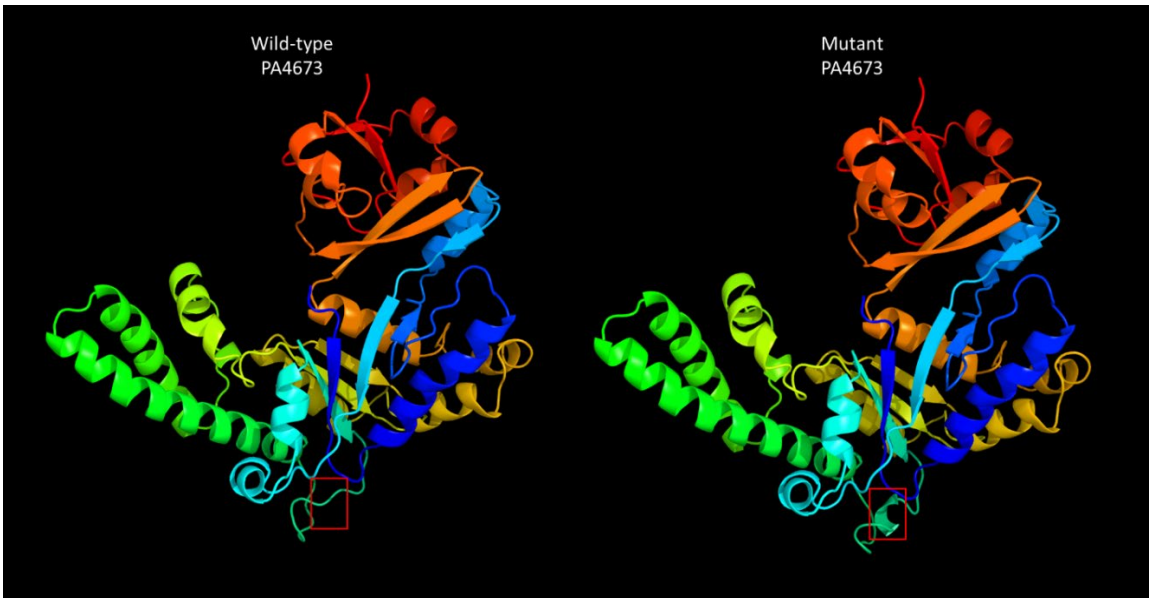

Figure 3.2 Protein structure of wild-type and mutant PA4673.

Protein structures were derived from the amino acid sequences of wild-type and mutant PA4673 using Phyre2. The red box indicates the structural change caused by the SNP. Functional domain identification in both PA4673 isoforms indicates that they likely function as GTP-binding proteins. As the SNP causes an amino acid change in the exterior portion of the predicted protein structure, it may lead to alteration of a binding site or protein function.

DEGs were Identified for Phoenix Colonies and VBNC-like Colonies

Due to the lack of clear genetic candidates for promoting alternative colony states, a transcriptomic approach was utilized to define gene regulation changes that are associated with each alternative colony type. RNA was isolated from samples at the edge of the ZOC at 72 hours, from multiple colony populations at 96 hours (phoenix colonies, VBNC-like colonies, and the outer background lawn), and from a 72 hour unexposed lawn as a control, and prepared for Illumina-based sequencing (Figure 3.1).

Differential gene expression of either phoenix colonies or VBNC-like colonies was performed to define transcriptional profiles that distinguish each phenotype. First, a multi-dimensional scaling (MDS) plot was generated using expression of all genes to examine the relationships between all samples (Figure 3.3). This plot shows compact clustering among biological replicates of each colony phenotype with the exception of 96 hour outer-edge populations. While the edge of ZOC group, control, and outer background lawn samples clustered on their own. The phoenix colonies and VBNC-like colonies overlap heavily, indicating highly similar transcriptomic profiles. Differential gene expression between the control lawn and phoenix colonies, as well as the control lawn and VBNC-like colonies, identified 1630 and 750 DEGs, respectively. Out of these DEGs, 46 and 59 genes, respectively, were identified to have significantly different transcript abundance (>2x fold change, $p<0.01$, Figure 3.4). These genes were split with 26 down-regulated and 20 up-regulated genes when comparing phoenix colonies to the control lawn, and 37 down-regulated and 22 up-regulated genes for VBNC-like colonies compared to the control (Table 3.1, Table 3.2). The DEGs were submitted for both

DAVID and KEGG pathway analysis, but no significant pathway correlation was identified.

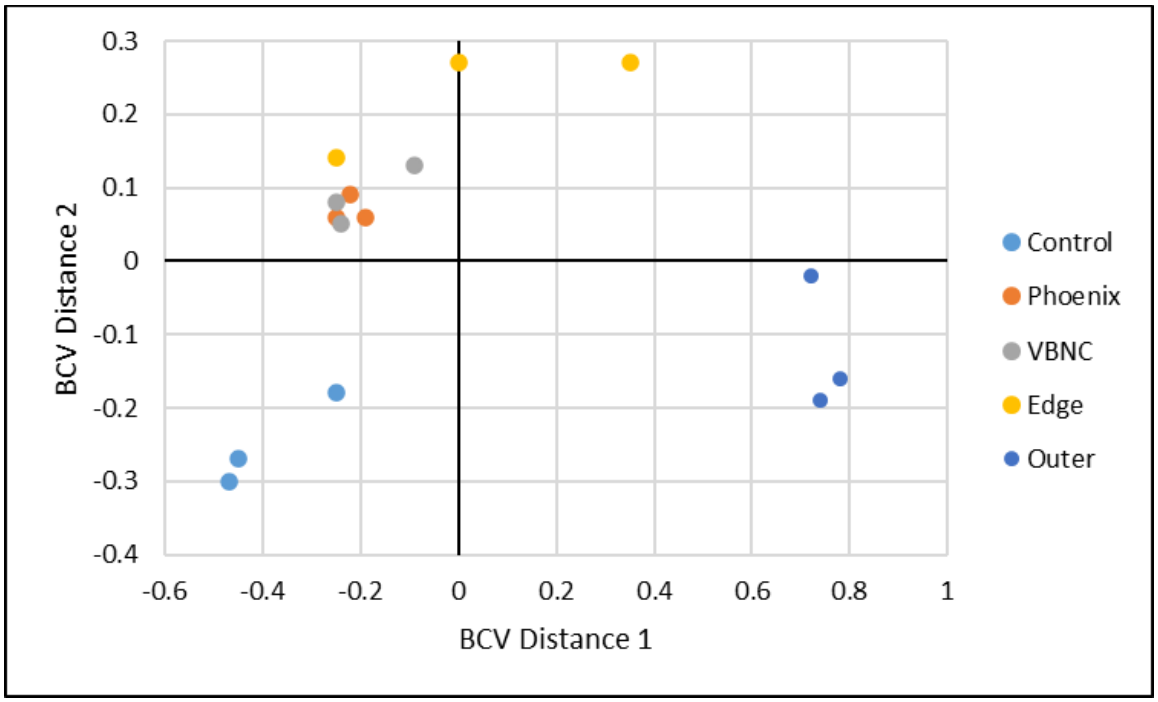

Figure 3.3 Multi-dimensional scaling (MDS) plot showing clustering of isolates. An MDS plot was generated using biological coefficients of variation (BCV) from transcript counts for each isolate sample. Samples from each group cluster well together aside from the Edge samples (yellow), and the phoenix colonies and VBNC-like colonies overlap considerably. Control lawn, edge, and outer samples cluster on their own and separately from the phoenix and VBNC-like samples.

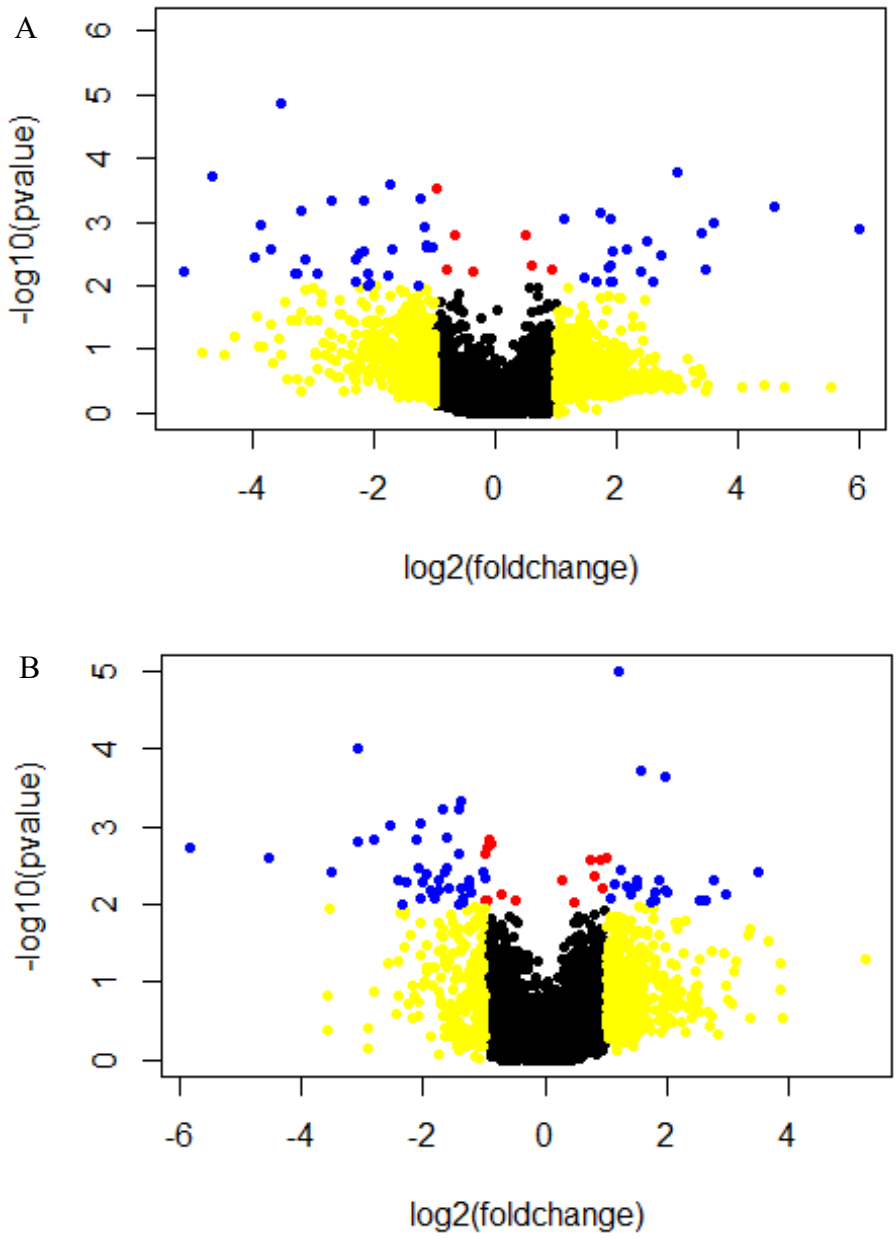

Figure 3.4 Volcano plots of DEGs.

A. Comparison of phoenix colony transcript counts to control lawn transcript counts showed 1630 DEGs. B. Comparison of VBNC-like colony transcript counts to control lawn transcript counts showed 750 DEGs. A-B. Yellow dots indicate genes with at least a two-fold change. Red dots indicate a p-value of 0.01 or less. Blue dots indicate both at

least a two-fold change and p-value less than 0.01. Black dots indicate genes with no-significant difference in transcription.

Table 3.1 Statistically significant DEGs of phoenix colonies.

Phoenix colony transcripts were compared to the control lawn to identify genes which were significantly up or down regulated. Red indicates genes which were significantly upregulated.

Gene	Fold Change	p-value	Protein Product Annotation
PA0526	63.273	0.001	hypothetical protein PA0526
PA3609	24.304	0.001	polyamine ABC transporter permease PotC
PA3038	11.912	0.001	porin
PA4712	10.947	0.005	hypothetical protein PA4712
PA4713	10.403	0.001	hypothetical protein PA4713
PA3355	7.94	0	hypothetical protein PA3355
PA2926	6.669	0.003	histidine ABC transporter ATP-binding protein
PA2576	5.677	0.002	hypothetical protein PA2576
PA2482	5.204	0.006	cytochrome C
PA4492	4.449	0.003	hypothetical protein PA4492
PA0103a	3.814	0.009	hypothetical protein PA0103a
PA2843	3.796	0.003	aldolase
PA4591	3.739	0.005	hypothetical protein PA4591
PA3611	3.715	0.009	hypothetical protein PA3611
PA5210	3.712	0.001	secretion pathway ATPase
PA4272.1	3.647	0.005	P27
PA2948	3.299	0.001	precorrin-4 C(11)-methyltransferase
PA0846	3.147	0.009	sulfate transporter CysZ
PA3626	2.749	0.007	tRNA pseudouridine synthase D
PA2792	2.17	0.001	hypothetical protein PA2792
PA2583	1.916	0.006	sensor/response regulator hybrid protein
PA0394	1.506	0.005	hypothetical protein PA0394
PA3143	1.401	0.002	hypothetical protein PA3143

Table 3.2 Statistically significant DEGs of VBNC-like colonies.

VBNC-like colony transcripts were compared to the control lawn to identify genes which were significantly up or down regulated. Red indicates genes which were significantly upregulated and blue indicates genes which were significantly downregulated.

Gene	Fold Change	p-value	Protein Product Annotation
PA1470	11.187	0.004	short-chain dehydrogenase
PA4056	7.686	0.008	riboflavin-specific deaminase/reductase
PA1289	6.795	0.005	hypothetical protein PA1289
PA0444	6.18	0.009	allantoate amidohydrolase
PA1166	5.758	0.009	hypothetical protein PA1166
PA3677	4.033	0.007	resistance-nodulation-cell division (RND) efflux membrane fusion protein
PA1239	3.942	0.006	hypothetical protein PA1239
PA0513	3.866	0	heme d1 biosynthesis protein NirG
PA2507	3.677	0.005	catechol 1,2-dioxygenase
PA1238	3.503	0.007	multidrug efflux pump outer membrane protein
PA2016	3.455	0.009	liu genes regulator
PA3202	3.376	0.009	hypothetical protein PA3202
PA1514	3.288	0.01	ureidoglycolate hydrolase
PA0170	2.963	0	hypothetical protein PA0170
PA5538	2.855	0.006	N-acetylmuramoyl-L-alanine amidase
PA2928	2.821	0.005	hypothetical protein PA2928
PA5502	2.667	0.007	hypothetical protein PA5502
PA3409	2.539	0.006	transmembrane sensor
PA1521	2.328	0.004	guanine deaminase
PA1282	2.29	0	major facilitator superfamily transporter
PA4516	2.213	0.005	hypothetical protein PA4516
PA4302	2.112	0.008	ATPase TadA
PA0527	0.017	0.002	transcriptional regulator Dnr
PA3620	0.043	0.002	DNA mismatch repair protein MutS
PA3048	0.089	0.004	ribosomal RNA large subunit methyltransferase K/L
PA4727	0.119	0	poly(A) polymerase
PA3212	0.12	0.002	ABC transporter ATP-binding protein

PA4728	0.143	0.001	2-amino-4-hydroxy-6-hydroxymethyldihydropteridine pyrophosphokinase
PA2936	0.171	0.001	hypothetical protein PA2936
PA3398	0.19	0.005	transcriptional regulator
PA0668.5	0.197	0.01	5S ribosomal RNA
PA2492	0.208	0.005	transcriptional regulator MexT
PA2584	0.229	0.002	CDP-diacylglycerol--glycerol-3-phosphate 3-phosphatidyltransferase
PA1149	0.237	0.003	hypothetical protein PA1149
PA2736	0.239	0.009	hypothetical protein PA2736
PA5228	0.243	0.001	hypothetical protein PA5228
PA0109	0.245	0.005	hypothetical protein PA0109
PA5349	0.256	0.004	rubredoxin reductase
PA2513	0.271	0.006	anthranilate dioxygenase small subunit
PA1839	0.277	0.007	RNA methyltransferase
PA5369.5	0.281	0.008	16S ribosomal RNA
PA3942	0.285	0.007	acyl-CoA thioesterase
PA3621.1	0.296	0.005	regulatory RNA RsmZ
PA2958	0.297	0.005	hypothetical protein PA2958
PA3806	0.298	0.006	dual-specificity RNA methyltransferase RlmN
PA3621	0.311	0.001	ferredoxin I
PA0103a	0.317	0.004	hypothetical protein PA0103a
PA0112	0.324	0.001	hypothetical protein PA0112
PA0039	0.326	0.003	hypothetical protein PA0039
PA3416	0.336	0.006	pyruvate dehydrogenase E1 component subunit beta
PA1157	0.371	0.002	two-component response regulator
PA5527	0.373	0.01	hypothetical protein PA5527
PA5435	0.374	0.001	pyruvate carboxylase subunit B
PA2818	0.384	0.006	aminoglycoside response regulator
PA4401	0.385	0	glutathione S-transferase
PA0107	0.391	0.008	cytochrome C oxidase assembly protein
PA0373	0.394	0.009	signal recognition particle receptor FtsY
PA1530.1	0.416	0.005	4.5S ribosomal RNA
PA2941	0.417	0.006	hypothetical protein PA2941
PA4047	0.426	0.007	GTP cyclohydrolase II
PA0633	0.49	0.004	hypothetical protein PA0633
PA4280.5	0.499	0.005	16S ribosomal RNA

Phoenix Colony Emergence is Eliminated by Disruption of PA0394 and PA3626

Transposon mutants for each DEG identified in comparisons between the control and either phoenix or VBNC-like colonies were screened for change in the frequency of phoenix colonies emergence. Three DEGs did not have a corresponding transposon mutant available for screening: two hypothetical proteins (PA0103a and PA0526), and the sRNA P27 which directly inhibits *rhlI* (PA4272.1) (Table 3.3). Yet, disruption of two genes, PA0394 and PA3626, produced a complete lack of phoenix colony emergence when exposed to tobramycin (n=6). PA0394 encodes an uncharacterized, hypothetical protein that lacks any annotated function, while PA3626 encodes for the pseudouridine synthase D (TruD) (144). In addition, complementation of PA3626 into the PA3626 transposon mutant, using a pUCP18::PA3626 plasmid, showed rescue of the phoenix phenotype to wild-type levels (Figure 3.5), indicating the importance of TruD in phoenix colony emergence.

Table 3.3 Phoenix colony DEGs remaining after transposon mutant screen.

After screening DEG associated transposon mutants, PA0394 and PA3626 were found to have a complete loss of phoenix colony emergence in the presence of tobramycin (n=6). PA0103a, PA0526, and PA4272.1 had no available transposon mutant for screening. Red indicates genes which were significantly upregulated.

Gene	Fold Change	p-value	Protein Product
PA0526	63.273	0.001	hypothetical protein
PA0103a	3.814	0.009	hypothetical protein
PA4272.1	3.647	0.005	P27 (sRNA)
PA3626	2.749	0.007	tRNA pseudouridine synthase D
PA0394	1.506	0.005	hypothetical protein

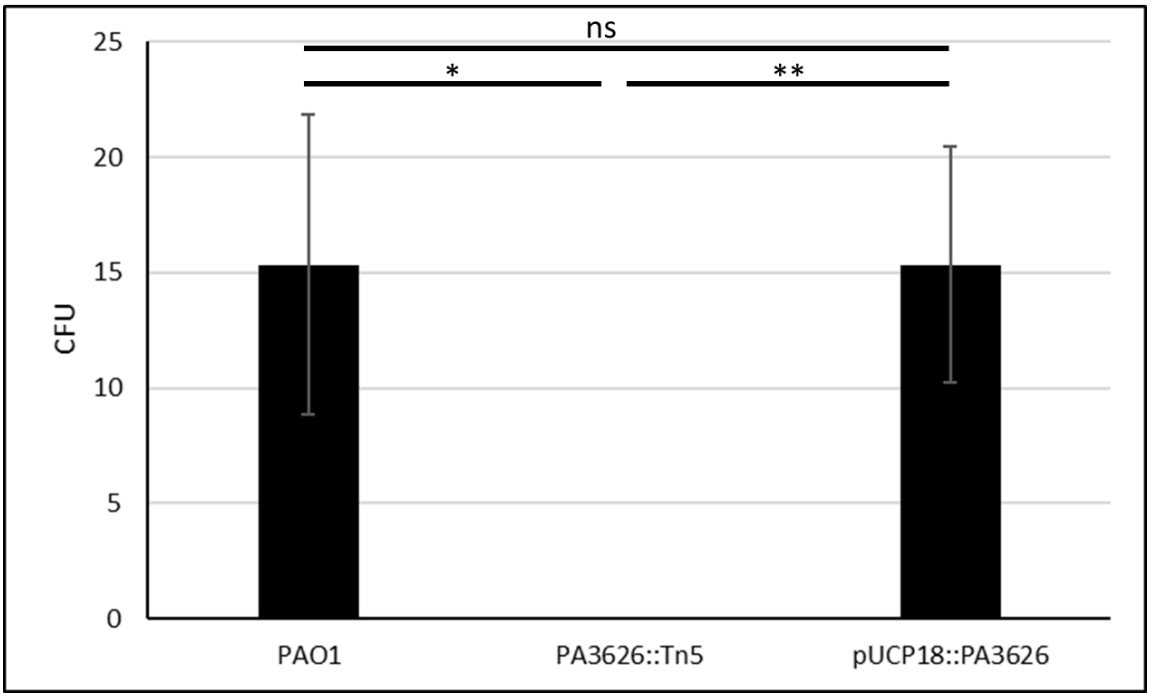

Figure 3.5 Complementation of PA3626 shows rescue of the phoenix phenotype. Phoenix colony counts were obtained for wild-type *P. aeruginosa* PAO1, the PA3626 transposon mutant, and the PA3626 complementation strain. After complementation of the transposon mutant, phoenix colony counts returned to wild-type levels (p=1), further confirming the importance of the tRNA pseudouridine synthase D in the emergence of phoenix colonies. *p<0.05, **p<0.01, n=3.

PA0394 is Predicted to Encode for a PLP-binding Protein

To gain greater insight into putative functions for PA0394, whose disruption alters phoenix colony formation, protein structure and functional analysis was performed in order to gain a better understand of how this gene may play a role in phoenix colony emergence. Structural modeling was performed on PA0394, which displays strong homology to pyridoxal 5'-phosphate (PLP) binding proteins (94% coverage at 100% confidence, Figure 3.6). PLP-binding proteins play an important role in the transamination of amino acids as well as act as a transcriptional regulator (145, 146).

Figure 3.6 Structural modeling of the hypothetical protein associated with phoenix colony emergence.

Phyre2 structure predictions were generated for the hypothetical protein PA0394, which showed an elimination of phoenix colony emergence.

3.5. Discussion

P. aeruginosa is an important bacterial pathogen implicated in both superficial and life-threatening infections that has readily developed tolerance and resistance to multiple antibacterial drugs. In this study, both the genomes and transcriptomes of both phoenix colonies and VBNC-like colonies were examined. Whole genome sequencing with pooling of the samples was used to identify conserved driver mutations. While VBNC-like isolates are genotypically identical to wild-type *P. aeruginosa*, phoenix colonies have a SNP in the PA4673 gene which is predicted to encode a GTP-binding protein similar to YchF in *S. pombe* (142, 143). This SNP leads to a modification of the protein structure in an external region of the gene and could possibly lead to a change in a binding site. GTP binding proteins, also known as G proteins, are molecular switches which hydrolyze GTP to GDP and are bound to the membrane to allow for downstream effects to be stimulated by extracellular stimuli (147). A modification in the ability of a G protein to bind to a substrate may have a major impact to downstream effectors within the pathway and may allow phoenix colonies to transiently tolerate the presence of high concentrations of antibiotic.

Transcriptionally, both phoenix colonies and VBNC-like colonies were found to cluster separately from the control lawn which had not been exposed to antibiotics, the edge of the ZOC, and the outer background lawn controls, while clustering well with each other. It is interesting that both the phoenix colonies and VBNC-like colonies are transcriptomically similar to each other despite appearing as two distinct phenotypes. It is possible that VBNC-like colonies could be a subset of phoenix colonies which lack the

ability to be cultured due to a dependence on a metabolite in the initial environment from either the original biofilm lawn or surrounding variant colonies. It is also interesting to note that no significant metabolic pathway changes were found in phoenix colonies or VBNC-like colonies which could account for the antibiotic tolerance exhibited by these phenotypes. This contrasts the typical tolerance phenotypes found in *P. aeruginosa* including persister cells, small colony variants, and adaptive resistance colonies, which enter a state of dormancy, have growth defects, or are otherwise metabolically driven (50, 52, 65, 67, 83, 85).

Upon further examination of the DEGs associated with phoenix colonies, two genes were found that when screened showed a lack of phoenix colony emergence, PA0394 which is predicted to encode for a PLP-binding protein and PA3626 which encodes for tRNA pseudouridine synthase D (TruD). PLP-binding proteins are important for both transamination of amino acids as well as transcriptional regulation (145, 146). Tobramycin, the antibiotic associated with the emergence of phoenix colonies (86), is an aminoglycoside. Aminoglycosides bind irreversibly to the 30S portion of the bacterial ribosome, leading to mismatching binding of tRNA to the mRNA due to a steric hindrance during translation (148). Antibiotic resistance to aminoglycosides can be conferred through modification of the ribosomal target site (20). Additionally, it has been shown that aminoglycosides also interact directly with tRNA and can lead to a loss of interaction between the T- and D- loops as well as unfolding of the D-stem (149, 150). TruD converts uracil-13 in the D-loop to pseudouridine which may influence the way that aminoglycosides are able to interact with the tRNA (151). Knockout of TruD by

transposon mutagenesis led to an elimination of phoenix colony emergence which was able to be rescued to wild-type levels by plasmid complementation. This finding is interesting as it leads us to believe that, in addition to the ribosome, tobramycin may also be interacting with tRNA leading to cell death. Phoenix colonies may then be modifying their tRNA with TruD to increase tRNA stability and allow for survival with exposure to tobramycin, although this is something that will need to be followed up on for confirmation.

Three additional genes from the phoenix colony DEG list lacked a transposon mutant to be screened: two hypothetical proteins (PA0103a and PA0526) and PA4272.1 which encodes for the sRNA P27. P27 has been found in a previous study to bind and directly inhibit *rhlI*. *rhlI* is important within the RhlR pathway of *Pseudomonas*, which control a large portion of quorum sensing associated genes (152). This association is significant in that changes in quorum sensing pathways have been directly linked to antimicrobial tolerance (153-155). Additionally, differential expression of P27 could lead to modification of numerous metabolic pathways within *P. aeruginosa* and may alter the way the bacteria interact with tobramycin.

Further research, including epigenetic exploration, is needed to come to a complete understanding of both the phoenix colonies and VBNC-like colonies. By understanding how these and other bacterial phenotypes are able to survive in the presence of antibiotics, we will be better prepared to control the rise of antibiotic tolerant and resistant infections.

3.6. Acknowledgements

This work was supported in part by the Ohio State University College of Medicine and R01 NIH- GM124436 (PS), R01AI148788 (MZA), and the American Heart Association grant AHA 20PRE35200201, M.J.D., 2020. We would like to thank the Genomics Shared Resource of the Ohio State University Comprehensive Cancer Center for performing the RNA sequencing. We would also like to thank Robert Fillinger for technical assistance with the RNAseq data analysis. Additionally, we would like to thank the lab of Dr. Daniel Wozniak for providing strains from their stocks of Dr. Colin Manoil's *P. aeruginosa* transposon library. Conflict of interest - None declared.

Chapter 4. Exploration of the Pharmacodynamics for *Pseudomonas aeruginosa* Biofilm Eradication by Tobramycin

Devin Sindeldecker, Shaurya Prakash, and Paul Stoodley

Data and figures represented in this chapter have been previously published:
Sindeldecker, D., Prakash, S., & Stoodley, P. (2021). Exploration of the Pharmacodynamics for *Pseudomonas aeruginosa* Biofilm Eradication by Tobramycin. *Antimicrobial agents and chemotherapy*.

4.1. Abstract

Pseudomonas aeruginosa is a Gram-negative, opportunistic pathogen which is involved in numerous infections. It is of growing concern within the field of antibiotic resistant and tolerance and often exhibits multi-drug resistance. Previous studies have shown the emergence of antibiotic resistant and tolerant variants within the zone of clearance of a biofilm lawn after exposure to aminoglycosides. As concerning as the tolerant variant emergence is, there was also a zone of killing (ZOK) immediately surrounding the antibiotic source from which no detectable bacteria emerged or were cultured. In this study, the ZOK was analyzed using both *in vitro* and *in silico* methods to determine if there was a consistent antibiotic concentration versus time constraint (area under the curve, (AUC)) which is able to completely kill all bacteria in the lawn biofilms

in our *in vitro* model. Our studies revealed that by achieving an average AUC of 4,372.5 μg*hr/mL, complete eradication of biofilms grown on both agar and hydroxyapatite was possible. These findings show that appropriate antibiotic concentrations and treatment duration may be able to treat antibiotic resistant and tolerant biofilm infections.

4.2. Introduction

Pseudomonas aeruginosa is a Gram-negative bacterium and opportunistic pathogen. Most commonly, it is associated with cystic fibrosis (CF) related lung infections but is also implicated in chronic wounds and post-surgical site infections (2, 3, 110). Antimicrobial tolerance and resistance are also major concerns with *P. aeruginosa*, as the formation of biofilms, variant populations, and multidrug resistance mechanisms are also prevalent (5-8, 86). A recent study on the antibiotic resistance rates of *P. aeruginosa* have shown a minimum 20% rate of resistance for carbapenems, cephalosporins, aminoglycosides, and piperacillin/tazobactam (156). In addition, multi-drug resistance was also found in 20% of infections (156).

In a previous study, variant colony phenotypes of *P. aeruginosa* emerging within the region cleared by a tobramycin-loaded calcium sulfate bead were identified (86). This region of bacterial lawn clearance is referred to as the zone of clearance (ZOC, Figure 4.1). These variant colonies included classical resistance, persister cells, viable but non-culturable like colonies (VBNC-like), and newly identified, tolerant, phoenix colonies (86). While the significance of these emergent phenotypes may be of concern from a clinical standpoint, it is important to note that there was also a smaller, consistent region within the ZOC, immediately adjacent to the antibiotic source, from which no variants

emerged or were cultured (86, 113). This previously reported zone, referred to as the zone of killing (ZOK), represents a region of complete biofilm killing including antibiotic tolerant and resistant variants (Figure 4.1, (86, 113)).

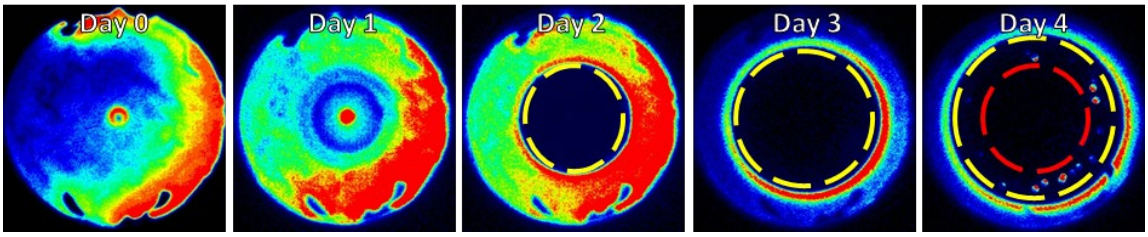

Figure 4.1 Emergence of ZOC and ZOK.

IVIS images of a representative *P. aeruginosa* Xen41 plate showing ZOC emergence after exposure to tobramycin. A biofilm lawn was grown for 24 hours before being exposed to tobramycin on Day 0. Over time, a ZOC (yellow dotted circle) can be seen as the antibiotic clears the background lawn. On Day 3, variant colonies begin to grow within the ZOC and a ZOK (red dotted circle) becomes apparent. The ZOK is the region in which there are no variant colonies or other discernable bacterial activity. In the images, red indicates high levels of metabolic activity, blue indicates low levels of metabolic activity, and black indicates no metabolic activity.

While pharmacodynamic studies have been done using planktonic *P. aeruginosa* exposed to antibiotics (157, 158), further research into the pharmacodynamics necessary to eliminate biofilms is needed. Currently, the primary method for measuring pharmacokinetics and pharmacodynamics (PK/PD) *in vitro* is the modified Calgary biofilm device method (159). This method is used to grow biofilms on pegs which are suspended in wells of a 96-well plate before exposing the biofilms to antibiotics (159). Use of this method can be complicated by contamination risks, variation in recovered biofilm after antibiotic exposure due to the rinsing steps necessary, and residual antibiotics left after rinses (159). In this study, the ZOK from which no bacteria could be cultured was further analyzed using a new method for exploring PK/PD *in vitro*. We hypothesized that the junction between the outer edge of the ZOK and the region containing the emergent variants represents an antibiotic concentration versus treatment time constraint in which complete bacterial biofilm eradication can be achieved. In order to evaluate our hypothesis, a combination of a biofilm plate *in vitro* model and an *in silico* approach was used to identify the concentration and time (AUC) necessary to eliminate a *P. aeruginosa* biofilm, including variants which can typically survive antibiotic therapy, using tobramycin. Additionally, substrates using both a tissue mimic (agar, (160, 161)) and a bone mimic (hydroxyapatite (HA), (162)) were used to determine if the biofilm substrate would affect the ability of an AUC to completely eradicate the biofilm.

4.3. Materials and Methods

Bacterial strains and culture conditions

The metabolically driven, bioluminescent strain *P. aeruginosa* Xen41 (Xenogen Corp., USA) was used for the imaging portion of this study. Additionally, *P. aeruginosa* PAO1 (15) which is both a standard lab strain and the parent strain for *P. aeruginosa* Xen41 was used in this study. Culture plates were prepared by from glycerol stock cultures stored at -80°C using Luria-Bertani (LB) agar plates. Streaked plates were incubated at 37°C for 24 hours to allow for individual colonies to grow. Individual colonies were examined for proper morphology and then isolated and transferred to 20 mL of LB broth. Broth cultures were incubated overnight in a shaking incubator set to 37°C and 200 rpm.

Generation of Biofilm Lawns

Overnight broth cultures of *P. aeruginosa* Xen41 were diluted to an OD_{600} of 0.1 in LB broth and 100 µL aliquots were spread onto plates containing 20 mL of sterile, LB agar. These plates were incubated at 37°C with 5% CO_2 for 24 hours to allow for biofilm lawns to generate. Lawn generation was confirmed both visually and by using *in vitro* imaging system (IVIS) imaging.

Bioluminescence Imaging

Bioluminescence imaging was completed using thirty second exposures in an IVIS system. A pseudo-color heatmap was overlaid to aid in visualization of the metabolic activity of the biofilms. The scale for the heatmap is as follows: red indicates

high levels of metabolic activity, blue indicates low levels of metabolic activity, and black indicates no metabolic activity.

Exposure of Biofilm Lawns to Antibiotic

After lawn generation, the biofilms were exposed to set masses of tobramycin (250 µg, 500 µg, 1000 µg, and 2000 µg). Briefly, a 100 mg/mL stock solution of tobramycin was created using tobramycin powder (TCI America, USA) and sterile water. This solution was then used to create dilutions for the other necessary masses of tobramycin. A sterile, filter paper disk was placed in the center of each of the lawn biofilms and then 20 µL of the appropriate tobramycin solution was placed on the disk to allow for exposure of the biofilm lawns to the desired masses of tobramycin. After antibiotic placement, the plates continued to be incubated at 37°C with 5% CO_2 for five additional days. IVIS images were taken and the zones of killing measured daily.

Time-kill Curve Generation

In order to measure the CFUs within the ZOK over time, time-kill curves were generated. Biofilm lawns were generated as above and were either exposed to 1 mg of tobramycin on a filter paper disk or not exposed for controls. At various time points, a 1 cm x 1 cm area of biofilm lawn, located between 1 and 2 cm from the disk, was scraped using a sterile loop and placed into 1 mL of sterile PBS. A dilution series was then made and plated. CFUs were counted for each sample and curves were generated.

Computational Modeling

In order to calculate the antibiotic concentration versus time necessary for development of the ZOK, an analytical solution was used to estimate the tobramycin concentration, *c(r, t)* for a 120 hour treatment time. The solution for the diffusion of antibiotic bead or disk in an agar plate is given by:

$$c(r,\ t) = \frac{m}{h_0}\frac{1}{4\pi D(t+t_o)}\exp\left(-\frac{r^2}{4D(t+t_o)}\right),$$

where the diffusion coefficient of tobramycin in agar is D and was experimentally determined to be 3.84×10^{-10} m^2/s, m is the mass of antibiotic added to the source, h_0 is the height of the agar, and r is the position coordinate relative to the center of a paper disk (118, 161, 163, 164). The model assumes that antibiotic source is finite with a radius, r_o = 3 mm. The model assumed that the inner *radius* of the petri dish, 70 mm (inner diameter is 140 mm), was >10 times the radius of the paper disks (3 mm) used, whereas the depth of agar layer was ~3.6 mm. After model generation, an area under the curve (AUC) value was calculated in MATLAB for each curve using the trapezoidal rule function, and the mean of the AUCs was also calculated.

Testing of AUC on Hydroxyapatite

In order to assess whether the AUC required for *P. aeruginosa* biofilm eradication could be translated to biofilms grown on alternative surfaces, biofilms of *P. aeruginosa* PAO1 were grown on 0.5 inch hydroxyapatite (HA) coupons (Biosurface Technologies, USA). Overnight LB broth cultures of *P. aeruginosa* PAO1 were prepared as above.

Overnight cultures were diluted to an OD_{600} of 0.1 in LB broth. HA coupons were added to the wells of a 12 well plate before 3 mL of the diluted overnight culture were also added to the wells. The well plate was incubated at 37°C with 5% CO_2 for 24 hours to allow biofilms to form on the HA coupons. Three coupons were then exposed to tobramycin, and three coupons were exposed to PBS only as a control. Briefly, the coupons were removed from the well plate and rinsed in PBS to remove any planktonic bacteria. The coupons were then placed in a fresh 12 well plate for exposure to tobramycin or PBS only. Three mL of a tobramycin solution was used for antibiotic exposure of the coupons for 24 hours at a concentration of 182 µg/mL in order to equal the mean AUC value of 4,368 µg*hr/mL. During the tobramycin exposure, the coupons continued to be incubated at 37°C with 5% CO_2. After 24 hours, coupons were removed from the well plate to obtain CFU counts. The coupons were rinsed in PBS before being placed into wells of a fresh 12 well plate containing 3 mL of PBS. This plate was then placed into a water bath sonicator and sonicated for 30 minutes. After sonication, the PBS was removed from each well and centrifuged in order to pellet the bacteria. The pellet was then resuspended in 200 µL of LB broth and a dilution series was created. The dilution series was plated on 20 mL of LB agar and CFU counts were obtained.

Testing of AUC on Plastic and Agar

In addition to AUC validation on HA coupons, the AUC was also validated on plastic pegs of an MBEC assay biofilm inoculator plate (Innovotech, Canada) as well as MBEC assay biofilm inoculator plate pegs coated in LB agar. Briefly, LB agar coated

pegs were prepared as follows. 200 µL of molten LB agar was placed into the wells of a 96 well plate. The MBEC plate, which had previously been cooled to -80°C, was then placed onto the 96 well plate to allow the pegs to dip into the molten LB agar. After 3 seconds, the plate was removed and the agar was allowed to finish cooling in a coating on the pegs. After LB agar coating, both LB agar coated pegs and uncoated pegs were exposed to *P. aeruginosa* PAO1 to allow biofilms to form. An overnight culture of PAO1 was diluted in LB broth at a ratio of 1:1000. 150 µL of the diluted culture was added to wells of 96 well plates. MBEC plates both coated in LB agar and uncoated were placed onto the 96 well plates with diluted culture. These plates were then incubated at 37°C with 110 rpm shaking for 24 hours to allow biofilms to develop. After incubation, the pegs were rinsed in 200 µL of PBS for 10 seconds. After rinsing, the MBEC plates were placed on 96 well plates containing either 200 µL of 182 µg/mL tobramycin or 200 µL of PBS as a control. These plates were then incubated for an additional 24 hours at 37°C with 110 rpm shaking. After incubation, the MBEC plates were rinsed in wells containing 200 µL PBS and then placed on a fresh 96 well plate with wells containing 200 µL PBS. These plates were then sonicated in a water bath sonicator for 30 minutes. After sonication, the bacteria containing PBS was removed and plated in a dilution series. CFU counts were obtained for each sample.

Statistical analysis

All experiments were replicated in triplicate. ANOVA analysis was completed by GraphPad Prism (v8.2.1) with a p-value of 0.05 being considered significant.

4.4. Results

Zones of Clearance of Biofilms Exhibit Dose-dependency

In order to begin assessing the possible correlation between the ZOK and an antibiotic concentration versus time constraint, twenty-four hour biofilm lawns of *P. aeruginosa* Xen41 were generated as reported previously (86, 160) before being exposed to various weight quantities of tobramycin (Figure 4.2). *In vitro* Imaging System (IVIS) evaluation of the biofilm lawns post tobramycin exposure showed the emergence of dose-dependent ZOCs which continued to expand over time. Within the ZOC, variant colonies began to emerge and encroach on the ZOC which had formed. However, there was also a dose-dependent ZOK within the ZOC from which no discernable bacterial activity was detected (Figure 4.2). It should also be noted that the luminescence which appears to overly the antibiotic disks is likely due to surface associated biofilm growth. The presence of the disk likely provides an additional substrate for biofilm growth and allows for initial levels of high bioluminescence before the tobramycin ultimately is able to clear the formed biofilm.

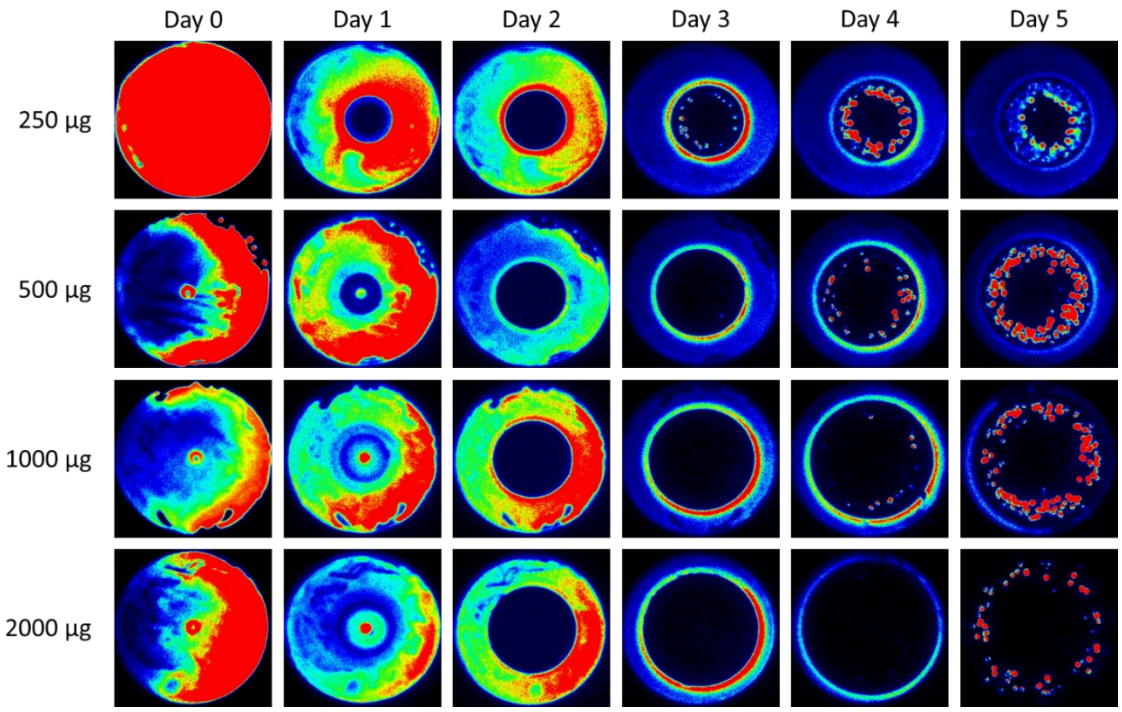

Figure 4.2 IVIS imaging of *P. aeruginosa* biofilms exposed to tobramycin.

Biofilm lawns of *P. aeruginosa* Xen41 were generated on agar before being exposed to various amounts of tobramycin for a total of five days. Zones of clearance (ZOC) can be seen growing over time for each mass of tobramycin. Although variant colonies emerge from the ZOC, there is a distinct region immediately adjacent to the antibiotic source from which nothing grows, marked explicitly in Figure 4.1, known as the zone of killing (ZOK). In the images, red indicates high levels of metabolic activity, blue indicates low levels of metabolic activity, and black indicates no metabolic activity.

Profiling of the ZOC/ZOK Confirms Dose-dependency

After exposure of the biofilm lawns to tobramycin, the plates were further analyzed to obtain measurements of the ZOK over time. These measurements were used to generate plots (Figure 4.3) which show the linear generation of the ZOC, followed by a ZOC peak right before variant colonies began to emerge. The peak of the plot for each weight quantity of tobramycin shifts to a later time point as the weight quantity increases. This is likely due to the time necessary for the antibiotic to diffuse to low enough concentrations to allow variant colonies to begin to emerge. As variant colonies began to emerge and grow within the ZOC, this allows the ZOK to be visualized. The plots then plateaued as the ZOK became more apparent in which no detectable bacteria emerged or grew. Once the ZOK stabilized, the radius of the edge of the ZOK was noted, as this is the point likely to represent the minimum antibiotic concentration away from the antibiotic source versus time constraint necessary for complete biofilm eradication including the killing of any antibiotic tolerant or resistant variants. These radii values and time points were then used to generate antibiotic diffusion plots using numerical modeling. In addition, a time-kill curve was generated for the ZOK of a 1 mg tobramycin loaded disk. At 40 hours post tobramycin exposure, a slight decrease in CFUs/cm^2 can be seen which further decreases and becomes significant ($p=0.017$) by 48 hours. At 72 hours of tobramycin exposure and thereafter, no CFUs are able to be recovered from within the ZOK (Figure 4.4).

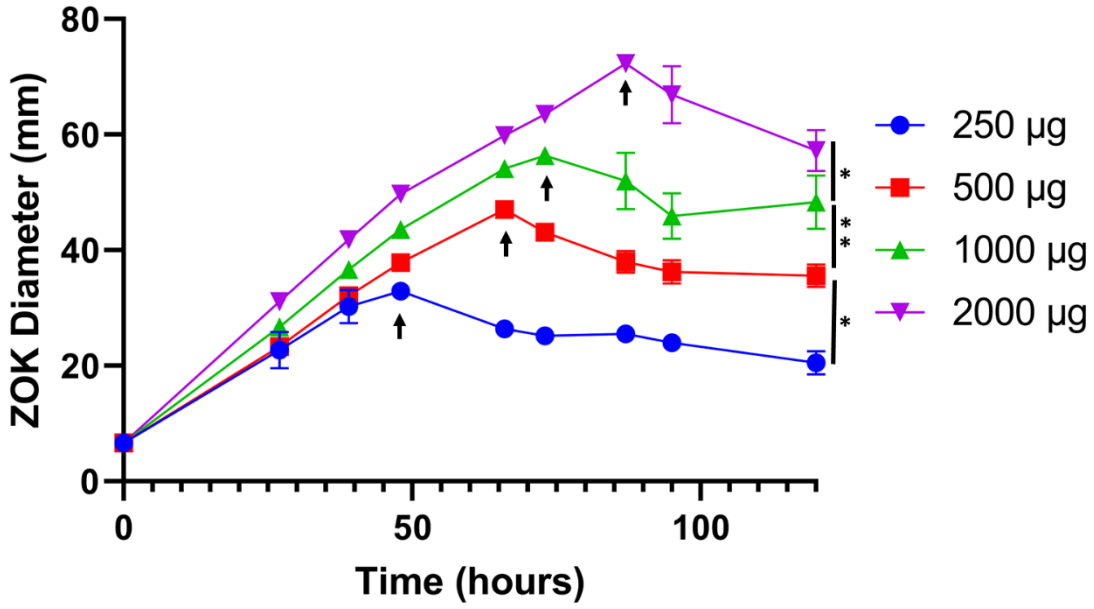

Figure 4.3 ZOK expansion curves for tobramycin.

The ZOK of the plates from Figure 4.2 were measured over time. The zones follow linearly until the peak (indicated by black arrows), which occurs as variant colonies begin to emerge within the ZOC, and the diameter of the ZOK becomes evident. As these variant colonies continue to emerge and begin to grow, the ZOK reduces. After the peak, the ZOK continues to become more apparent as the area lacking emergence of variant colonies. The ZOK decrease continues as variant colonies emerge until the plot begins to plateau, at which point the ZOK was stable. Data are reported as mean ± SD (n=3). *p<0.05, **p<0.01.

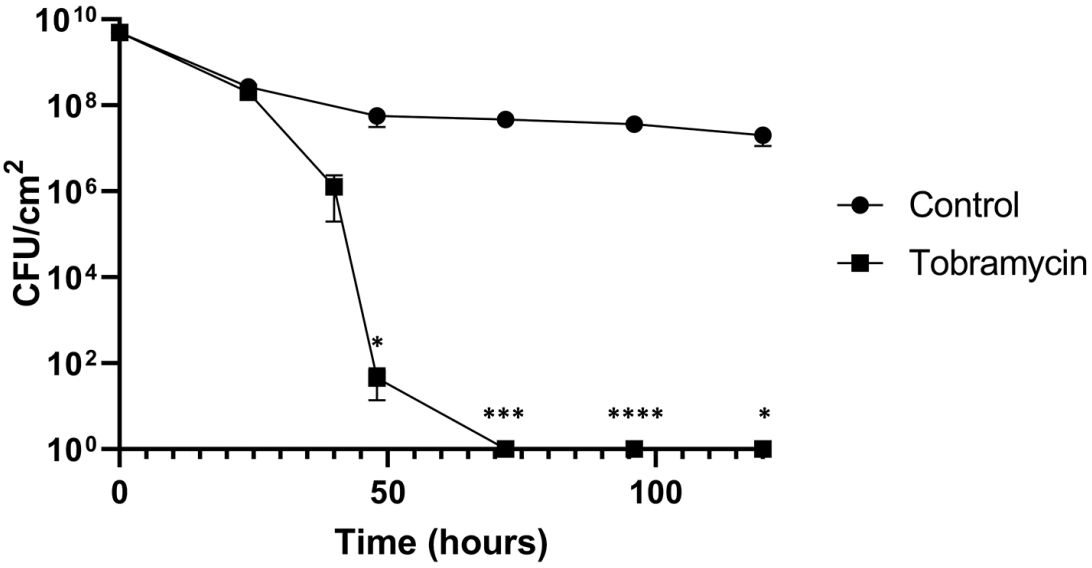

Figure 4.4 Time-kill curve for the ZOK.

CFUs within the ZOK of 1 mg of tobramycin were measured over time. Controls CFUs were measured for plates without tobramycin exposure. At 48 hours post tobramycin exposure, a decrease in CFUs begins to be seen, and by 72 hours post tobramycin exposure, no CFUs were able to be recovered from within the ZOK. Data are reported as mean±SD. *$p<0.05$, ***$p<0.001$, ****$p<0.0001$, n=3.

Computational Modeling Identified an Area Under the Curve Value for Biofilm Eradication

Using the data collected from the profiling of the ZOC and ZOK, a model was used (163) to predict the tobramycin concentration over time at the ZOK radius identified for each mass of tobramycin used (Figure 4.5). The model calculates the concentration of tobramycin over time assuming Fickian diffusion in a finite space (118, 163). The plots in Figure 3 show a dose-dependent increase in the antibiotic concentration after antibiotic placement until concentrations for each weight quantity of antibiotic peaked (120.9, 241.9, 483.8, and 967.5 μg/mL, respectively). The concentration then gradually begins to decrease and plateau as the system continues to approach equilibrium (12.5, 25, 50, 100 mg/mL, respectively) for each weight quantity (250, 500, 1000, 2000 μg, respectively). An AUC (μg*hr/mL) was calculated for each plot to determine the necessary minimum value necessary for ZOK generation for each of the amounts of tobramycin (Table 4.1). Interestingly, despite a 4-fold change in the starting tobramycin weight quantity, the AUCs for each were relatively similar. This observation highlights the importance of an AUC being taken into consideration during antibiotic dosing as opposed to purely relying on the antibiotic concentration alone. The mean of the AUC values was also calculated to determine that the average minimum value necessary for biofilm eradication, including antibiotic tolerant and resistant variants, was approximately 4,372.5 μg*hr/mL. The concentration of antibiotic needed here is much higher than standard minimum inhibitory concentrations (MIC) for tobramycin and *P. aeruginosa* PAO1 (4 μg/mL). Additionally, by dividing the AUC by the MIC, an AUC/MIC ratio of 46 can be calculated when

normalizing for 24 hours. This higher concentration ratio is likely responsible for the ability to kill even antibiotic resistant and tolerant variants.

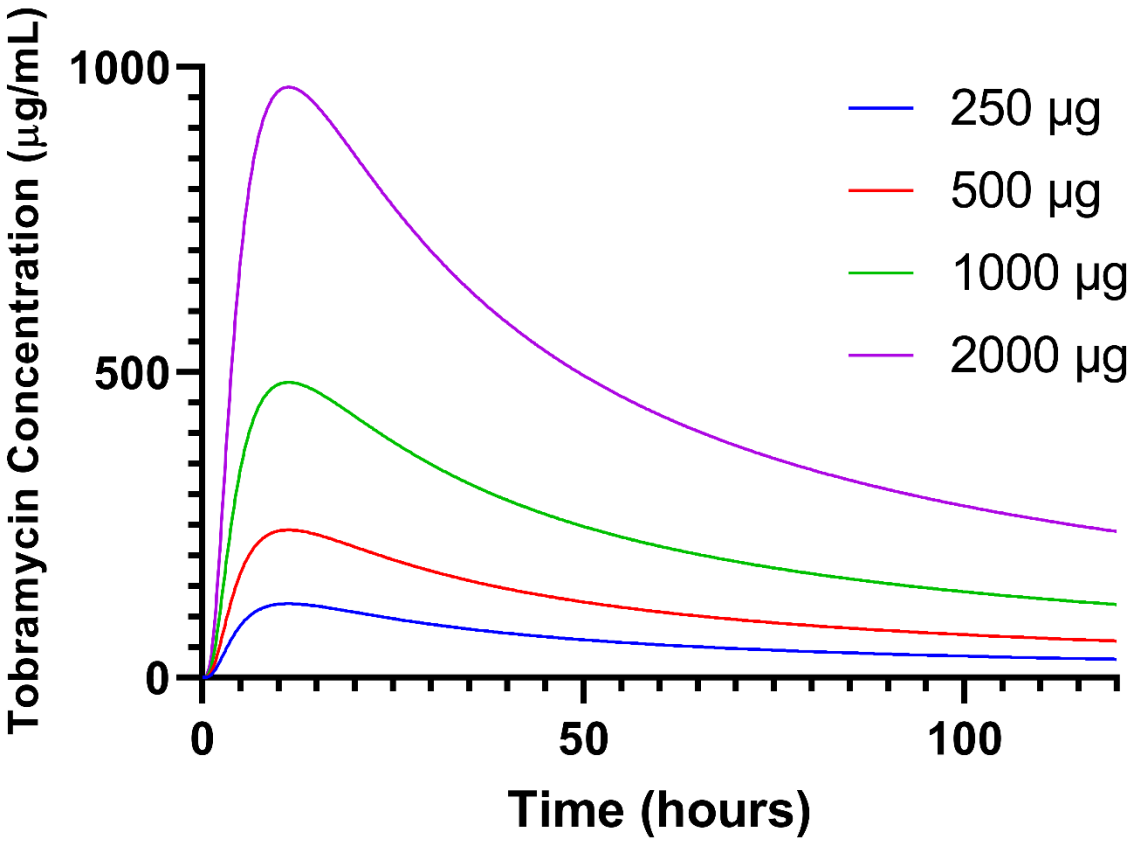

Figure 4.5 Computational modeling of antibiotic diffusion.

The diffusion model shows the spread of tobramycin over time. The radii used to determine the zones of killing for each antibiotic quantity was experimentally measured (Figure 4.2) and used as an input to the model for the computation of the concentration. All plots show an increase in tobramycin concentration followed by a decrease following the Fickian diffusion model.

Table 4.1 AUC values associated with complete biofilm eradication.

Values for the AUC (µg*hr/mL) for each mass of tobramycin were calculated from the plots of Figure 4.3. The mean of each of these values was also calculated and likely represents the minimum AUC necessary for complete eradication of biofilms, including antibiotic resistant and tolerant variants.

	250 µg	500 µg	1000 µg	2000 µg	Average
AUC	3560 µg*hr/mL	4730 µg*hr/mL	4330 µg*hr/mL	4870 µg*hr/mL	4372.5 µg*hr/mL

Identified AUC Can Eradicate Biofilms Grown on an Alternate Substrate

In order to test the AUC value associated with complete *P. aeruginosa* biofilm eradication by tobramycin, biofilms were grown on LB agar coated pegs, as well as HA coupons and plastic pegs as alternate biofilm substrates. Biofilm colony forming units (CFUs) were measured for biofilms exposed to tobramycin at the approximate 4,372.5 µg*hr/mL AUC. LB agar coated peg, HA coupon, and plastic peg biofilms were exposed to tobramycin for 24 hours at a stable concentration of 182 µg/mL (Figure 4.6) which equals an approximate AUC value of 4372.5 µg*hr/mL. In all tobramycin exposure samples, no CFUs were recovered, indicating a complete eradication of the biofilms. Additionally, a control was run at a 0.1 AUC equivalent on agar grown biofilms. The control samples showed full lawns of growth after tobramycin treatment, indicating minimal effectiveness of biofilm clearance. These results confirm that by obtaining a

high concentration of antibiotics for at least 24 hours, complete eradication of a *P. aeruginosa* lawn biofilm including any antibiotic resistant or tolerant variants was possible and, substrate differences were not relevant.

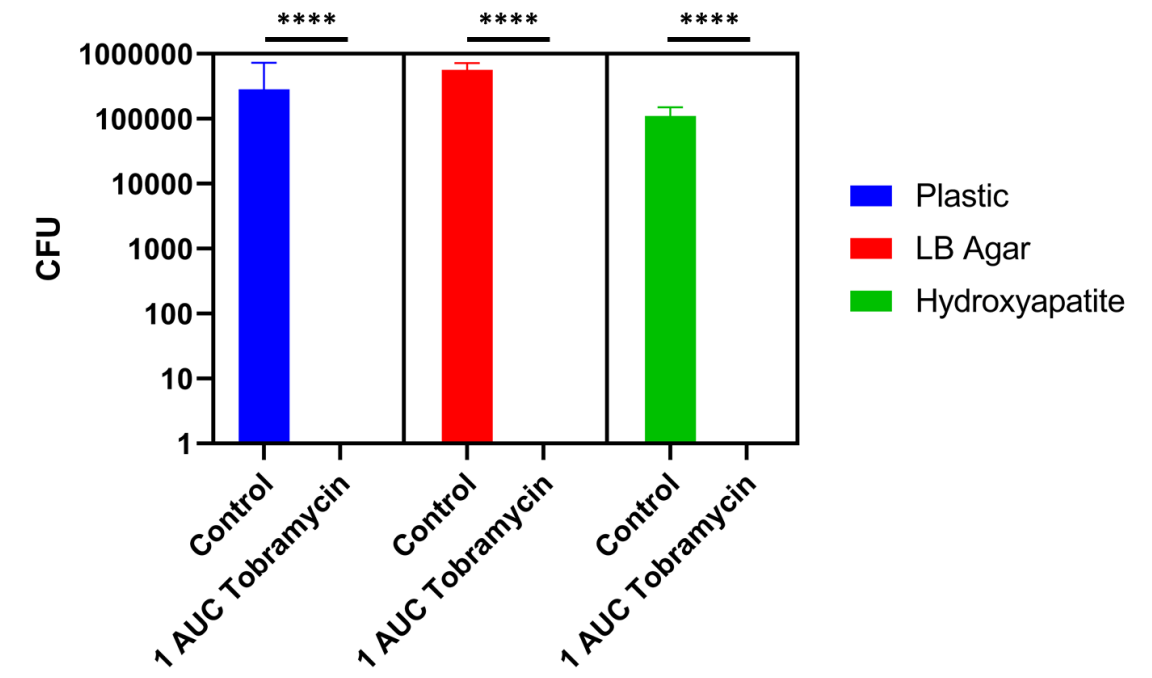

Figure 4.6 Eradication of *P. aeruginosa* biofilms grown on plastic, LB agar, and hydroxyapatite.

P. aeruginosa PAO1 biofilms grown on plastic pegs, LB agar coated pegs, and hydroxyapatite coupons were exposed to 182 µg/mL of tobramycin for 24 hours, equaling an AUC value of approximately 4372.5 µg*hr/mL. Complete biofilm eradication was seen in all of the tobramycin treated samples. ****$p<0.0001$, n=3.

4.5. Discussion

P. aeruginosa is an opportunistic, bacterial pathogen which has been associated with numerous infection sites. It has also been shown to readily develop tolerance and resistance to multiple antibacterial drugs leading to an increased concern for complicated and difficult to treat infections (4, 107, 108). Previously, the antibiotic tolerant phoenix and the VBNC-like phenotypes were identified, in addition to classically resistant colonies and persister cells, within the ZOC of produced by antibiotics released from tobramycin loaded Kirby-Bauer filter disks and $CaSO_4$ beads (86). While the emergence of these variant colonies is concerning, it was also shown that there was a consistent ZOK immediately adjacent to the antibiotic source from which no bacteria emerged or were cultured. Replica plating was also performed on these plates and showed no growth within the ZOK, indicating that this region is sterile (86). In these studies, both the ZOC and ZOK were measured since it is not possible to differentiate between the two zones at early time points before variant colonies begin to emerge. The distinct ZOK within the ZOC indicates a smaller region where we may be able to eliminate antibiotic resistance and tolerance with high enough concentrations of antibiotics over extended time frames. By understanding how antibiotic kinetics effect biofilms and antibiotic resistant and tolerant variants, we will be better prepared to control and prevent the rise of these dangerous biofilm infections.

In this study, the ZOK of *P. aeruginosa* biofilms was analyzed to determine the antibiotic pharmacodynamics necessary for its generation. For our study, a combination of a biofilm plate model and numerical modeling was used as a simpler alternative to the

modified Calgary biofilm plate model (159). The methods presented here could be adapted for further *in vitro* biofilm PK/PD studies including the use of other bacterial species and antibiotics. Previous studies have shown the importance of not only the concentration of antibiotic used but also the exposure time of the biofilm-growing bacteria to the antibiotic. These studies on the antibiotic AUC have shown that as exposure time increases, the minimum concentration needed for biofilm eradication (MBEC) decreases (165). In addition, pharmacodynamic studies on the efficacy of antibiotics against bacteria have shown an importance in the ratio of AUC/MIC (166, 167). The AUC/MIC ratio necessary for bactericidal activity against *P. aeruginosa* by tobramycin has been shown to be approximately 42. For our studies, various weight quantities of tobramycin were used which allowed for a more complete understanding of these required pharmacodynamics. While the varying masses of antibiotic used showed large, dose-dependent variations in the ZOK diameters, it was interesting that the AUCs calculated for each mass did not scale similar to the weight of the antibiotic, ranging from 3560-4870 μg*hr/mL, although there was a nearly 8-fold increase in antibiotic dosing (250-2000 μg). At an approximate AUC of 4372.5 μg*hr/mL and an MIC of 4 μg/mL, the AUC/MIC ratio for biofilm eradication by tobramycin would be approximately 46 when normalized for a 24-hour timeframe. Previous studies on local tobramycin concentrations achieved when treating orthopedic infections with tobramycin loaded methylmethacrylate bone cement has shown that the concentrations peak at approximately 40 μg/mL around 1 hour after beginning exposure. The concentration then drops to approximately 20 μg/mL through 24 hours (168). These lower concentrations

may explain the prevalence of post-surgical infection treatment failure, as antibiotic tolerant or resistant variants may be able to survive. In addition, while C_{max}/MIC is the metric typically used in relation to tobramycin (166), it has been shown that by using AUC/MIC, better clinical outcomes are able to be achieved (167). This may be especially true when treating biofilm infections as biofilms are inherently more tolerant of antibiotics due to slow diffusion of the antibiotic into the biofilm matrix as well as heterogeneity in the biofilm metabolism (106), increasing the importance of time-dependence. Our observations suggest that a minimum AUC representing the total treatment effect (concentration x time) may be used to facilitate the complete eradication of *P. aeruginosa* biofilms, including variants that without this treatment could re-seed infection (121). It is also important to note that although VBNC-like colonies may be present in our systems, they would not be apparent as they are unable to be cultured by nature. However, this characteristic also would likely prevent re-emergence in a clinical environment.

In addition to using different weight quantities of tobramycin, different substrates were also used to provide breadth to the relevance of the identified 4,372.5 µg*hr/mL necessary for biofilm eradication. It is possible that biofilms grown on different substrates could have differing phenotypes, including variations in metabolic pathways which may play a role in the efficacy of antibiotics (94, 169). Although biofilm phenotypic variations can occur, the identified AUC was able to eradicate biofilms grown on both a tissue mimic such as agar (160, 161) and a material commonly known to be important for bone infections (HA, (162)), indicating that the use of the AUC metric for

biofilm treatment is independent of the substrate rigidity and providing relevance to other fields such as dentistry and orthopedics. The observation evaluating the clearance of biofilms from two distinct substrates is important clinically as biofilms are able to grow in the human body on soft tissues such as lung tissue or skin and on hard substrates such as bone or implanted devices (109, 162, 170). Clearly, optimizing the AUC as a treatment effect metric needs further work, but the values reported here provide a specific evaluation for tobramycin and *P. aeruginosa*. Therefore, further research, including studies involving other antibiotic classes and bacterial species, is needed for a more complete understanding of the ability to eradicate bacterial biofilm infections.

4.6. Acknowledgements

This work was supported in part by the Ohio State University College of Medicine and R01 NIH- GM124436 (PS). We also acknowledge partial support from the National Heart, Lung, and Blood Institute (R01HL141941: SP). Conflict of interest - None declared.

Chapter 5. Discussion

Pseudomonas aeruginosa is an opportunistic pathogen commonly acquired in the hospital setting and is able to cause infections in numerous human-associated environments including the lungs of CF patients, wounds, and post-surgical sites (2, 3, 171). It has also been shown to rapidly develop tolerance and resistance to antimicrobial agents (4, 107, 108). In addition to its many antibiotic survival mechanisms and multidrug resistance, it is also able to form biofilms which not only increase antimicrobial tolerance but also provide high density populations which increase the chances of antibiotic resistance and tolerance phenotypes to develop (5, 7, 9, 10, 119, 120).

Antibiotic impregnated beads, cements, and bone fillers are routinely used during orthopedic revision surgeries to provide local therapy at high antibiotic concentrations (111). While these methods may effectively kill the majority of planktonic or biofilm bacteria, the antibiotic gradients which they produce may lead to the emergence of antibiotic resistant or tolerant variants, potentially resulting in complicated and difficult to treat infections (121). While these variants may develop, it has also been shown that by spacing the antibiotic sources appropriately, proper coverage can be attained which may prevent antibiotic resistant or tolerant variants from emerging (113).

In Chapter 2, variant colonies emerging within the ZOC of tobramycin were isolated. In addition to the well documented antibiotic resistant colonies of *P. aeruginosa* which can occur by a number of mechanisms (6, 13, 16, 29, 122, 123), two new variant colony phenotypes of *P. aeruginosa* were also identified: phoenix colonies and VBNCs. While the VBNCs were difficult to characterize further since it is not possible to culture them, the characterization of the phoenix colony phenotype was feasible. Phoenix colonies exist as a small population within the biofilm lawn and are unable to out compete the background lawn bacteria, thus they only emerge once the background lawn has been cleared away. The phoenix colonies are able to maintain high levels of metabolic activity and growth despite high concentrations of tobramycin in the local environment but are able to revert to a wild-type level of susceptibility once removed from the antibiotic laden environment (Figure 2.11). While previous studies in *P. aeruginosa* have shown that adaptive resistance is regulated by a transient upregulation of efflux pumps with a return to wild-type levels of antibiotic susceptibility when the antibiotic pressure is removed (48), it is likely that phoenix colonies fall into the category of adaptive resistance but utilize a different mechanism as indicated by phoenix colony emergence in the presence of a broad spectrum efflux pump inhibitor. A previous study showed that an anaerobic environment can induce an alternate metabolism which could lead to antibiotic tolerance in *P. aeruginosa* (83). Due to the presence of anaerobic and microaerobic environments contained in the deeper layers of a biofilm, it is possible that phoenix colonies could develop in an oxygen deficient portion of the biofilm lawn and then enter an alternate metabolic state, conferring the antibiotic tolerance which the

phoenix colony phenotype exhibits. Once isolated from the environment and cultured, it is likely that the phoenix colonies would return to a wild-type metabolism which could explain the change in antibiotic susceptibility as well.

The studies in Chapter 2 also provided some possible clues as to the mechanism behind their development. Due to the transient, non-heritable nature of phoenix colony antibiotic tolerance, the mechanism behind their emergence is likely due to epigenetics at either the transcriptional or translational level. When emerging within the ZOC, phoenix colonies exhibit a non-heritable alteration in pigmentation from yellow-green to white. The loss of pigmentation indicates a lack of pyocyanin production, which is regulated by RhlR, a major transcription factor in *P. aeruginosa* (172). Additionally, aminoglycoside antibiotics were the only antibiotic class tested which show emergence of the phoenix colony phenotype (Figure 2.1, Figures 2.2, Figure 2.3), indicating that the ribosome may play a significant role in phoenix colony development. However, in Chapter 3, upon completion of RNAseq, there was no significant difference in transcripts for pyocyanin, other genes downstream of RhlR, or major ribosomal genes. It is possible that these genes could be regulated post-transcriptionally, and evidence of this possibility can be found in the DEGs which did not have a transposon mutant which could be screened. PA4272.1 encodes the sRNA P27, which binds and directly inhibit *rhlI*, an important enzyme in the RhlR signaling pathway of *P. aeruginosa* (152). P27 may also regulate other cellular pathways which have yet to be identified, but this is purely speculative. Although there were not any major ribosome related genes differentially expressed, PA3626, which encodes for tRNA pseudouridine synthase D (TruD), was significantly upregulated.

Additionally, when TruD was knocked out there was a complete loss of phoenix colony emergence which was rescued to wild-type levels by complementation. Previous studies have shown interaction between aminoglycosides and tRNA which leads to a loss of interaction between the T- and D- loops as well as unfolding of the D-stem (149, 150). TruD is able to convert uracil-13 located within the D-loop to pseudouridine (151). This change may stabilize the tRNA and influence the interaction between aminoglycosides and the tRNA. Our findings lead us to believe that, in addition to the ribosome binding by aminoglycosides, tobramycin may also be interacting with tRNA leading to cell death. Phoenix colonies may modify tRNA with TruD to increase tRNA stability and allow for survival of exposure to aminoglycosides. Additionally, it is possible that TruD may be able to convert other uridines to pseudouridine in *P. aeruginosa* leading to modification of other tRNA sites or the rRNA. As aminoglycosides bind to the ribosome, modification of the rRNA may provide another avenue for the antibiotic tolerance exhibited by phoenix colonies. Although complementation of truD was able to be achieved, there where difficulties in production of a PA0394 complementation strain and thus further work is needed to follow up on the possibility of this gene being involved in phoenix colony emergence.

In addition to the DEGs, it is interesting that both the phoenix colonies and VBNC-like colonies are transcriptionally similar despite appearing as two distinct phenotypes. It is possible that VBNC-like colonies may be a subset of phoenix colonies which are unable to be cultured due to a dependence on a metabolite in the initial environment, either from the background lawn or the surrounding variant colonies.

Further research, including metabolic and epigenetic studies, is needed to enhance our understanding of the mechanisms behind the emergence of both the phoenix colonies and VBNC-like colonies.

Although phoenix colonies, VBNC-like colonies, resistant mutants, and persister cells could emerge in an infection, it is promising to note that high concentrations of tobramycin in our studies, found immediately adjacent to the tobramycin sources, were able to eradicate all variant colonies. This is supported not only by the lack of colony emergence within the ZOC but also by the lack of growth on replica plates and swabs taken directly from the ZOK. The ZOK provides evidence that it is possible to eliminate antibiotic resistance and tolerance assuming that there are high enough concentrations of antibiotic present over an appropriate time frame. This metric, known as the AUC, was measured in the studies found in Chapter 4. Here, the pharmacodynamics of the ZOK were measured and calculated. It is interesting to note that although the variation in starting mass of tobramycin was as large as 8-fold, the AUCs were all similar to each other. This strengthens the idea that an AUC is an important metric when determining dosing regimens for treatment of bacteria with an antibiotic. In addition to the different mass quantities of tobramycin, the use of differing substrates allows the calculated AUC to be more broadly applicable. Although biofilm phenotypic variations can occur, the identified AUC was successfully able to kill all detectable bacteria on agar, plastic, and HA, making the findings relevant to a wide variety of microbial research areas.

In conclusion, our work here has identified another phenotype which *P. aeruginosa* may use to evade killing by antibiotics. These studies have also improved our

understand of the pharmacodynamics necessary to prevent antibiotic resistant and tolerant variant colony emergence. These findings not only have important implications for the field of *P. aeruginosa* biofilm infections and aminoglycosides but also provide support for continued research using other bacterial species and antibiotic classes. As this work is built upon, we will be better informed and better prepared to deal with the ever-rising concerns of antibiotic resistance and antibiotic tolerance.

Bibliography

1. Malhotra S, Hayes D, Jr., Wozniak DJ. 2019. Cystic Fibrosis and Pseudomonas aeruginosa: the Host-Microbe Interface. Clin Microbiol Rev 32.
2. Shah NB, Osmon DR, Steckelberg JM, Sierra RJ, Walker RC, Tande AJ, Berbari EF. 2016. Pseudomonas Prosthetic Joint Infections: A Review of 102 Episodes. J Bone Jt Infect 1:25-30.
3. Serra R, Grande R, Butrico L, Rossi A, Settimio UF, Caroleo B, Amato B, Gallelli L, de Franciscis S. 2015. Chronic wound infections: the role of Pseudomonas aeruginosa and Staphylococcus aureus. Expert Rev Anti Infect Ther 13:605-13.
4. Ciofu O, Tolker-Nielsen T. 2019. Tolerance and Resistance of Pseudomonas aeruginosa Biofilms to Antimicrobial Agents-How P. aeruginosa Can Escape Antibiotics. Front Microbiol 10:913.
5. Lewis K. 2008. Multidrug tolerance of biofilms and persister cells. Curr Top Microbiol Immunol 322:107-31.
6. Zavascki AP, Carvalhaes CG, Picao RC, Gales AC. 2010. Multidrug-resistant Pseudomonas aeruginosa and Acinetobacter baumannii: resistance mechanisms and implications for therapy. Expert Rev Anti Infect Ther 8:71-93.
7. Hall-Stoodley L, Stoodley P. 2005. Biofilm formation and dispersal and the transmission of human pathogens. Trends Microbiol 13:7-10.
8. Lewis K. 2010. Persister cells. Annu Rev Microbiol 64:357-72.
9. Cross AS, Opal S, Kopecko DJ. 1983. Progressive increase in antibiotic resistance of gram-negative bacterial isolates. Walter Reed Hospital, 1976 to 1980: specific analysis of gentamicin, tobramycin, and amikacin resistance. Arch Intern Med 143:2075-80.
10. Blahova J, Kralikova K, Krcmery V, Sr., Schafer V. 2001. Sudden increase in Pseudomonas aeruginosa nosocomial strains with broad host range transfer of antibiotic resistance. J Chemother 13:607-10.
11. Zignol M, Hosseini MS, Wright A, Weezenbeek CL, Nunn P, Watt CJ, Williams BG, Dye C. 2006. Global incidence of multidrug-resistant tuberculosis. J Infect Dis 194:479-85.
12. Keen EF, 3rd, Robinson BJ, Hospenthal DR, Aldous WK, Wolf SE, Chung KK, Murray CK. 2010. Prevalence of multidrug-resistant organisms recovered at a military burn center. Burns 36:819-25.
13. Tam VH, Chang KT, Abdelraouf K, Brioso CG, Ameka M, McCaskey LA, Weston JS, Caeiro JP, Garey KW. 2010. Prevalence, resistance mechanisms, and susceptibility of multidrug-resistant bloodstream isolates of Pseudomonas aeruginosa. Antimicrob Agents Chemother 54:1160-4.
14. Oliver A, Canton R, Campo P, Baquero F, Blazquez J. 2000. High frequency of hypermutable Pseudomonas aeruginosa in cystic fibrosis lung infection. Science 288:1251-4.

15. Gilleland LB, Gilleland HE, Gibson JA, Champlin FR. 1989. Adaptive resistance to aminoglycoside antibiotics in Pseudomonas aeruginosa. J Med Microbiol 29:41-50.
16. Poole K. 2005. Aminoglycoside resistance in Pseudomonas aeruginosa. Antimicrob Agents Chemother 49:479-87.
17. Prickett MH, Hauser AR, McColley SA, Cullina J, Potter E, Powers C, Jain M. 2017. Aminoglycoside resistance of Pseudomonas aeruginosa in cystic fibrosis results from convergent evolution in the mexZ gene. Thorax 72:40-47.
18. Levin-Reisman I, Ronin I, Gefen O, Braniss I, Shoresh N, Balaban NQ. 2017. Antibiotic tolerance facilitates the evolution of resistance. Science 355:826-830.
19. Jalal S, Ciofu O, Hoiby N, Gotoh N, Wretlind B. 2000. Molecular mechanisms of fluoroquinolone resistance in Pseudomonas aeruginosa isolates from cystic fibrosis patients. Antimicrob Agents Chemother 44:710-2.
20. Bryan LE, Haraphongse R, Van den Elzen HM. 1976. Gentamicin resistance in clinical-isolates of Pseudomonas aeruginosa associated with diminished gentamicin accumulation and no detectable enzymatic modification. J Antibiot (Tokyo) 29:743-53.
21. Doi O, Ogura M, Tanaka N, Umezawa H. 1968. Inactivation of kanamycin, neomycin, and streptomycin by enzymes obtained in cells of Pseudomonas aeruginoa. Appl Microbiol 16:1276-81.
22. Brzezinska M, Benveniste R, Davies J, Daniels PJ, Weinstein J. 1972. Gentamicin resistance in strains of Pseudomonas aeruginosa mediated by enzymatic N-acetylation of the deoxystreptamine moiety. Biochemistry 11:761-5.
23. Kobayashi F, Yamaguchi M, Mitsuhashi S. 1971. Inactivation of dihydrostreptomycin by Pseudomonas aeruginosa. Jpn J Microbiol 15:381-2.
24. Seupt A, Schniederjans M, Tomasch J, Haussler S. 2020. Expression of the MexXY Aminoglycoside Efflux Pump and Presence of an Aminoglycoside-Modifying Enzyme in Clinical Pseudomonas aeruginosa Isolates Are Highly Correlated. Antimicrob Agents Chemother 65.
25. Kashfi MH, A.; Eslami, G.; Sadredin Amin, M.; Tarashi, S.; Taki, E. 2017. The prevalence of aminoglycoside-modifying enzyme genes among Pseudomonas aeruginosa strains isolated from burn patients. Arch Clin Infect Dis 12.
26. Rodriguez Esparragon F, Gonzalez Martin M, Gonzalez Lama Z, Sabatelli FJ, Tejedor Junco MT. 2000. Aminoglycoside resistance mechanisms in clinical isolates of Pseudomonas aeruginosa from the Canary Islands. Zentralbl Bakteriol 289:817-26.
27. Thirumalmuthu K, Devarajan B, Prajna L, Mohankumar V. 2019. Mechanisms of Fluoroquinolone and Aminoglycoside Resistance in Keratitis-Associated Pseudomonas aeruginosa. Microb Drug Resist 25:813-823.
28. Pan X, Dong Y, Fan Z, Liu C, Xia B, Shi J, Bai F, Jin Y, Cheng Z, Jin S, Wu W. 2017. In vivo Host Environment Alters Pseudomonas aeruginosa Susceptibility to Aminoglycoside Antibiotics. Front Cell Infect Microbiol 7:83.

29. Terzi HA, Kulah C, Ciftci IH. 2014. The effects of active efflux pumps on antibiotic resistance in Pseudomonas aeruginosa. World J Microbiol Biotechnol 30:2681-7.
30. Rampioni G, Pillai CR, Longo F, Bondi R, Baldelli V, Messina M, Imperi F, Visca P, Leoni L. 2017. Effect of efflux pump inhibition on Pseudomonas aeruginosa transcriptome and virulence. Sci Rep 7:11392.
31. Horna G, Lopez M, Guerra H, Saenz Y, Ruiz J. 2018. Interplay between MexAB-OprM and MexEF-OprN in clinical isolates of Pseudomonas aeruginosa. Sci Rep 8:16463.
32. Laborda P, Alcalde-Rico M, Blanco P, Martinez JL, Hernando-Amado S. 2019. Novel Inducers of the Expression of Multidrug Efflux Pumps That Trigger Pseudomonas aeruginosa Transient Antibiotic Resistance. Antimicrob Agents Chemother 63.
33. Halfon Y, Jimenez-Fernandez A, La Rosa R, Espinosa Portero R, Krogh Johansen H, Matzov D, Eyal Z, Bashan A, Zimmerman E, Belousoff M, Molin S, Yonath A. 2019. Structure of Pseudomonas aeruginosa ribosomes from an aminoglycoside-resistant clinical isolate. Proc Natl Acad Sci U S A 116:22275-22281.
34. Sanz-Garcia F, Alvarez-Ortega C, Olivares-Pacheco J, Blanco P, Martinez JL, Hernando-Amado S. 2019. Analysis of the Pseudomonas aeruginosa Aminoglycoside Differential Resistomes Allows Defining Genes Simultaneously Involved in Intrinsic Antibiotic Resistance and Virulence. Antimicrob Agents Chemother 63.
35. Freschi L, Vincent AT, Jeukens J, Emond-Rheault JG, Kukavica-Ibrulj I, Dupont MJ, Charette SJ, Boyle B, Levesque RC. 2019. The Pseudomonas aeruginosa Pan-Genome Provides New Insights on Its Population Structure, Horizontal Gene Transfer, and Pathogenicity. Genome Biol Evol 11:109-120.
36. Andersson DI, Nicoloff H, Hjort K. 2019. Mechanisms and clinical relevance of bacterial heteroresistance. Nat Rev Microbiol 17:479-496.
37. Hermes DM, Pormann Pitt C, Lutz L, Teixeira AB, Ribeiro VB, Netto B, Martins AF, Zavascki AP, Barth AL. 2013. Evaluation of heteroresistance to polymyxin B among carbapenem-susceptible and -resistant Pseudomonas aeruginosa. J Med Microbiol 62:1184-1189.
38. He J, Jia X, Yang S, Xu X, Sun K, Li C, Yang T, Zhang L. 2018. Heteroresistance to carbapenems in invasive Pseudomonas aeruginosa infections. Int J Antimicrob Agents 51:413-421.
39. Xu Y, Zheng X, Zeng W, Chen T, Liao W, Qian J, Lin J, Zhou C, Tian X, Cao J, Zhou T. 2020. Mechanisms of Heteroresistance and Resistance to Imipenem in Pseudomonas aeruginosa. Infect Drug Resist 13:1419-1428.
40. El-Halfawy OM, Valvano MA. 2015. Antimicrobial heteroresistance: an emerging field in need of clarity. Clin Microbiol Rev 28:191-207.
41. Band VI, Weiss DS. 2019. Heteroresistance: A cause of unexplained antibiotic treatment failure? PLoS Pathog 15:e1007726.

42. Band VI, Satola SW, Burd EM, Farley MM, Jacob JT, Weiss DS. 2018. Carbapenem-Resistant Klebsiella pneumoniae Exhibiting Clinically Undetected Colistin Heteroresistance Leads to Treatment Failure in a Murine Model of Infection. mBio 9.
43. Anderson SE, Sherman EX, Weiss DS, Rather PN. 2018. Aminoglycoside Heteroresistance in Acinetobacter baumannii AB5075. mSphere 3.
44. Nicoloff H, Hjort K, Levin BR, Andersson DI. 2019. The high prevalence of antibiotic heteroresistance in pathogenic bacteria is mainly caused by gene amplification. Nat Microbiol 4:504-514.
45. Band VI, Hufnagel DA, Jaggavarapu S, Sherman EX, Wozniak JE, Satola SW, Farley MM, Jacob JT, Burd EM, Weiss DS. 2019. Antibiotic combinations that exploit heteroresistance to multiple drugs effectively control infection. Nat Microbiol 4:1627-1635.
46. Barclay ML, Begg EJ, Chambers ST, Thornley PE, Pattemore PK, Grimwood K. 1996. Adaptive resistance to tobramycin in Pseudomonas aeruginosa lung infection in cystic fibrosis. J Antimicrob Chemother 37:1155-64.
47. Alford MA, Baquir B, An A, Choi KG, Hancock REW. 2021. NtrBC Selectively Regulates Host-Pathogen Interactions, Virulence, and Ciprofloxacin Susceptibility of Pseudomonas aeruginosa. Front Cell Infect Microbiol 11:694789.
48. Skiada A, Markogiannakis A, Plachouras D, Daikos GL. 2011. Adaptive resistance to cationic compounds in Pseudomonas aeruginosa. Int J Antimicrob Agents 37:187-93.
49. Coleman SR, Blimkie T, Falsafi R, Hancock REW. 2020. Multidrug Adaptive Resistance of Pseudomonas aeruginosa Swarming Cells. Antimicrob Agents Chemother 64.
50. Brauner A, Fridman O, Gefen O, Balaban NQ. 2016. Distinguishing between resistance, tolerance and persistence to antibiotic treatment. Nat Rev Microbiol 14:320-30.
51. Grassi L, Di Luca M, Maisetta G, Rinaldi AC, Esin S, Trampuz A, Batoni G. 2017. Generation of Persister Cells of Pseudomonas aeruginosa and Staphylococcus aureus by Chemical Treatment and Evaluation of Their Susceptibility to Membrane-Targeting Agents. Front Microbiol 8:1917.
52. Renbarger TL, Baker JM, Sattley WM. 2017. Slow and steady wins the race: an examination of bacterial persistence. AIMS Microbiol 3:171-185.
53. Hobby GL MK, Chaffee E. 1942. Observations on the mechanism of action of penicillin. Proc Soc Exp Biol Med 50:281-285.
54. Bigger J. 1944. Treatment of staphylococcal infections with penicillin by intermittent sterilisation. Lancet 244:497-500.
55. Soares A, Roussel V, Pestel-Caron M, Barreau M, Caron F, Bouffartigues E, Chevalier S, Etienne M. 2019. Understanding Ciprofloxacin Failure in Pseudomonas aeruginosa Biofilm: Persister Cells Survive Matrix Disruption. Front Microbiol 10:2603.

56. Zhou J, Li S, Li H, Jin Y, Bai F, Cheng Z, Wu W. 2021. Identification of a Toxin-Antitoxin System That Contributes to Persister Formation by Reducing NAD in Pseudomonas aeruginosa. Microorganisms 9.
57. Andersen SB, Ghoul M, Griffin AS, Petersen B, Johansen HK, Molin S. 2017. Diversity, Prevalence, and Longitudinal Occurrence of Type II Toxin-Antitoxin Systems of Pseudomonas aeruginosa Infecting Cystic Fibrosis Lungs. Front Microbiol 8:1180.
58. Kim Y, Wood TK. 2010. Toxins Hha and CspD and small RNA regulator Hfq are involved in persister cell formation through MqsR in Escherichia coli. Biochem Biophys Res Commun 391:209-13.
59. Dorr T, Vulic M, Lewis K. 2010. Ciprofloxacin causes persister formation by inducing the TisB toxin in Escherichia coli. PLoS Biol 8:e1000317.
60. Brown BL, Grigoriu S, Kim Y, Arruda JM, Davenport A, Wood TK, Peti W, Page R. 2009. Three dimensional structure of the MqsR:MqsA complex: a novel TA pair comprised of a toxin homologous to RelE and an antitoxin with unique properties. PLoS Pathog 5:e1000706.
61. Gonzalez Barrios AF, Zuo R, Hashimoto Y, Yang L, Bentley WE, Wood TK. 2006. Autoinducer 2 controls biofilm formation in Escherichia coli through a novel motility quorum-sensing regulator (MqsR, B3022). J Bacteriol 188:305-16.
62. Ren D, Bedzyk LA, Thomas SM, Ye RW, Wood TK. 2004. Gene expression in Escherichia coli biofilms. Appl Microbiol Biotechnol 64:515-24.
63. Hong SH, Wang X, O'Connor HF, Benedik MJ, Wood TK. 2012. Bacterial persistence increases as environmental fitness decreases. Microb Biotechnol 5:509-22.
64. Mulcahy LR, Burns JL, Lory S, Lewis K. 2010. Emergence of Pseudomonas aeruginosa strains producing high levels of persister cells in patients with cystic fibrosis. J Bacteriol 192:6191-9.
65. Lewis K. 2007. Persister cells, dormancy and infectious disease. Nat Rev Microbiol 5:48-56.
66. Zierdt CH, Schmidt PJ. 1964. Dissociation in Pseudomonas aeruginosa. J Bacteriol 87:1003-10.
67. Haussler S, Tummler B, Weissbrodt H, Rohde M, Steinmetz I. 1999. Small-colony variants of Pseudomonas aeruginosa in cystic fibrosis. Clin Infect Dis 29:621-5.
68. Melter OR, B. 2010. Small colony variants of staphylococcus aureus - review. Folia Microbiol 55.
69. Boles BR, Thoendel M, Singh PK. 2004. Self-generated diversity produces "insurance effects" in biofilm communities. Proc Natl Acad Sci U S A 101:16630-5.
70. Pestrak MJC, S.B.; Eggleston, H.C.; Dellos-Nolan, S.; Dixit, S.; Mathew-Steiner, S.S.; Roy, S.; Parsek, M.R.; Sen, C.K.; Wozniak, D.J. 2018. Pseudomonas aeruginosa rugose small-colony variants evade host clearance, are hyper-inflammatory, and persist in multiple host environments. PLoS Pathog 14.

71. Drenkard E, Ausubel FM. 2002. Pseudomonas biofilm formation and antibiotic resistance are linked to phenotypic variation. Nature 416:740-3.
72. D'Argenio DA, Calfee MW, Rainey PB, Pesci EC. 2002. Autolysis and autoaggregation in Pseudomonas aeruginosa colony morphology mutants. J Bacteriol 184:6481-9.
73. Ross P, Weinhouse H, Aloni Y, Michaeli D, Weinberger-Ohana P, Mayer R, Braun S, de Vroom E, van der Marel GA, van Boom JH, Benziman M. 1987. Regulation of cellulose synthesis in Acetobacter xylinum by cyclic diguanylic acid. Nature 325:279-81.
74. Boyd CD, O'Toole GA. 2012. Second messenger regulation of biofilm formation: breakthroughs in understanding c-di-GMP effector systems. Annu Rev Cell Dev Biol 28:439-62.
75. Hickman JW, Harwood CS. 2008. Identification of FleQ from Pseudomonas aeruginosa as a c-di-GMP-responsive transcription factor. Mol Microbiol 69:376-89.
76. Baraquet C, Murakami K, Parsek MR, Harwood CS. 2012. The FleQ protein from Pseudomonas aeruginosa functions as both a repressor and an activator to control gene expression from the pel operon promoter in response to c-di-GMP. Nucleic Acids Res 40:7207-18.
77. Malone JG, Jaeger T, Spangler C, Ritz D, Spang A, Arrieumerlou C, Kaever V, Landmann R, Jenal U. 2010. YfiBNR mediates cyclic di-GMP dependent small colony variant formation and persistence in Pseudomonas aeruginosa. PLoS Pathog 6:e1000804.
78. Starkey M, Hickman JH, Ma L, Zhang N, De Long S, Hinz A, Palacios S, Manoil C, Kirisits MJ, Starner TD, Wozniak DJ, Harwood CS, Parsek MR. 2009. Pseudomonas aeruginosa rugose small-colony variants have adaptations that likely promote persistence in the cystic fibrosis lung. J Bacteriol 191:3492-503.
79. Blanka A, Duvel J, Dotsch A, Klinkert B, Abraham WR, Kaever V, Ritter C, Narberhaus F, Haussler S. 2015. Constitutive production of c-di-GMP is associated with mutations in a variant of Pseudomonas aeruginosa with altered membrane composition. Sci Signal 8:ra36.
80. Kirisits MJ, Prost L, Starkey M, Parsek MR. 2005. Characterization of colony morphology variants isolated from Pseudomonas aeruginosa biofilms. Appl Environ Microbiol 71:4809-21.
81. Hickman JW, Tifrea DF, Harwood CS. 2005. A chemosensory system that regulates biofilm formation through modulation of cyclic diguanylate levels. Proc Natl Acad Sci U S A 102:14422-7.
82. Jennings LKS, K.M.; Ledvina, H.E.; Coulon, C.; Marmont, L.S.; Sadovskaya, I.; Secor, P.R.; Tseng, B.S.; Scian, M.; Filloux, A.; et al. . 2015. Pel is a cationic exopolysaccharide that cross-links extracellular DNA in the Pseudomonas aeruginosa biofilm matrix. Proc Natl Acad Sci U S A 112.
83. Schiessl KT, Hu F, Jo J, Nazia SZ, Wang B, Price-Whelan A, Min W, Dietrich LEP. 2019. Phenazine production promotes antibiotic tolerance and metabolic heterogeneity in Pseudomonas aeruginosa biofilms. Nat Commun 10:762.

84. Glasser NRK, S.E.; Newman, D.K. 2014. Phenazine redox cycling enhances anaerobic survival in Pseudomonas aeruginosa by facilitating generation of ATP and a proton-motive force. Mol Microbiol 92.
85. McCurtain JL, Gilbertsen AJ, Evert C, Williams BJ, Hunter RC. 2019. Agmatine accumulation by Pseudomonas aeruginosa clinical isolates confers antibiotic tolerance and dampens host inflammation. J Med Microbiol 68:446-455.
86. Sindeldecker D, Moore K, Li A, Wozniak DJ, Anderson M, Dusane DH, Stoodley P. 2020. Novel Aminoglycoside-Tolerant Phoenix Colony Variants of Pseudomonas aeruginosa. Antimicrob Agents Chemother 64.
87. Satola SW, Farley MM, Anderson KF, Patel JB. 2011. Comparison of detection methods for heteroresistant vancomycin-intermediate Staphylococcus aureus, with the population analysis profile method as the reference method. J Clin Microbiol 49:177-83.
88. Tolker-Nielsen T. 2015. Biofilm Development. Microbiol Spectr 3:MB-0001-2014.
89. Skariyachan S, Sridhar VS, Packirisamy S, Kumargowda ST, Challapilli SB. 2018. Recent perspectives on the molecular basis of biofilm formation by Pseudomonas aeruginosa and approaches for treatment and biofilm dispersal. Folia Microbiol (Praha) 63:413-432.
90. Maurice NM, Bedi B, Sadikot RT. 2018. Pseudomonas aeruginosa Biofilms: Host Response and Clinical Implications in Lung Infections. Am J Respir Cell Mol Biol 58:428-439.
91. Marmont LS, Whitfield GB, Rich JD, Yip P, Giesbrecht LB, Stremick CA, Whitney JC, Parsek MR, Harrison JJ, Howell PL. 2017. PelA and PelB proteins form a modification and secretion complex essential for Pel polysaccharide-dependent biofilm formation in Pseudomonas aeruginosa. J Biol Chem 292:19411-19422.
92. Jones CJ, Wozniak DJ. 2017. Psl Produced by Mucoid Pseudomonas aeruginosa Contributes to the Establishment of Biofilms and Immune Evasion. mBio 8.
93. Jenal U, Reinders A, Lori C. 2017. Cyclic di-GMP: second messenger extraordinaire. Nat Rev Microbiol 15:271-284.
94. Song F, Wang H, Sauer K, Ren D. 2018. Cyclic-di-GMP and oprF Are Involved in the Response of Pseudomonas aeruginosa to Substrate Material Stiffness during Attachment on Polydimethylsiloxane (PDMS). Front Microbiol 9:110.
95. Kahl LJ, Price-Whelan A, Dietrich LEP. 2020. Light-Mediated Decreases in Cyclic di-GMP Levels Inhibit Structure Formation in Pseudomonas aeruginosa Biofilms. J Bacteriol 202.
96. Mukherjee S, Moustafa D, Smith CD, Goldberg JB, Bassler BL. 2017. The RhlR quorum-sensing receptor controls Pseudomonas aeruginosa pathogenesis and biofilm development independently of its canonical homoserine lactone autoinducer. PLoS Pathog 13:e1006504.
97. Kostylev M, Kim DY, Smalley NE, Salukhe I, Greenberg EP, Dandekar AA. 2019. Evolution of the Pseudomonas aeruginosa quorum-sensing hierarchy. Proc Natl Acad Sci U S A 116:7027-7032.

98. Walters MC, 3rd, Roe F, Bugnicourt A, Franklin MJ, Stewart PS. 2003. Contributions of antibiotic penetration, oxygen limitation, and low metabolic activity to tolerance of Pseudomonas aeruginosa biofilms to ciprofloxacin and tobramycin. Antimicrob Agents Chemother 47:317-23.
99. Tseng BS, Zhang W, Harrison JJ, Quach TP, Song JL, Penterman J, Singh PK, Chopp DL, Packman AI, Parsek MR. 2013. The extracellular matrix protects Pseudomonas aeruginosa biofilms by limiting the penetration of tobramycin. Environ Microbiol 15:2865-78.
100. Bernier SP, Lebeaux D, DeFrancesco AS, Valomon A, Soubigou G, Coppee JY, Ghigo JM, Beloin C. 2013. Starvation, together with the SOS response, mediates high biofilm-specific tolerance to the fluoroquinolone ofloxacin. PLoS Genet 9:e1003144.
101. Nguyen D, Joshi-Datar A, Lepine F, Bauerle E, Olakanmi O, Beer K, McKay G, Siehnel R, Schafhauser J, Wang Y, Britigan BE, Singh PK. 2011. Active starvation responses mediate antibiotic tolerance in biofilms and nutrient-limited bacteria. Science 334:982-6.
102. Stewart PS, Zhang T, Xu R, Pitts B, Walters MC, Roe F, Kikhney J, Moter A. 2016. Reaction-diffusion theory explains hypoxia and heterogeneous growth within microbial biofilms associated with chronic infections. NPJ Biofilms Microbiomes 2:16012.
103. Nicholle LE. 2014. Catheter associated urinary tract infections. Antimicrob Resist Infect Control 25.
104. Xu WH, L.; Liu, C.; Rong, J.; Shi, Y.; Song, W.; Zhang, T.; Wang, L. 2015. The effect of infection control nurses on the occurence of Pseudomonas aeruginosa healthcare-acquired infection and multidrug-resistant strains in critically ill children. PLoS One 10.
105. Mulcahy LRI, V.M.; Lewis, K. 2014. Pseudomonas aeruginosa biofilms in disease. Microb Ecol 68.
106. Stewart PS. 2002. Mechanisms of antibiotic resistance in bacterial biofilms. Int J Med Microbiol 292:107-13.
107. Pachori P, Gothalwal R, Gandhi P. 2019. Emergence of antibiotic resistance Pseudomonas aeruginosa in intensive care unit; a critical review. Genes Dis 6:109-119.
108. Pang Z, Raudonis R, Glick BR, Lin TJ, Cheng Z. 2019. Antibiotic resistance in Pseudomonas aeruginosa: mechanisms and alternative therapeutic strategies. Biotechnol Adv 37:177-192.
109. Hoiby N, Bjarnsholt T, Moser C, Jensen PO, Kolpen M, Qvist T, Aanaes K, Pressler T, Skov M, Ciofu O. 2017. Diagnosis of biofilm infections in cystic fibrosis patients. APMIS 125:339-343.
110. Hoiby N, Ciofu O, Bjarnsholt T. 2010. Pseudomonas aeruginosa biofilms in cystic fibrosis. Future Microbiol 5:1663-74.
111. Wentao Z, Lei G, Liu Y, Wang W, Song T, Fan J. 2017. Approach to osteomyelitis treatment with antibiotic loaded PMMA. Microb Pathog 102:42-44.

112. Dusane DH, Diamond SM, Knecht CS, Farrar NR, Peters CW, Howlin RP, Swearingen MC, Calhoun JH, Plaut RD, Nocera TM, Granger JF, Stoodley P. 2017. Effects of loading concentration, blood and synovial fluid on antibiotic release and anti-biofilm activity of bone cement beads. J Control Release 248:24-32.
113. Devendra H. Dusane JRB, Devin Sindeldecker, Casey W. Peters, Anthony Li, Nicholas R. Farrar, Scott M. Diamond, Cory S. Knecht, Roger D. Plaut, Craig Delury, Sean S. Aiken, Phillip A. Laycock, Anne Sullivan, Jeffrey F. Granger, and Paul Stoodley. 2019. Complete Killing of Agar Lawn Biofilms by Systematic Spacing of Antibiotic-Loaded Calcium Sulfate Beads. Materials.
114. Howlin RP, Brayford MJ, Webb JS, Cooper JJ, Aiken SS, Stoodley P. 2015. Antibiotic-loaded synthetic calcium sulfate beads for prevention of bacterial colonization and biofilm formation in periprosthetic infections. Antimicrob Agents Chemother 59:111-20.
115. Lederberg J, Lederberg EM. 1952. Replica plating and indirect selection of bacterial mutants. J Bacteriol 63:399-406.
116. Stefani S, Campana S, Cariani L, Carnovale V, Colombo C, Lleo MM, Iula VD, Minicucci L, Morelli P, Pizzamiglio G, Taccetti G. 2017. Relevance of multidrug-resistant Pseudomonas aeruginosa infections in cystic fibrosis. Int J Med Microbiol 307:353-362.
117. Waters V, Smyth A. 2015. Cystic fibrosis microbiology: Advances in antimicrobial therapy. J Cyst Fibros 14:551-60.
118. Gefen O, Chekol B, Strahilevitz J, Balaban NQ. 2017. TDtest: easy detection of bacterial tolerance and persistence in clinical isolates by a modified disk-diffusion assay. Sci Rep 7:41284.
119. Hall-Stoodley L, Stoodley P. 2009. Evolving concepts in biofilm infections. Cell Microbiol 11:1034-43.
120. Lima J, Alves LR, Paz J, Rabelo MA, Maciel MAV, Morais MMC. 2017. Analysis of biofilm production by clinical isolates of Pseudomonas aeruginosa from patients with ventilator-associated pneumonia. Rev Bras Ter Intensiva doi:10.5935/0103-507X.20170039:0.
121. Swearingen MC, Granger JF, Sullivan A, Stoodley P. 2016. Elution of antibiotics from poly(methyl methacrylate) bone cement after extended implantation does not necessarily clear the infection despite susceptibility of the clinical isolates. Pathog Dis 74:ftv103.
122. Aeschlimann JR. 2003. The role of multidrug efflux pumps in the antibiotic resistance of Pseudomonas aeruginosa and other gram-negative bacteria. Insights from the Society of Infectious Diseases Pharmacists. Pharmacotherapy 23:916-24.
123. Wang DD, Sun TY, Hu YJ. 2007. Contributions of efflux pumps to high level resistance of Pseudomonas aeruginosa to ciprofloxacin. Chin Med J (Engl) 120:68-70.
124. Ramamurthy T, Ghosh A, Pazhani GP, Shinoda S. 2014. Current Perspectives on Viable but Non-Culturable (VBNC) Pathogenic Bacteria. Front Public Health 2:103.

125. Jacobs MA, Alwood A, Thaipisuttikul I, Spencer D, Haugen E, Ernst S, Will O, Kaul R, Raymond C, Levy R, Chun-Rong L, Guenthner D, Bovee D, Olson MV, Manoil C. 2003. Comprehensive transposon mutant library of Pseudomonas aeruginosa. Proc Natl Acad Sci U S A 100:14339-44.
126. Wick R. 2018. Porechop. https://github.com/rrwick/Porechop. Accessed
127. Winsor GL, Griffiths EJ, Lo R, Dhillon BK, Shay JA, Brinkman FS. 2016. Enhanced annotations and features for comparing thousands of Pseudomonas genomes in the Pseudomonas genome database. Nucleic Acids Res 44:D646-53.
128. Sovic I, Sikic M, Wilm A, Fenlon SN, Chen S, Nagarajan N. 2016. Fast and sensitive mapping of nanopore sequencing reads with GraphMap. Nat Commun 7:11307.
129. Li H, Handsaker B, Wysoker A, Fennell T, Ruan J, Homer N, Marth G, Abecasis G, Durbin R, Genome Project Data Processing S. 2009. The Sequence Alignment/Map format and SAMtools. Bioinformatics 25:2078-9.
130. Sedlazeck FJ, Rescheneder P, Smolka M, Fang H, Nattestad M, von Haeseler A, Schatz MC. 2018. Accurate detection of complex structural variations using single-molecule sequencing. Nat Methods 15:461-468.
131. Li H. 2011. A statistical framework for SNP calling, mutation discovery, association mapping and population genetical parameter estimation from sequencing data. Bioinformatics 27:2987-93.
132. Andrews S. FastQC. https://www.bioinformatics.babraham.ac.uk/projects/fastqc/. Accessed
133. Dobin A, Davis CA, Schlesinger F, Drenkow J, Zaleski C, Jha S, Batut P, Chaisson M, Gingeras TR. 2013. STAR: ultrafast universal RNA-seq aligner. Bioinformatics 29:15-21.
134. Robinson JT, Thorvaldsdottir H, Winckler W, Guttman M, Lander ES, Getz G, Mesirov JP. 2011. Integrative genomics viewer. Nat Biotechnol 29:24-6.
135. Anders S, Pyl PT, Huber W. 2015. HTSeq--a Python framework to work with high-throughput sequencing data. Bioinformatics 31:166-9.
136. Robinson MD, McCarthy DJ, Smyth GK. 2010. edgeR: a Bioconductor package for differential expression analysis of digital gene expression data. Bioinformatics 26:139-40.
137. Huang da W, Sherman BT, Lempicki RA. 2009. Systematic and integrative analysis of large gene lists using DAVID bioinformatics resources. Nat Protoc 4:44-57.
138. Huang da W, Sherman BT, Lempicki RA. 2009. Bioinformatics enrichment tools: paths toward the comprehensive functional analysis of large gene lists. Nucleic Acids Res 37:1-13.
139. Kanehisa M, Sato Y. 2020. KEGG Mapper for inferring cellular functions from protein sequences. Protein Sci 29:28-35.
140. Kelley LA, Mezulis S, Yates CM, Wass MN, Sternberg MJ. 2015. The Phyre2 web portal for protein modeling, prediction and analysis. Nat Protoc 10:845-58.
141. Sayle RA, Milner-White EJ. 1995. RASMOL: biomolecular graphics for all. Trends Biochem Sci 20:374.

142. R.K. Kniewel JAB, C.D. Lima. Structure of the S. pombe YchF GTP-binding protein.
143. Teplyakov A, Obmolova G, Chu SY, Toedt J, Eisenstein E, Howard AJ, Gilliland GL. 2003. Crystal structure of the YchF protein reveals binding sites for GTP and nucleic acid. J Bacteriol 185:4031-7.
144. Kaya Y, Ofengand J. 2003. A novel unanticipated type of pseudouridine synthase with homologs in bacteria, archaea, and eukarya. RNA 9:711-21.
145. Belitsky BR. 2004. Bacillus subtilis GabR, a protein with DNA-binding and aminotransferase domains, is a PLP-dependent transcriptional regulator. J Mol Biol 340:655-64.
146. Ito T, Yamamoto K, Hori R, Yamauchi A, Downs DM, Hemmi H, Yoshimura T. 2019. Conserved Pyridoxal 5'-Phosphate-Binding Protein YggS Impacts Amino Acid Metabolism through Pyridoxine 5'-Phosphate in Escherichia coli. Appl Environ Microbiol 85.
147. Rosenbaum DM, Rasmussen SG, Kobilka BK. 2009. The structure and function of G-protein-coupled receptors. Nature 459:356-63.
148. Jana S, Deb JK. 2006. Molecular understanding of aminoglycoside action and resistance. Appl Microbiol Biotechnol 70:140-50.
149. Walter F, Putz J, Giege R, Westhof E. 2002. Binding of tobramycin leads to conformational changes in yeast tRNA(Asp) and inhibition of aminoacylation. EMBO J 21:760-8.
150. Wang B, Wilkinson KA, Weeks KM. 2008. Complex ligand-induced conformational changes in tRNA(Asp) revealed by single-nucleotide resolution SHAPE chemistry. Biochemistry 47:3454-61.
151. Kaya Y, Del Campo M, Ofengand J, Malhotra A. 2004. Crystal structure of TruD, a novel pseudouridine synthase with a new protein fold. J Biol Chem 279:18107-10.
152. Chen R, Wei X, Li Z, Weng Y, Xia Y, Ren W, Wang X, Jin Y, Bai F, Cheng Z, Jin S, Wu W. 2019. Identification of a small RNA that directly controls the translation of the quorum sensing signal synthase gene rhlI in Pseudomonas aeruginosa. Environ Microbiol 21:2933-2947.
153. Bjarnsholt T, Jensen PO, Burmolle M, Hentzer M, Haagensen JAJ, Hougen HP, Calum H, Madsen KG, Moser C, Molin S, Hoiby N, Givskov M. 2005. Pseudomonas aeruginosa tolerance to tobramycin, hydrogen peroxide and polymorphonuclear leukocytes is quorum-sensing dependent. Microbiology (Reading) 151:373-383.
154. Kayama S, Murakami K, Ono T, Ushimaru M, Yamamoto A, Hirota K, Miyake Y. 2009. The role of rpoS gene and quorum-sensing system in ofloxacin tolerance in Pseudomonas aeruginosa. FEMS Microbiol Lett 298:184-92.
155. Viducic D, Murakami K, Amoh T, Ono T, Miyake Y. 2016. RpoN Modulates Carbapenem Tolerance in Pseudomonas aeruginosa through Pseudomonas Quinolone Signal and PqsE. Antimicrob Agents Chemother 60:5752-64.
156. Appaneal HJ, Caffrey AR, Jiang L, Dosa D, Mermel LA, LaPlante KL. 2018. Antibiotic resistance rates for Pseudomonas aeruginosa clinical respiratory and

bloodstream isolates among the Veterans Affairs Healthcare System from 2009 to 2013. Diagn Microbiol Infect Dis 90:311-315.
157. MacGowan AP, Wootton M, Holt HA. 1999. The antibacterial efficacy of levofloxacin and ciprofloxacin against Pseudomonas aeruginosa assessed by combining antibiotic exposure and bacterial susceptibility. J Antimicrob Chemother 43:345-9.
158. Madaras-Kelly KJ, Ostergaard BE, Hovde LB, Rotschafer JC. 1996. Twenty-four-hour area under the concentration-time curve/MIC ratio as a generic predictor of fluoroquinolone antimicrobial effect by using three strains of Pseudomonas aeruginosa and an in vitro pharmacodynamic model. Antimicrob Agents Chemother 40:627-32.
159. Hengzhuang W, Hoiby N, Ciofu O. 2014. Pharmacokinetics and pharmacodynamics of antibiotics in biofilm infections of Pseudomonas aeruginosa in vitro and in vivo. Methods Mol Biol 1147:239-54.
160. Dusane DH, Lochab V, Jones T, Peters CW, Sindeldecker D, Das A, Roy S, Sen CK, Subramaniam VV, Wozniak DJ, Prakash S, Stoodley P. 2019. Electroceutical Treatment of Pseudomonas aeruginosa Biofilms. Sci Rep 9:2008.
161. Lochab V, Jones TH, Dusane DH, Peters CW, Stoodley P, Wozniak DJ, Subramaniam VV, Prakash S. 2020. Ultrastructure imaging of Pseudomonas aeruginosa lawn biofilms and eradication of the tobramycin-resistant variants under in vitro electroceutical treatment. Sci Rep 10:9879.
162. Moley JP, McGrath MS, Granger JF, Stoodley P, Dusane DH. 2018. Reduction in Pseudomonas aeruginosa and Staphylococcus aureus biofilms from implant materials in a diffusion dominated environment. J Orthop Res 36:3081-3085.
163. Hoiby N, Henneberg KA, Wang H, Stavnsbjerg C, Bjarnsholt T, Ciofu O, Johansen UR, Sams T. 2019. Formation of Pseudomonas aeruginosa inhibition zone during tobramycin disk diffusion is due to transition from planktonic to biofilm mode of growth. Int J Antimicrob Agents 53:564-573.
164. Nichols WW, Dorrington SM, Slack MP, Walmsley HL. 1988. Inhibition of tobramycin diffusion by binding to alginate. Antimicrob Agents Chemother 32:518-23.
165. Castaneda P, McLaren A, Tavaziva G, Overstreet D. 2016. Biofilm Antimicrobial Susceptibility Increases With Antimicrobial Exposure Time. Clin Orthop Relat Res 474:1659-64.
166. Burkhardt O, Lehmann C, Madabushi R, Kumar V, Derendorf H, Welte T. 2006. Once-daily tobramycin in cystic fibrosis: better for clinical outcome than thrice-daily tobramycin but more resistance development? J Antimicrob Chemother 58:822-9.
167. Smith PF, Ballow CH, Booker BM, Forrest A, Schentag JJ. 2001. Pharmacokinetics and pharmacodynamics of aztreonam and tobramycin in hospitalized patients. Clin Ther 23:1231-44.
168. Gonzalez Della Valle A, Bostrom M, Brause B, Harney C, Salvati EA. 2001. Effective bactericidal activity of tobramycin and vancomycin eluted from acrylic bone cement. Acta Orthop Scand 72:237-40.

169. Dutta Sinha S, Chatterjee S, Maiti PK, Tarafdar S, Moulik SP. 2017. Evaluation of the role of substrate and albumin on Pseudomonas aeruginosa biofilm morphology through FESEM and FTIR studies on polymeric biomaterials. Prog Biomater 6:27-38.
170. Wilkinson HN, Iveson S, Catherall P, Hardman MJ. 2018. A Novel Silver Bioactive Glass Elicits Antimicrobial Efficacy Against Pseudomonas aeruginosa and Staphylococcus aureus in an ex Vivo Skin Wound Biofilm Model. Front Microbiol 9:1450.
171. Davies JC. 2002. Pseudomonas aeruginosa in cystic fibrosis: pathogenesis and persistence. Paediatr Respir Rev 3:128-34.
172. Groleau MC, de Oliveira Pereira T, Dekimpe V, Deziel E. 2020. PqsE Is Essential for RhlR-Dependent Quorum Sensing Regulation in Pseudomonas aeruginosa. mSystems 5.